THE DYNAMICS AND CONTROL OF LARGE-FLEXIBLE SPACE STRUCTURES - X

FINAL REPORT - Part II

NASA GRANT: NSG-1414, Supplement 9

by

Peter M. Bainum
Professor of Aerospace Engineering
Principal Investigator

and

A.S.S.R. Reddy
Assistant Professor
Co-Investigator

and

Cheick M. Diarra
Feiyue Li
Graduate Research Assistants

January 1988

DEPARTMENT OF MECHANICAL ENGINEERING
SCHOOL OF ENGINEERING
HOWARD UNIVERSITY
WASHINGTON, D.C. 20059

PREFACE

This volume represents the second part of the final report for NASA Grant NSG-1414, Suppl. 9. The first part, designated Part I, was published in August 1987 and focused on the stability analysis of large space structure control systems with delayed input and the minimum time attitude slewing maneuver of a rigid spacecraft system with numerical examples based on the rigidized model of the Spacecraft Control Laboratory Experiment (SCOLE) orbiting configuration.

This volume, designated as Part II, is based on the recently completed Ph.D. dissertation by Cheick Modibo Diarra, entitled, "On the Dynamics and Control of the Spacecraft Control Laboratory Experiment (SCOLE) Class of Offset Flexible Systems." First the open-loop dynamics of the orbiting SCOLE system are modeled to include the flexibility of the mast which connects the reflector to the Shuttle. The stability of system motion with respect to the nominal equilibrium during station keeping is considered for special cases, both for the 2-D and 3-D motion models. The control law synthesis is addressed for both small disturbances during station keeping operations and also during large amplitude preliminary slew maneuvers about the Shuttle's roll, pitch, and yaw axes, respectively.

Control law gains for both cases are based on linear quadratic regulator techniques. For the case of the rapid slew maneuvers the results presented here can form a basis of comparison with other results presented in Part I of this report and based on the application of two point boundary value problem techniques.

ABSTRACT

A mathematical model is developed to predict the dynamics of the proposed orbiting Spacecraft Control Laboratory Experiment during the station keeping phase. The Shuttle as well as the reflector are assumed to be rigid, the mast is flexible and is assumed to undergo elastic displacements very small as compared with its length. The equations of motion are derived using a Newton-Euler formulation. The model includes the effects of gravity, flexibility, and orbital dynamics. The control is assumed to be provided to the system through the Shuttle's three torquers, and through six actuators located by pairs at two points on the mast and at the mass center of the reflector. At each of the locations, an actuator acts parallel to the roll axis while the other one acts parallel to the pitch axis. The modal shape functions are derived using the fourth order beam equation. The generic mode equations are derived to account for the effects of the control forces on the modal shapes and frequencies. The equations are linearized about a nominal equilibrium position. When the interface point between the mast and the reflector is assumed to

coincide with the mass center of the reflector, it is seen that the pitch equation is decoupled from the roll and yaw motions. When the interface point is offset along the roll axis the pitch equation is still decoupled from the two other equations (roll and yaw). It is seen that the open loop system is unstable for both cases due to the (gravitationally) unfavorable moment of ineertia distribution. When, in addition to the roll axis offset, a pitch axis offset is introduced into the system, the equations describing the roll, pitch, and yaw motions are seen to be all coupled together. It is further seen that, in the presence of gravity gradient torques in the system dynamics, the system assumes a new equilibrium position about which the equations will have to be linearized. The linear regulator theory is used to derive control laws for both the linear model of the rigidized SCOLE as well as that of the actual SCOLE including the first four flexible modes. The control strategy previously derived for the linear model of the rigidized SCOLE is applied to the non-linear model of the same configuration of the system and preliminary single axis slewing maneuvers conducted. The results obtained confirm the applicability of the

intuitive and appealing two-stage control strategy which would slew the SCOLE system as if rigid to its desired position and then concentrate on damping out the residual flexible motions.

TABLE OF CONTENTS

Table of Contents cont'd

Table of Contents cont'd

LIST OF FIGURES

List of Figures cont'd

List of Figures cont'd

List of Figures cont'd

NOMENCLATURE

$[A]$	system state matrix with elements, A_{ij}
A	cross sectional area of beam
$A_n(t)$	time dependent amplitude of the nth mode
A_1, B_1, C_1, D_1	coefficients of x-z plane mode shape equation
A_2, B_2, C_2, D_2	coefficients of y-z plane mode shape equation
$A_3 B_3$	coefficients of torsinal mode shape equation
$\bar{a}$	inertial acceleration of a generic point in the system
$\bar{a}_o$	inertial acceleration of the system center of mass
$[B]$	control influence matrix with element, B_{ij}
c.m.	center of mass
Dx_0, Dy_0	c.m. displacements in x- and y-directions, respectively, at z = 0 on beam
Dx_L, Dy_L	c.m. displacements in x- and y-directions, respectively, at z = L on beam
EI	bending stiffness for beam when $(EI)_x = (EI)_y$
$(EI)_x$	x-z plane bending stiffness

$(EI)_y$	y-z plane bending stiffness
$\overline{F}i$	control force vectors
G	modulus of rigidity
$\overline{H}$	angular momentum vectors
I_p	polar moment of inertia
$[I_R]$	inertia tensor of the reflector with elements, I
$[I_S]$	inertia tensor of the shuttle elements, I_{Si}
I_{xx}, I_{yy}, I_{zz}	x-, y-, z-axis moments of inertia, respectively for the SCOLE system.
$I_{xx0}, I_{yy0}, I_{zz0}$	x-, y-, and z-axis moments of inertia, respectively, at z = 0
$I_{xxL}, I_{yyL}, I_{zzL}$	x-, y-, and z-axis moments of inertia, respectively, at z = L
I_{xy}	xy product of inertia for the SCOLE system
I_{xy0}	xy product of inertia at z = 0
I_{xyL}	xy product of inertia at L = 0
[K]	gain matrix with elements, k_{ij}
L	length of beam
M_x, M_y, M_z	moments about x-, y-, and z-axes, respectively.
M_{x0}, M_{y0}, M_{z0}	moments about x-, y-, and z-axes, respectively at z = 0 beam.
M_{xL}, M_{yL}, M_{zL}	moments about x-, y-, and z-axes, respectively at z = L beam.

M	mass of the beam
M_S	mass at z = 0 on beam (shuttle)
M_R	mass at z = L on beam (reflector)
$p(t)$	common time solution of partial D.E.'s
$P_x(t), P_y(t), P_z(t)$	separate time solutions of xz-plane, yz-plane, z-axis torsional P.D.E.'s, respectively.
$\bar{q}$	transverse elastic displacement vector
R	orbit radius
R_i	frames of reference
$\bar{r}_o$	position vector of the generic point of the undeformed system
$s_x(z), s_x(\ )$	xz-plane mode shape
$s_y(z), s_y(\ )$	yz-plane mode shape
t	time
$u(z,t)$	beam displacement in xz-plane
$v(z,t)$	beam displacement in yz-plane
V_x, V_y	shear forces in x- and y-directions, respectively
V_{xO}, V_{yO}	shear forces in x- and y-directions, respectively, at z = 0 on beams
V_{xL}, V_{yL}	shear forces in x- and y-directions, respectively, at z = L on beams
X, Y	offset variables
$z(\beta)$	eigenvalue matrix

α, γ, δ	phase angle (rad)
β_x	mode shape variable for x-z plane
β_Y	mode shape variable for yz-plane
β_z	mode shape variable for z-axis torsion
ε	dimensionless position variable ($\varepsilon = z/L$)
θ	pitch angle
θ_R	z-axis torsional mode shape
θ_x	angular displacement about x-axis
θ_y	angular displacement about y-axis
ρ	mass of the beam per unit length
ϕ	yaw angle
Φ_R	angular displacement about z-axis
$\vec{\Omega}_i$	angular velocity vectors
ω	natural frequency common to all three governing partial D.E.'s
ω_O	orbital angular velocity
$\omega_x, \omega_y, \omega_z$	natural frequency of vibration of xz-plane, yz-plane, and z-axis torsional bending modes, respectively
ψ	roll angle

CHAPTER ONE

INTRODUCTION

The problem of maneuvering a flexible spacecraft while suppressing the induced vibrations is becoming increasingly important. NASA is involved in studies which are concerned with the control of flexible bodies carried by a Shuttle in an Earth orbit. Similar experiments are being conducted in Earth-based laboratories. It is then desirable to derive a formulation which can accommodate both types of experiments.

NASA is currently involved in at least two experimental programs to test techniques derived for active control of flexible space structures.

In several versions of a recent paper, SCOLE[1] (Spacecraft Control Laboratory Experiment), Lawrence W. Taylor, Jr. and A.V. Balakrishnan have described the first which is ground based. It is a laboratory experiment based on a model of the Shuttle connected to a flexible beam with a reflecting grillage mounted at the end of the beam (Figure I.1). As a part of the design challenge, the authors stressed the need to directly compare competing control design techniques and discussed the

feasibility of such a direct comparison. Concern would be given to modeling order reduction, fault management, stability, and dynamic systems. Ground-based experimentation has its limitations because it is almost impossible to to duplicate the space environment in a laboratory. The second experimental program is known as Control of Flexible Spacecraft (COFS)[2] and consists of experiments designed to control flexible bodies carried by a Shuttle in an Earth orbit. Because of the cost and risks involved in testing control techniques in space, COFS includes laboratory simulations of similar experiments which will precede the space test. Therefore, in assuring the success of both SCOLE and COFS, mathematical modeling and computer simulation are required.

To accurately model and simulate flexible spacecraft, one needs a thorough knowledge of its structural behavior. In a paper[3], subsequent to the design challenge, the modal shapes and frequencies for the SCOLE system were derived. In the analysis of the mathematical model of reference 3, the SCOLE system is assumed to be described by partial differential equations in which the variables separate. The assumptions in that study did not create a

noticeable difference with the results previously derived[1]. Based on the equations describing the motion of the SCOLE system provided in reference 1, the expression for the reflector line-of-sight (LOS) error was expanded analytically ~~and studied~~ carefully[4]. Analytical results showed that the SCOLE's LOS error is independent of the Euler yaw attitude angle so, only two, instead of, originally three, angular parameters were needed to be concerned with in designing the pointing slew maneuvers.

Numerical simulation[4] test results indicated, then, that the single axis bang-bang or bang-pause-bang slew maneuvers work fairly well for pointing the LOS of SCOLE. The best pointing accuracy and shortest slew time were attained when using the Shuttle torquers and actuators placed on the reflector while imposing a 5 degree/second slew rate limit on the design.

Recently, a paper[5] concerned with the derivation of the equations of motion of the SCOLE class of flexible structures was published. The equations are supposed to describe a manuevering flexible spacecraft both in orbit and in an Earth based laboratory.[6] The analysis is based on a perturbation technique in which the large

rigid-body motion are regarded as the unperturbed motion of the spacecraft while the induced elastic motions and deviations from the nominal rigid motions are considered as perturbations. A maneuver force distribution on the SCOLE system corresponding to the least amount of elastic deformation is derived. The paper also highlights the coupling between the rigid and flexible modes.

With the aforementioned papers as a background, the present study commenced by first reviewing literature pertaining to Reference 1, together with texts and papers which treat structural dynamics modeling and boundary value problems[7].

Then, a mathematical model of the SCOLE system is developed assuming that: the space Shuttle is a rigid body; the reflector mast is a flexible beam type appendage; and that the reflector is a rigid plate. The mast shape functions and frequencies are obtained from the fourth order flexural beam partial differential equation with different boundary conditions assumed to be imposed on both the Shuttle and reflector grillage ends. The system is represented as a beam connected at both ends to bodies with inertia.

Frequencies and modal shapes are derived for in-plane and out-of-plane bending modes as well as for the shaft torsional vibrational modes.

The equation describing the in-plane dynamics of the system are developed based on an Eulerian formulation. This equation is linearized about a nominal motion where the Shuttle would have its velocity vector along the local horizontal.

Also undertaken in this study is the modeling of the three dimensional dynamics of the SCOLE configuration based on the Eulerian techniques already employed in the development of the in-plane (2-D) open-loop dynamics. The increased complexity of this three dimensional formulation should be emphasized. The techniques consist in isolating an elemental mass of the system in its deformed state and deriving its angular momentum taken at the mass center of the Orbiter.

The position vector extending from the origin of the coordinate system to the elemental mass of the mast or the reflector accounts for the elastic displacements. The expressions for these displacements are derived from the mode shape functions generated during the three

dimensional structural analysis of the system (see Appendix A).

The equations obtained for the elemental masses of the components of the system are integrated over the mass of the entire system to yield its angular momentum about the mass center of the Orbiter. The derivative of the system angular momentum with respect to time is equated with the gravity gradient torques[8] on the system about the same point (see Appendix C). Such a vectorial equation, when projected along the three axes of rotation, yields the system rotational equations of motion. These rotational equations of motion are then linearized to yield a model which provides the basis for the control law synthesis developed in this study. But first, the stability analysis is conducted in the three following steps:

first, when the mast is assumed to be rigid and to be connected to both end bodies, at their mass centers;

second, when the interface point between the mast and the reflector is offset with respect to the reflector mass center in the "x" direction while the mast is still assumed rigid; and

finally when the "y" offset is introduced into the rigid SCOLE configuration. The flexible model of the SCOLE system, which includes the effects of the first four flexible modes, is obtained by substituting the expressions for the acceleration of the modal amplitudes, obtained from the generic mode equations, into the rotational equations of motion. These expressions take into account the effects of the controllers on the modal shapes and frequencies of the structure.

The ORACLS[9] package is used to derive control laws for both the rigidized SCOLE (linearized model) and the linearized model of SCOLE with a flexible mast.

The control law, based on the linear regulator theory, derived for the linearized model of the rigidized SCOLE is also used for large amplitude rigid motion maneuvers. The non-linear equations describing the dynamics of that model are derived from the more general rotational equations of motion previously obtained. From the numerical results obtained from the simulations of all three models, conclusions are drawn regarding the modeling technique used herein, and the control efforts versus maneuver time of this strategy is compared with control laws previously presented for consideration for their

implementation in the laboratory model of the SCOLE. Under some additional assumptions, the equations describing the dynamics of the SCOLE system can be modified and adapted to systems with offsets proposed or currently under development such as the Wrap-Rib antenna[10] in which the attachment of the lower mast, to the rest of the system, is offset and the tether connected platform (Kinetic Isolation Tether Experiment)[11-13] in which the location of the interface point between the platform and the tether can vary.

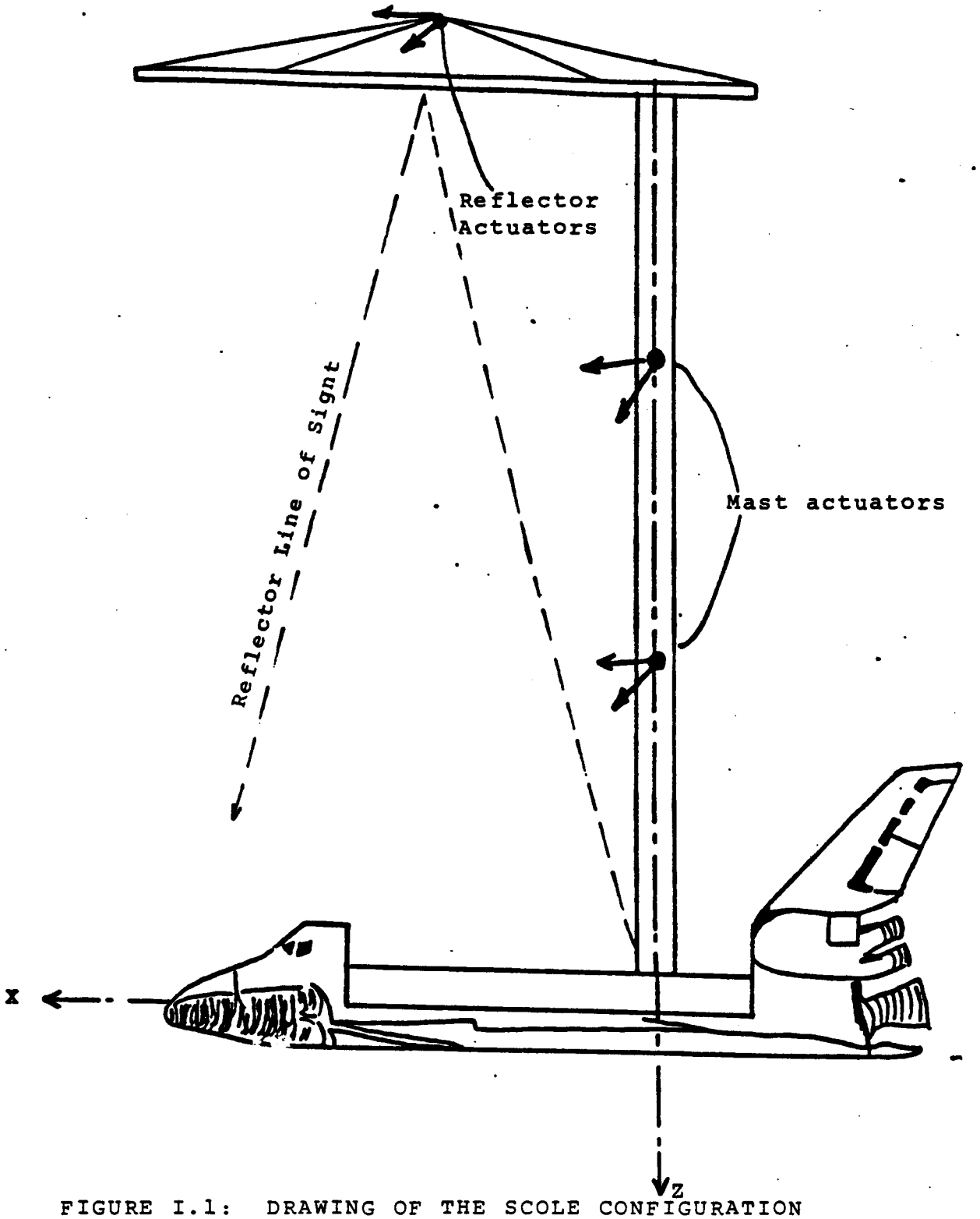

FIGURE I.1: DRAWING OF THE SCOLE CONFIGURATION

CHAPTER TWO

TWO DIMENSIONAL ANALYSIS OF THE SCOLE CONFIGURATION

In this chapter, the equation describing the in-plane (rotational) dynamics of the SCOLE configuration (Figure II.1) is derived using the Eulerian moment equation.

The folllowing main assumptions are made in the development:

a) the space Shuttle orbiter is assumed to be rigid;

b) the mast, treated as a 130 ft long beam, is rigidly connected to the Shuttle at G, mass center of the orbiter, and to the reflector at O_1, the interface point.

c) the reflector is considered to be a flat and rigid plate with its mass center at G_1;

d) the mast is assumed homogeneous and isotropic;

e) the elastic displacements are assumed small as compared with the length of the mast.

f) the analysis here is performed by assuming that the mast vibrates at only one of its flexible modal frequencies but can be extended, within the linear range, by superimposing the effects of several modes.

II.1. Angular Momentum of the Shuttle with Respect to its Center of Mass, G.

The center of mass of the Shuttle is considered to move in an orbit about a fixed point, the geocenter 0; its angular momentum about its center of mass is given by

$$\bar{H}_{S/G} = (\dot{\theta}-\omega_0)\, I_{S2}\, \hat{j} \qquad \text{(II.1)}$$

where $\dot{\theta}$ is the pitch rate, ω_0 the angular velocity of the orbit, I_{S2} the moment of inertia of the orbiter with respect to an axis passing through G and perpendicular to the the orbit plane.

II.2 Angular Momentum of the Mast With Respect to G, the Orbiter Center of Mass.

Consider here an element of the mast located at point P, with mass dm. The elemental angular momentum of such an element is given by

$$\vec{dH}_{M/G} = \vec{GP} \times \frac{d}{dt}(\vec{GP})\Big|_{R_0} dm \qquad \text{(II.2)}$$

where R_0 is the inertial frame centered at the geocenter, O.

If one notes that

$$\vec{GP} = \bar{r}_0 + \bar{q}; \qquad \text{(II.3)}$$

then, Equation (II.2) may be expanded according to:

$$\bar{H}_{M/G} = \int_M (\bar{r}_0+\bar{q}) \times (\dot{\bar{r}}_0+\dot{\bar{q}})\, dm \qquad \text{(II.4)}$$

$\frac{d\bar{R}}{dt}\Big|_{R_0}$ is expressed using the relationship between the time

rate of a vector in an inertial (R_0) and rotating (R_i) frames, i.e.

$$\frac{\vec{dR}}{dt}\Big|_{R_0} = \frac{\vec{dR}}{dt}\Big|_{R} + \vec{\Omega}_{R/R} \times \vec{R} \qquad \text{(II.5)}$$

The in-plane transverse elastic displacement vector, $\bar{q}$, (assuming a single mode of vibration) (see Appendix A) is found to be:

$$\bar{q} = \cos(\omega t+\phi)\{A\cos\beta z + B\sin\beta z + C\cosh\beta z + D\sinh\beta z\}\,\hat{i}_S \qquad \text{(II.6)}$$

After substitution of Equations (II.5) and (II.6) into Equation (II.4) and integration term by term, one can develop:

$$\vec{dH}_{M/G} = \{(\bar{r}_0+\bar{q})\times[\vec{\Omega}_{S/R} \times \bar{r}_0 + \dot{\bar{q}}_{/RM} + \vec{\Omega}_{S/RO}\times\bar{q}]\}dm$$

$$\simeq \{\bar{r}_0\times(\vec{\Omega}_{S/R}\times\bar{r}_0) + \dot{\bar{q}}_{/RM} + \vec{\Omega}_{S/RO}\times\bar{q}) + \bar{q}\times(\vec{\Omega}_{S/RO}\times\bar{r}_0)\}dm$$

where one assumes $\bar{q}\cdot\bar{q}$ and $\dot{\bar{q}}\cdot\dot{\bar{q}}$ small as compared with the other terms. This can be explicitly rewritten as:

$$\vec{dH}_{M/G} = \{\dot{\theta}+\dot{\theta}_R-\omega_0)z^2 - z\sin(\omega t+\phi)\{A\cos\beta z + B\sin\beta z + C\cosh\beta z + D\sinh\beta z\}\}\hat{j}\,dm$$

with $dm=\delta\,dz$ where δ is the mass per unit length of the mast, $\vec{\Omega}_{S/R_0} = (\dot{\theta}-\omega_0)\hat{j}$, the inertial angular velocity of

the Shuttle, $\dot{\bar{q}}|_{R_M}$ the velocity of the mast element as seen from , R_M, the frame moving with the mast, and

$$\dot{\theta}_R = \frac{d}{dt}\left[\frac{\partial q(z,t)}{\partial z}\right]_{z=-L}$$

$$\vec{H}_{M/G} = \int_M d\,\vec{H}_{M/G}$$

$$\vec{H}_{M/G} = (\dot{\theta} - \omega_0)\,\rho\frac{L^3}{3} + \rho\,\sin(\omega t+\phi)f)\,\hat{j}$$

where $f = A\left(L\frac{\sin\beta L}{\beta} + \frac{\cos\beta L}{\beta^2} - \frac{1}{\beta^2}\right) + B\left(L\frac{\cos\beta L}{\beta} - \frac{\sin\beta L}{\beta^2}\right)$

$$+ C\left(L\frac{\sinh\beta L}{\beta} - \frac{\cosh\beta L}{\beta^2} + \frac{1}{\beta^2}\right) + D\left(\frac{\sinh\beta L}{\beta^2} - L\frac{\cosh\beta L}{\beta}\right)$$

finally

$$\vec{H}_{M/G} = \left\{(\dot{\theta}+\dot{\theta}_R-\omega_0)\frac{ML^2}{3} + M\,\omega\sin(\omega t+\phi)\,(f/L)\right]\hat{j} \qquad \text{(II.7)}$$

II.3. Angular Momentum of the Rigid Reflector About G, the Orbiter Mass Center

The reflector being rigid, its angular momentum can be found at G by a simple application of the transfer theorem (see Appendix B).

$$\vec{H}_{R/G}=\vec{H}_R|_{G_1}+M_R\vec{GG}_1 \times \frac{d}{dt}(\vec{GG}_1)|_{R_0} \qquad \text{(II.8)}$$

$$\vec{H}_{R/G}=(\dot{\theta}+\dot{\theta}_R-\omega_0)I_{R2}\,\hat{j} \quad \text{where } \dot{\theta}_R=\frac{d}{dt}\left[\frac{\partial q}{\partial z}\right]_{z=L}$$

$$\dot{\theta}_R=-\omega\sin(\omega t+\phi)\beta[-A\sin\beta L+B\cos\beta L+C\sinh\beta L+D\cosh\beta L]$$

Because of the assumed magnitude of the transverse elastic displacement, it can be assumed that the length of the mast remains constant. Subsequently,

$$\frac{d\vec{GG}_1}{dt}|_{R_0} = \frac{d\vec{GO}}{dt}|_{R_0} + \frac{d}{dt}(\vec{O_1G_1})|_{R_0}$$

This can be expanded using Equation (II.5) with the result

$$\frac{d}{dt}\vec{OG}_1|_{R_0}=[L(\dot{\theta}-\omega_0+\dot{\theta}_R)]\,\hat{i}_M - X(\dot{\theta}-\omega_0+\dot{\theta}_R)\,\hat{k}_M$$

where X is the distance between O_1 and G_1

$$\vec{GG}_1 = -L\hat{k}_M + X\hat{i}_M$$

$$\vec{GG}_1 \times \frac{d}{dt}(\vec{GG}_1)|_{R_0}=[(\dot{\theta}+\dot{\theta}_R-\omega_0)L^2+X^2(\dot{\theta}+\dot{\theta}_R-\omega_0)\hat{j}]$$

$$\vec{H}_{R/G}=[(\dot{\theta}+\dot{\theta}_R-\omega_0)(I_{R2}+M_R(L^2+X^2))]\hat{j} \qquad \text{(II.9)}$$

II.4. Angular Momentum of the System About G.

$$\vec{H}_{syst/G} = \sum_{i=1} \vec{H}_{i/G} \qquad \text{(II.10)}$$

$$\vec{H}_{syst/G} = \{(\dot{\theta} - \omega_0)\, I_{S2} + (\dot{\theta} - \omega_0 + \dot{\theta}_R) ML^2/3 + M\omega \sin(\omega t + \phi)\, f/L + (\dot{\theta} + \dot{\theta}_R - \omega_0)\, (I_{R2} + M_R[L^2 + X^2])\}\hat{j} \qquad \text{(II.11)}$$

II.5. Rotational Equation of Motion of the Open Loop System

The rotational equation of motion is obtained by equating the rate of change of the angular momentum of the system about G with the external torques acting on the system taken at G. Here it will be assumed that the only external torque is due to the gravity - gradient. (The effect of control torques will be treated later in Chapter Five).

$$\frac{d}{dt}\left(\vec{H}_{syst/G}\right)\Big|_{R_0} \cdot \hat{j} = \vec{N} \cdot \hat{j} \qquad \text{(II.12)}$$

which can be explicitly written as:

$$\ddot{\theta}(I_{S2} + ML^2/3 + I_{R2} + M_R(X^2 + L^2)) + \ddot{\theta}_R(I_{R2} + ML^2/3 + M_R(X^2 + L^2)) - M\omega^2 \cos(\omega t + \phi)\, f/L = -3\omega_0^2[I_1 - I_3]\theta \qquad \text{(II.13)}$$

where $-3\omega_0^2\,\theta\,(I_1-I_3)$ is the y component of the gravity-gradient torque acting on the system at its center of mass, G (see Appendix C).

II.6. Linearization of the Rotational Equations of Motion

Let τ, the dimensionless time, be equal to $\omega_0\,t$.

Then $\frac{d\theta}{dt} = \omega_0 \frac{d\theta}{d\tau} = \omega_0\theta'$, and $\frac{d^2\theta}{dt^2} = \omega_0^2 \frac{d^2\theta}{d\tau^2} = \omega_0^2\,\theta''$

Equation (II.13) can be rewritten as

$$\omega_0^2\theta''(I_{S2}+ML^2/3+I_{R2}+M_R(X^2+L^2))+\theta_R''\,\omega_0^2(I_{R2}+ML^2/3+M_R(X^2+L^2))$$

$$-M\omega^2\cos(\omega t+\phi)f/L + 3\omega_0^2\,(I_1-I_3)=0 \qquad \text{(II.14)}$$

Dividing Equation (II.14) by ML^2 yields

$$\theta''(I_{S2}/ML^2+1/3+I_{R2}/ML^2+\frac{M_R}{M}[(X/L)^2+1])$$

$$+\theta''_R\,(I_{R2}/ML^2+1/3+\frac{M_R}{M}[(X/L)^2+1])$$

$$-(\omega/\omega_0)^2\cos(\omega t+\phi)\,f/L^3+3\theta(I_1-I_3)/ML^2=0 \qquad \text{(II.15)}$$

Equation (II.15) can be recast as

$$C_1\,\theta'' + C_2\theta = f(\tau) \qquad \text{(II.16)}$$

if $\omega/\omega_0 = W$, $M_R/M = \mu$ and $X/L = \lambda$

$$\text{then, } C_1 = I_{S2}/ML^2 + 1/3 + I_{R2}/ML^2 + \mu\ (\lambda^2 + 1)$$

$$C_2 = 3(I_1 - I_3)/ML^2$$

$$f(\tau) = W^2 \cos(W\tau + \phi)\ (f/L^3) - \theta''_R\ (I_{R2}/ML^2 + 1/3 + (1 + \lambda^2))$$

II.7. Stability Analysis of the In-plane Motion

The stability analysis will be conducted in two phases: first in a torque free situation and second in the presence of gravity gradient torques.

II.7.A. Stability Analysis in the Torque-Free Configuration

In this case, Equation (II.16) becomes

$$C_1\theta'' = f(\tau)$$

which is integrated twice to yield

$$\theta(\tau) = \frac{1}{C_1}[-\cos(W\tau+\theta)\ (f/L^3) - \theta_R(I_{R2}/ML^2 + 1/3\ \mu(\lambda^2+1)) + K_0\tau + K_1]$$

The value of the constants K_0 and K_1 are derived from the initial conditions (assuming $\theta = 0$) i.e.

when $\tau = 0$, $\theta(0) = \theta_0$ and $\theta'(0) = \theta_0'$

$$C_1 \theta_0 = (-f / L^3) - \theta_R(0) (I_{R2}/ML^2+1/3+ \mu (\lambda^2+1))+ K_1$$

or $$K_1 = C_1 \theta_0 + \theta_R(0) (I_{R2}/ML^2+1/3+ (\lambda^2+1)) + (f/L^3)$$

and

$$C_1 \theta_0 = - \theta_R'(0)(I_{R2}/ML^2+1/3+ \mu(\lambda^2+1))+K_0$$

or $$K_0 = C_1\theta_0' + \theta_R'(0) (I_{R2}/ML^2+1/3 + (\lambda^2 + 1))$$

finally, $$\theta(\tau)= \frac{1}{C_1} \{((f/ L^3)(1-\cos(W\tau)) + C_1(\theta_0 + \theta_0') + (I_{R2}/ML^2+1/3+ \mu (\lambda^2+1)) (\theta_R'(0)\tau + \theta_R(0)-\theta_R)\}$$

(II.17)

A numerical simulation of Equation (II.17) (Figures II.2 - II.6) for different values of the x offset and frequencies has shown that:

a) the system oscillates about an equilibrium position, in the absence of gravity-gradient torques and disturbances, different from zero due to the forcing effects of the flexibility and the related coupling due to the offset. (Figures II.2 and II.3)

b) the amplitudes of the oscillations increase with the offset (Figure II.4 and II.6), according to

the coefficient of the second group of terms in Equation (II.17).

c) finally, given an offset and an initial disturbance, the amplitude and the frequency of oscillation about the equilibrium position increase with the frequency of the mode of vibration of the system (Figures II.4 and II.6) Note that the coefficients in f (A-D) are related to the modal amplitude functions.

II.7.B. Stability Analysis of the System in the Presence of Gravity Gradient Torque

In the presence of the gravity-gradient torques, the two dimensional motion of the SCOLE system is described by Equation (II.16):

$$C_1 \theta'' + C_2 \theta = f(\tau)$$

In the absence of flexibility, $f(\tau)=0$, this equation reduces to

$$C_1 \theta'' + C_2 \theta = 0$$

Since $C_2 = 3(I_1-I_3)/ML^2$ is negative for the SCOLE configuration, the solution, $\theta(\tau)$, for this case is unstable. The case will be reconsidered in chapter IV where the three dimensional dynamics of the rigidized SCOLE is analyzed.

Here, Equation (II.16) is numerically integrated and the motion simulated for two different values of the offset (X= 18.75 ft and X= 37.5 ft): Figures II.7, II.8, and II.9.

In addition to the tendencies depicted earlier for the case of the torque free configuration, it is now seen that the SCOLE system, with the presence of gravity-gradient torques in its dynamics, is unstable. This is due to the inertia distribution of the system in the configuration considered here.

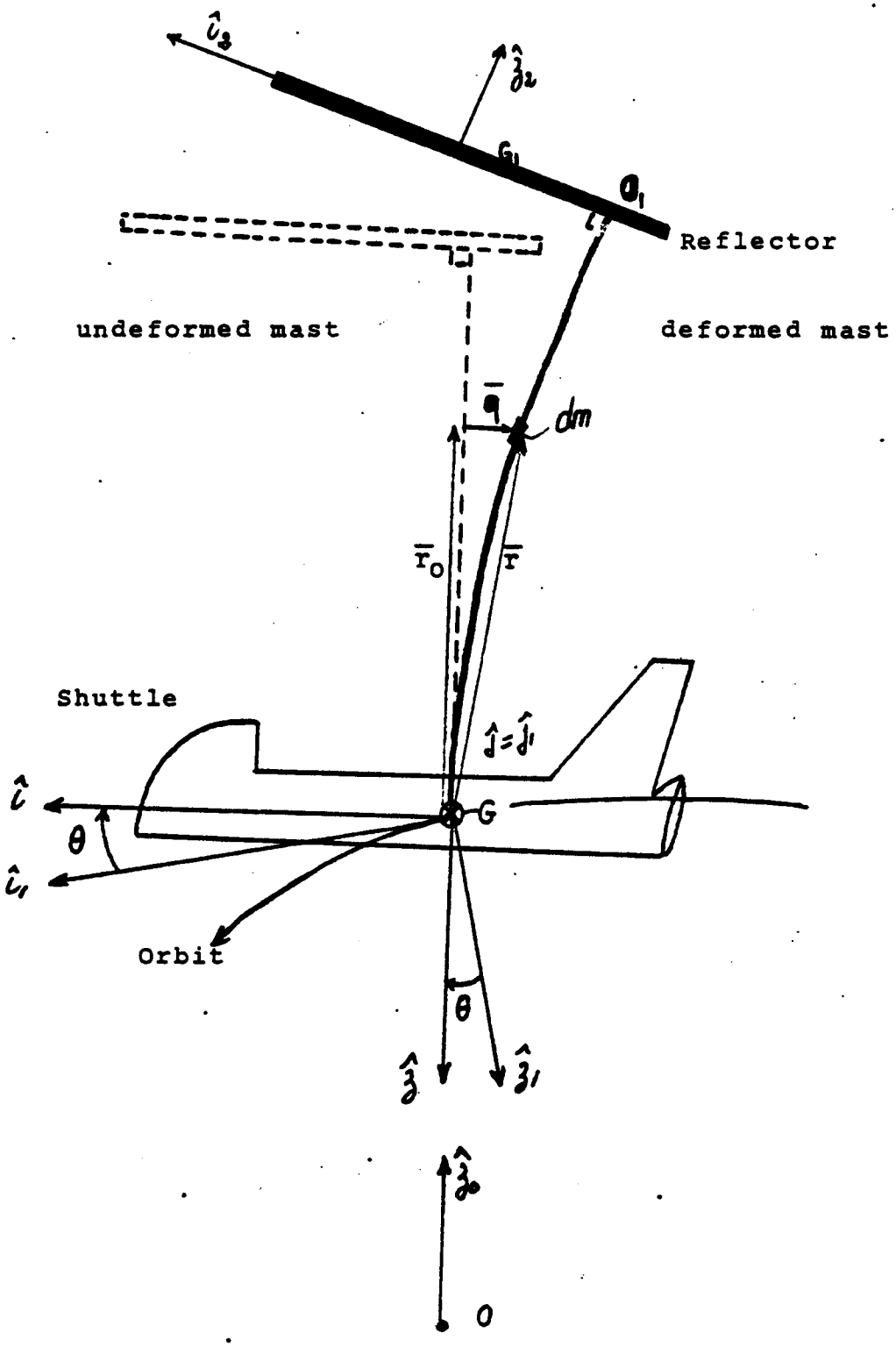

Figure (II.1) System Geometry in 2-D

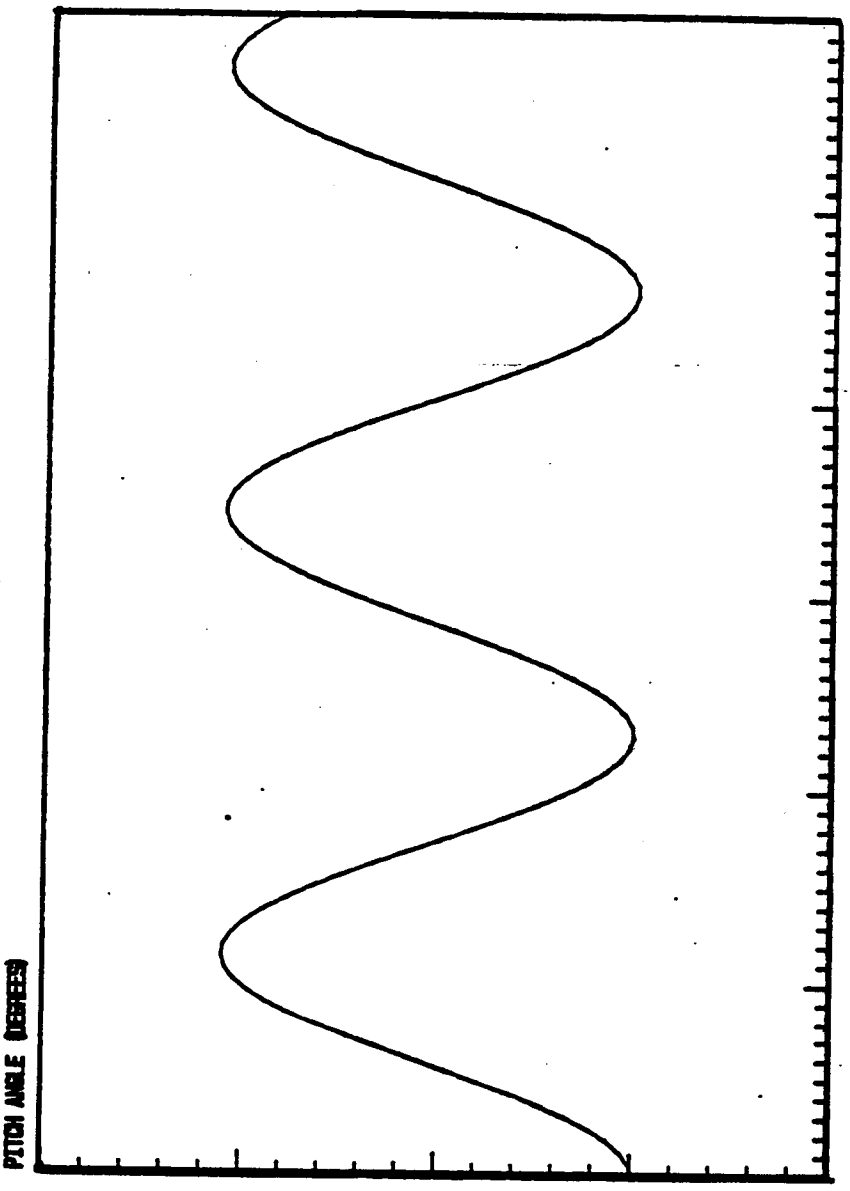
SCOLE 2-D (NO GRAVITY-GRADIENT TORQUE)
FREQUENCY=.274 Hz.; THETA(0)=0.
PITCH ANGLE (DEGREES)
1.5
1.0
0.5
0.0
-0.5
0
10
20
30
40
50
60
TIME (SECONDS)
X=10.76

FIGURE II.2:

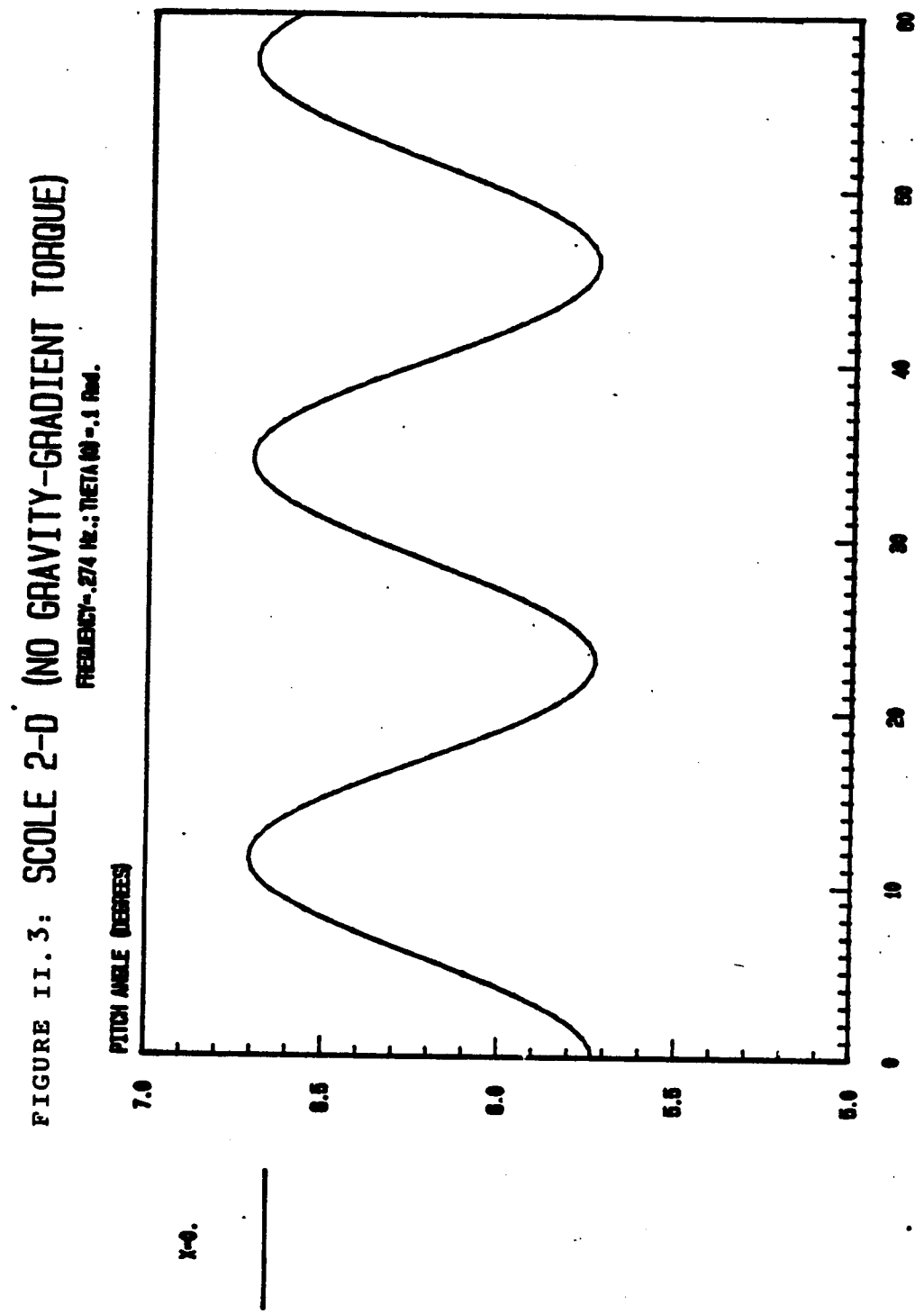
SCOLE 2-D (NO GRAVITY-GRADIENT TORQUE)
FREQUENCY=.274 Hz.; THETA(0)=.1 Rad.
PITCH ANGLE (DEGREES)
7.0
6.5
6.0
5.5
5.0
0
10
20
30
40
50
60
TIME (SECONDS)
X=0.

FIGURE II.3:

FIGURE II.4: SCOLE 2-D (NO GRAVITY-GRADIENT TORQUE)

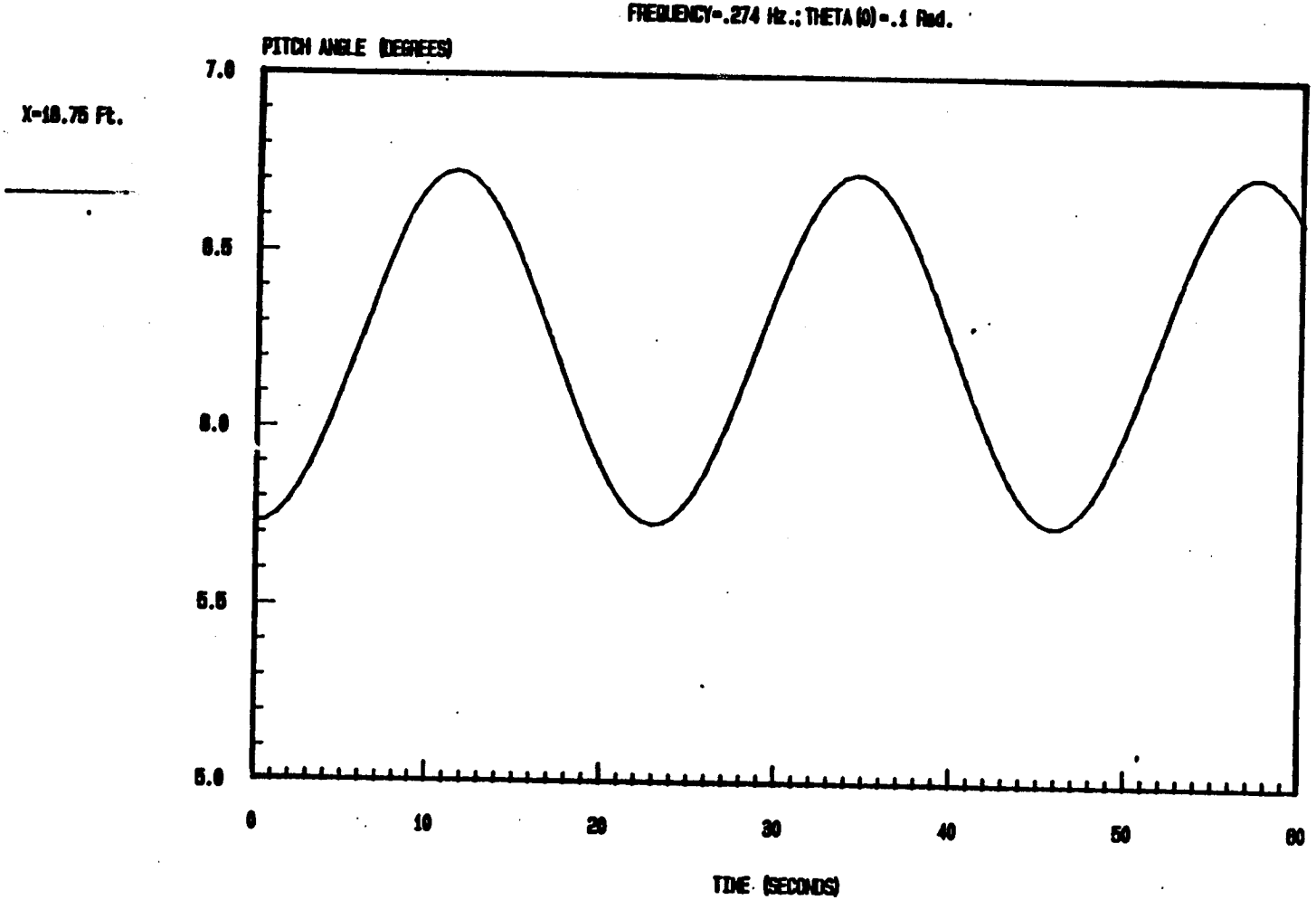

FIGURE II.5: SCOLE 2-D (NO GRAVITY-GRADIENT TORQUE)

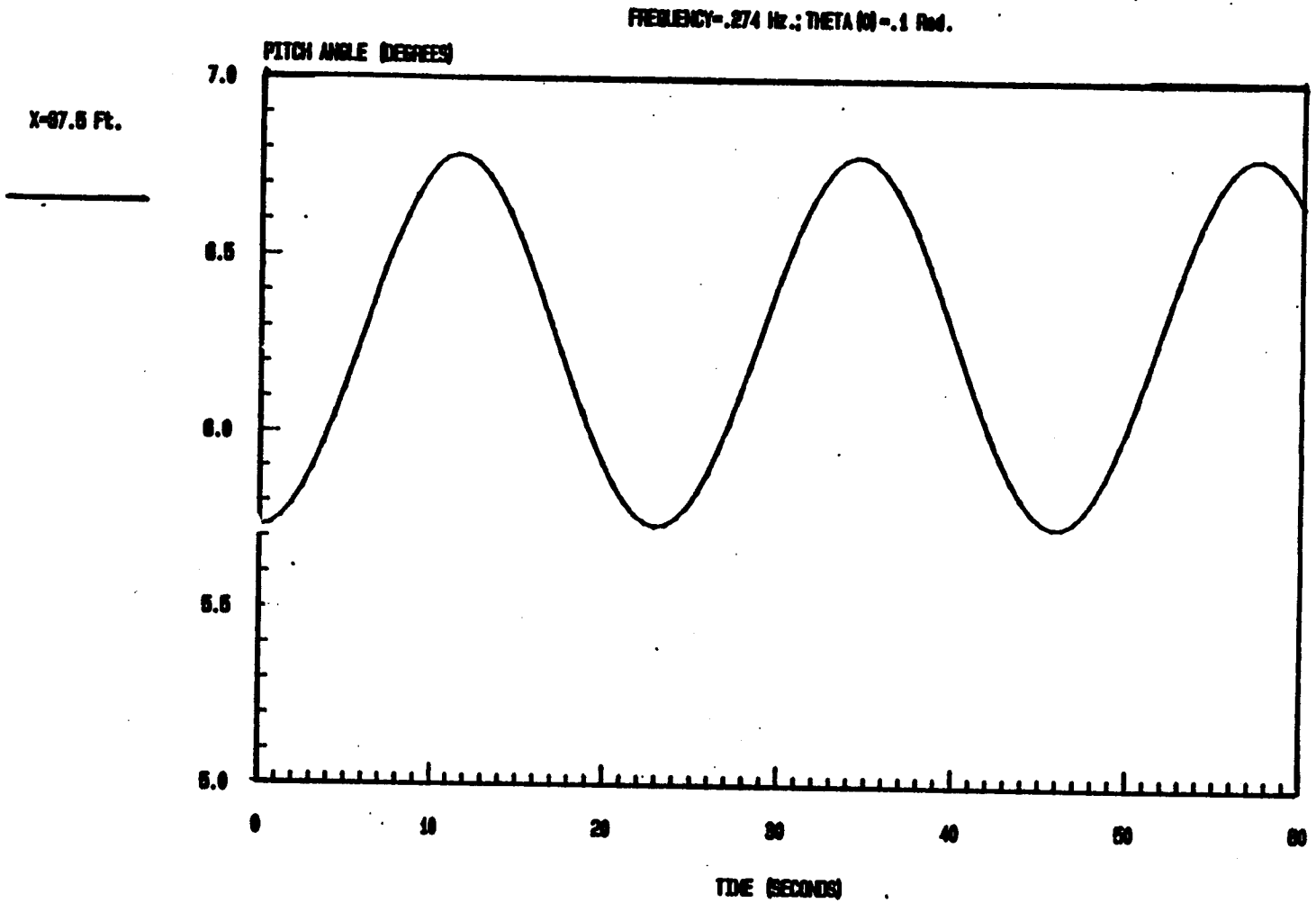

FIGURE II.6; SCOLE 2-D (NO GRAVITY-GRADIENT TORQUE)

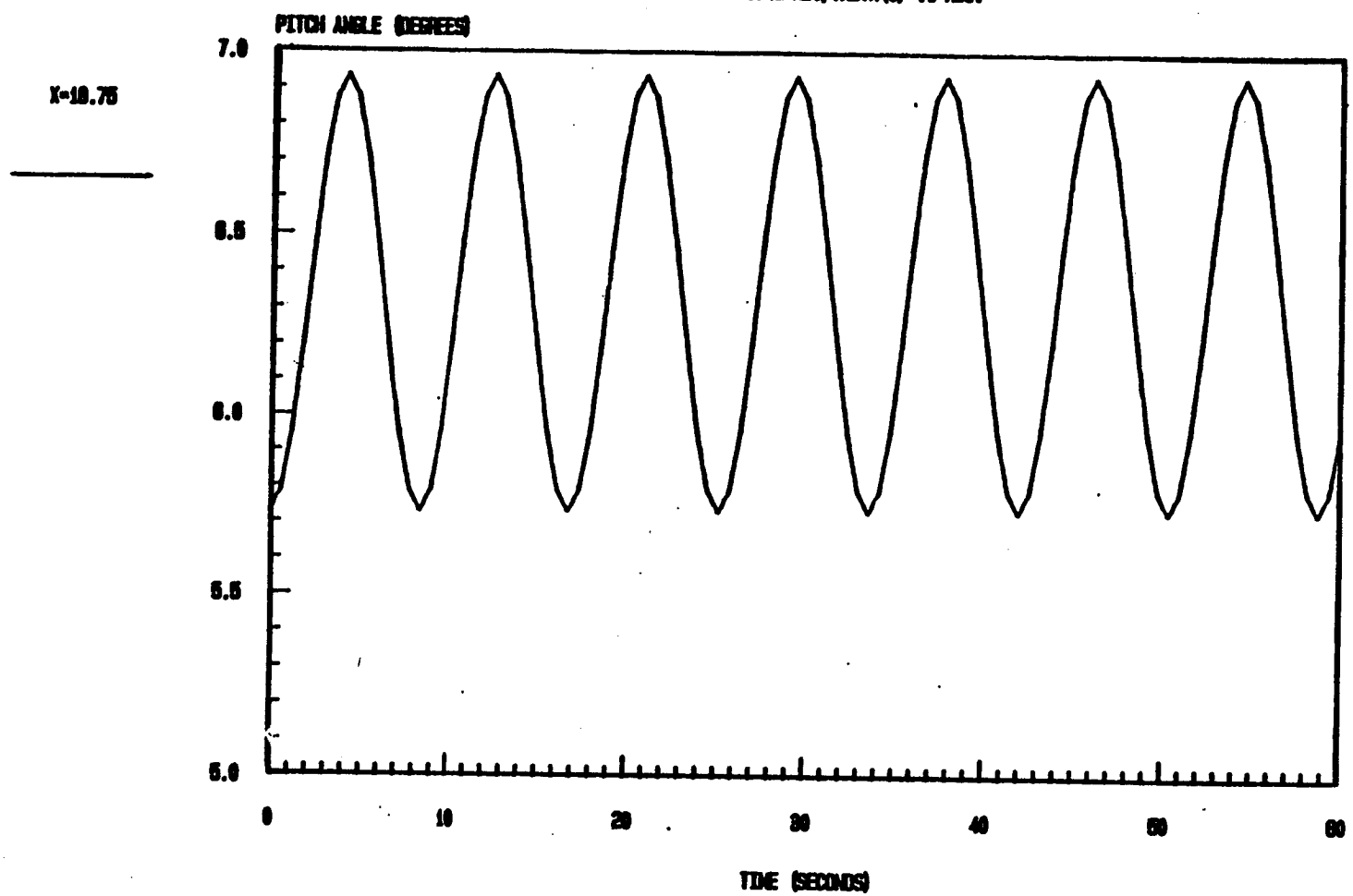

FIGURE II.7: SCOLE 2-D (WITH GRAVITY-GRADIENT TORQUE)

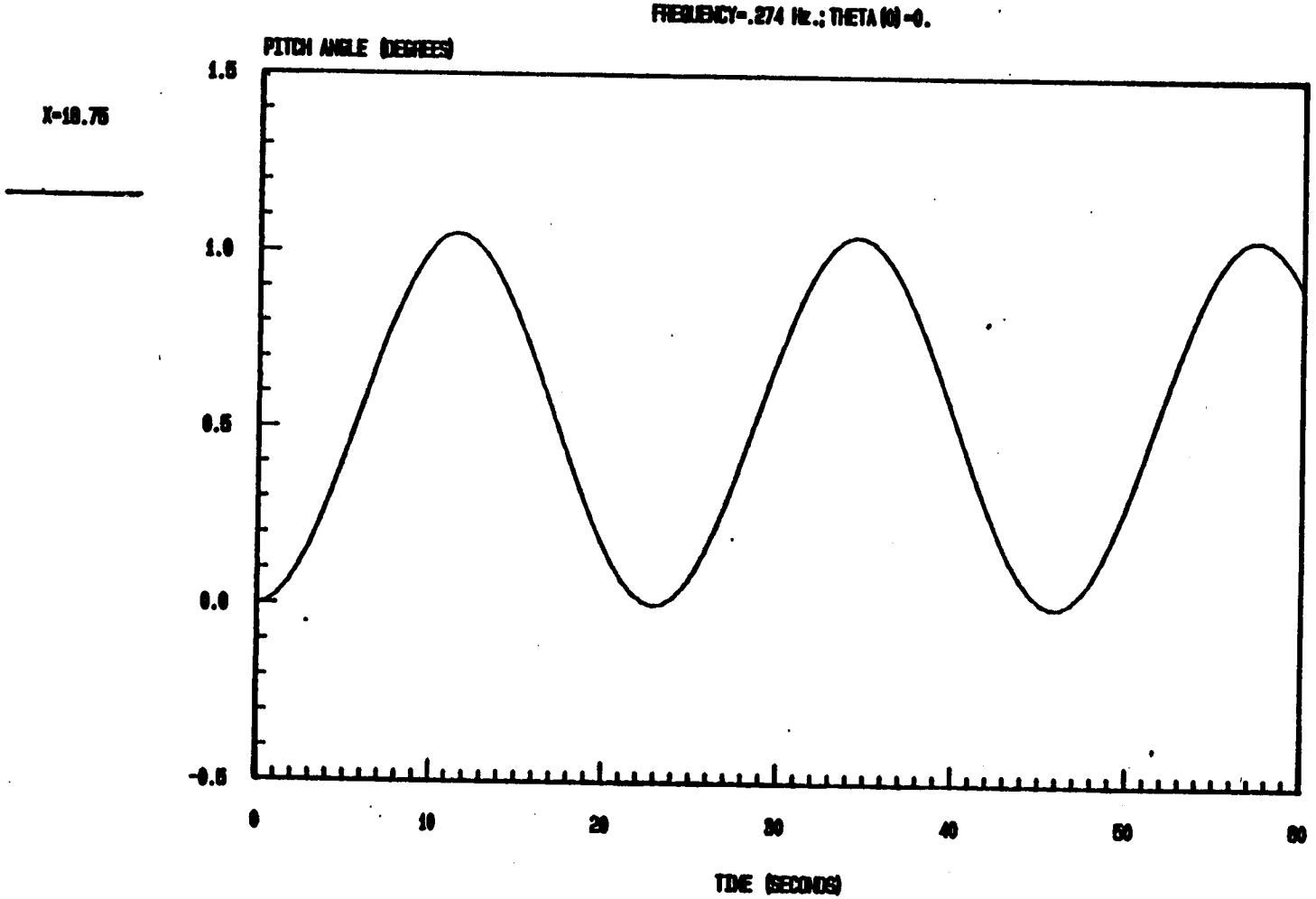

FIGURE II.8 : SCOLE 2-D (WITH GRAVITY-GRADIENT TORQUE)

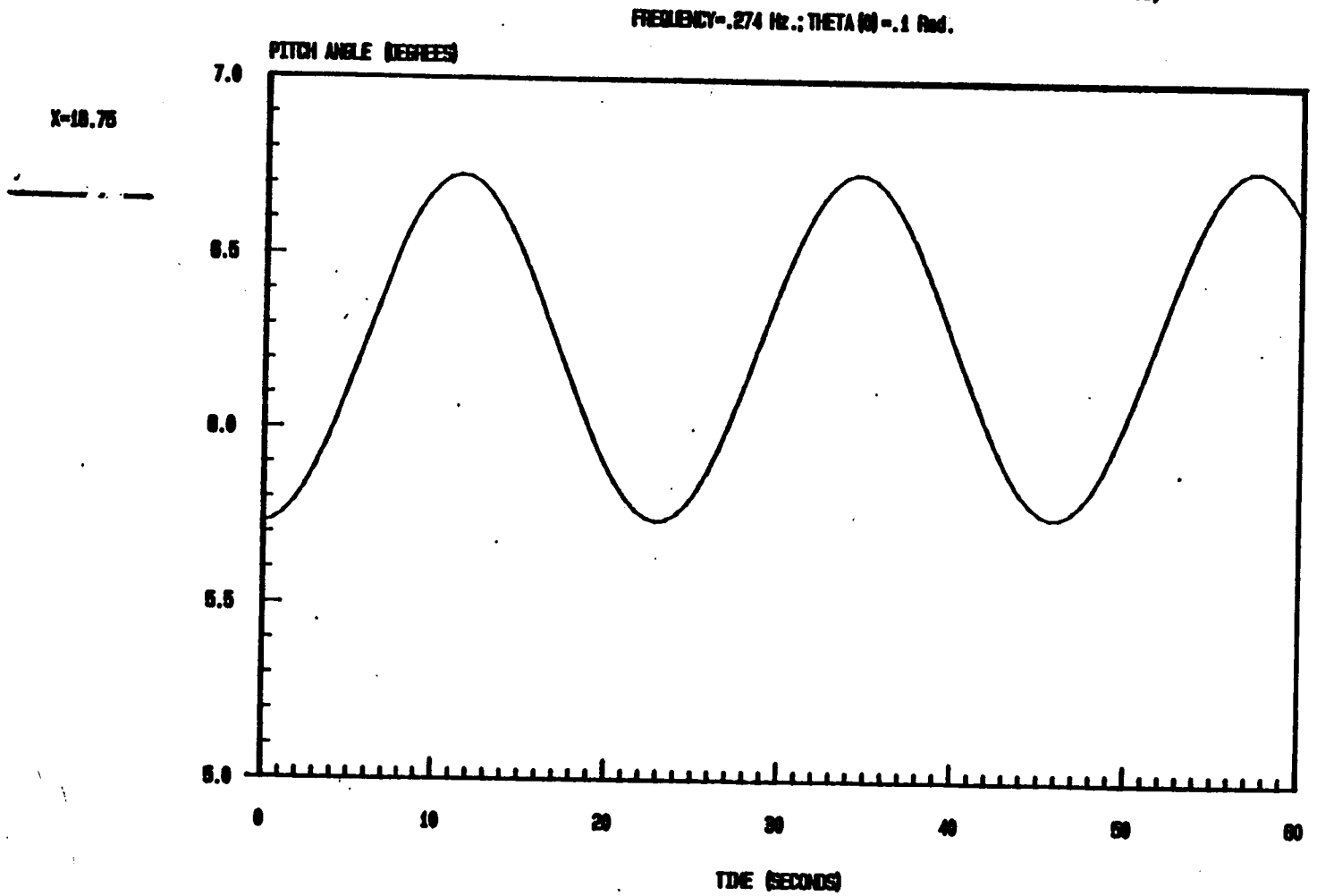

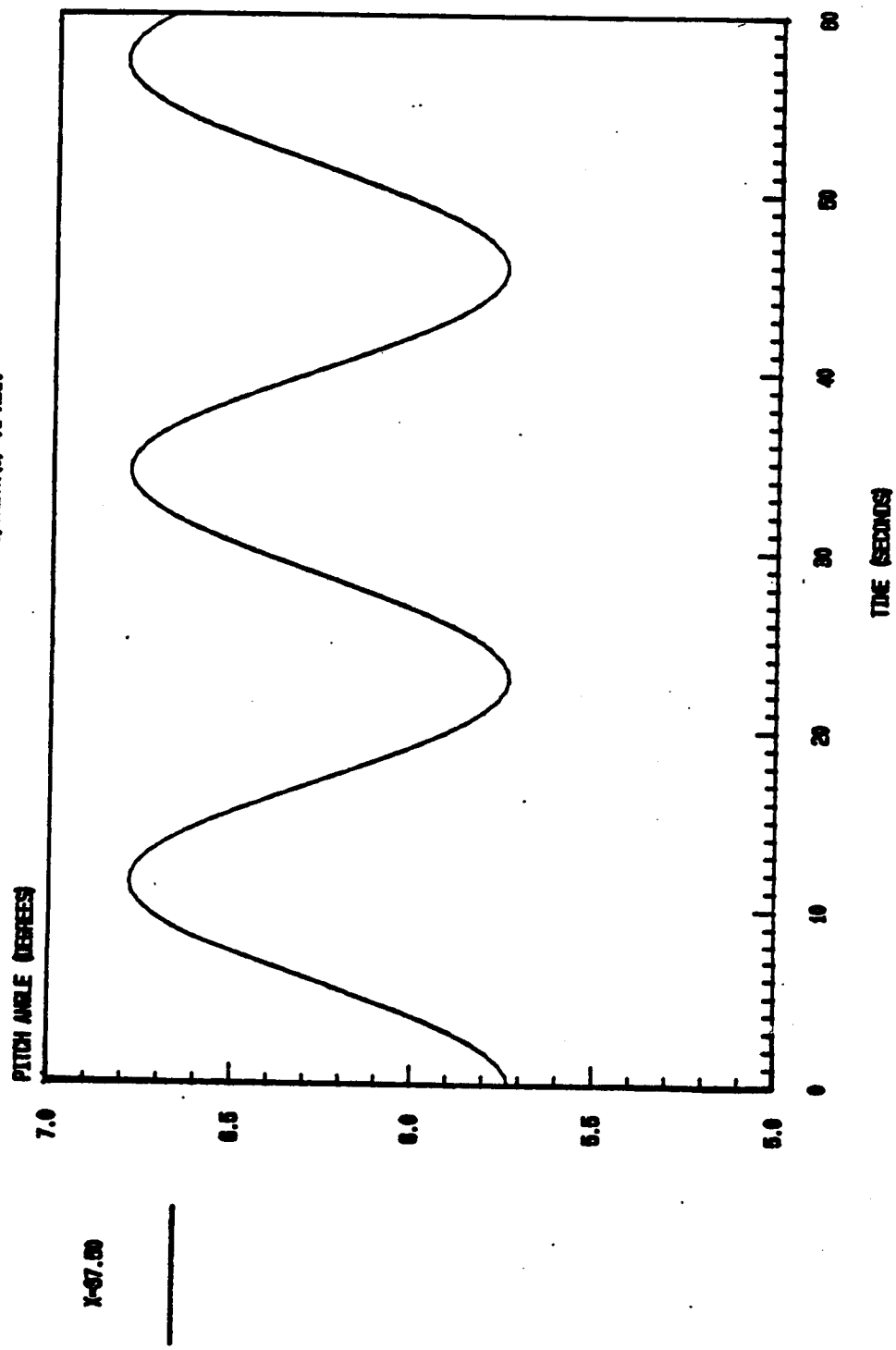
SCOLE 2-D (WITH GRAVITY-GRADIENT TORQUE)
FREQUENCY=.274 Hz.; THETA(0)=.1 Rad.
PITCH ANGLE (DEGREES)
7.0
6.5
6.0
5.5
5.0
0
10
20
30
40
50
60
TIME (SECONDS)
X=57.00

FIGURE II.9:

CHAPTER THREE

THREE DIMENSIONAL EQUATIONS OF MOTION: THE ACTUAL SCOLE CONFIGURATION

In this chapter, the three dimensional formulation of the SCOLE dynamics is developed based on a Newton - Eulerian formulation. The Shuttle and the reflector are assumed to be rigid bodies and the mast is modelled as a connecting flexible beam.

The expressions for the general displacement (See Appendix A) of an elemental mass on the mast are derived from the three dimensional mode shape functions consistent with the boundary conditions on the mass. The three dimensional rotational equations are obtained by taking the moment of all the external forces acting on each elemental mass, at some arbitrary point, and equating it with the moment, about the same point, of the inertial forces acting on the element.

These equations must then be integrated over the entire system and then projected on the three axes of rotation in order to obtain the rotational equations of motion. Similarly, generic modal equations (See Appendix

D) for the flexible mast modes are obtained for the SCOLE system.

III.1. SCOLE System Geometry

Since the SCOLE system has three components with some relative degrees of freedom, it takes at least four coordinate systems to describe its geometry in its deformed state.

Let therefore, R_0 be an inertial frame centered at the geocenter; R_1 ($\hat{i}_1$, $\hat{j}_1$, $\hat{k}_1$), a frame connected and moving with the orbit with $\hat{j}_1$ parallel to the angular momentum vector of the center of mass of the Shuttle and with $\hat{i}_1$ directed along the positive orbit; $R(\hat{i}, \hat{j}, \hat{k})$, a frame centered at G, mass center of the orbiter; $R_2(\hat{i}_2, \hat{j}_2, \hat{k}_2)$ a frame moving with the reflector and centered at G, its center of mass. (See Figure III.1).

If $\bar{\omega}_0$ is the orbital angular velocity of the Shuttle, then

$$\bar{\omega}_0 = -\omega_0 \hat{j}_1 \qquad \text{(III.1)}$$

Let us assume the following Euler angle sequence

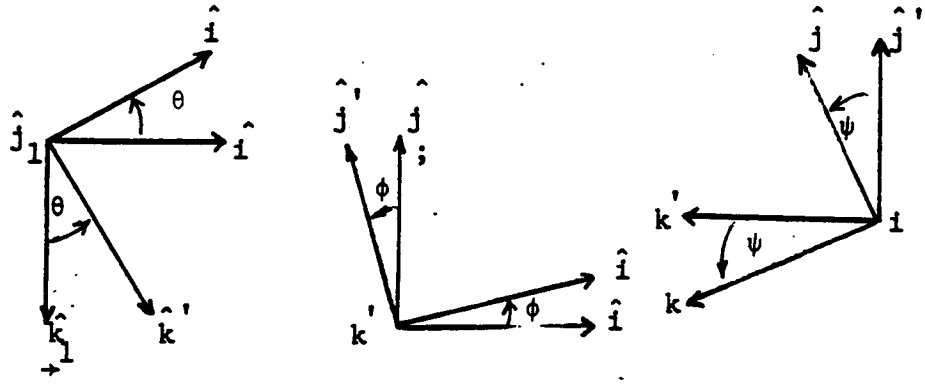

then, $\vec{\Omega}_{S/R}$, the inertial angular velocity of the Orbiter can be expressed as

$$\vec{\Omega}_{S/R_0} = (\dot{\theta}-\omega_0)\,\hat{j}_1 + \dot{\phi}\hat{k}' + \dot{\psi}\,\hat{i} \qquad \text{(III.2)}$$

Since, $\hat{k}' = \cos\psi\ \hat{k} + \sin\psi\ \hat{j}$ and

$$\hat{j}_1 = \sin\phi\,\hat{i} + \cos\phi\ \cos\psi\ \hat{j} - \cos\phi\sin\psi\ \hat{k},$$

$\vec{\Omega}_{S/R}$ can be rewritten in the body frame as:

$$\vec{\Omega}_{S/R_0} = \Omega_x\,\hat{i} + \Omega_y\hat{j} + \Omega_z\hat{k}$$

$$= [(\dot{\theta}-\omega_0)\sin\phi + \dot{\psi}]\hat{i} + [(\dot{\theta}-\omega_0)\cos\phi\cos\psi + \dot{\phi}\sin\psi]\hat{j}$$

$$+ [\dot{\phi}\cos\psi - (\dot{\theta}-\omega_0)\cos\phi\sin\psi]\hat{k} \qquad \text{(III.3)}$$

The reflector is assumed to be rigidly connected to the beam, its angular velocity is that of the end, O_1, of

the beam. The angular velocity, $\vec{\Omega}_{R/S}$, of the reflector with respect to the Shuttle can be expressed as

$$\vec{\Omega}_{R/S} = \dot{\psi}_R \hat{i} + \dot{\theta}_R j_1 + \dot{\Phi}_R \hat{k}_2 \qquad \text{(III.4)}$$

where

$$\dot{\psi}_R = \frac{d}{dt} \left[-\frac{\partial v(z,t)}{\partial z}\right]_{|z=-L}$$

$$\dot{\theta}_R = \frac{d}{dt} \left[\frac{\partial u(z,t)}{\partial z}\right]_{|z=-L} \qquad \text{(III.5)}$$

and $$\dot{\Phi}_R = \frac{d}{dt} \Phi_R(z,t)_{|z=-L}$$

$u(z,t)$, $v(z,t)$, and $\Phi(z,t)$ are the in-plane, the out of plane, and the torsional bending mode shape functions of the beam, respectively.

Assuming the following sequence in the beam motion relative to the orbiter:

i. Out of orbit plane bending;

ii. Bending in a plane parallel to the orbit plane;

iii. Torsion about $\hat{k}_2$,

the unit vectors in the intermediate coordinate systems are expressed as:

$$\hat{i}_2 = \cos\ \Phi_R \cos\ \theta_R\, \hat{i} + \sin\ \Phi_R \cos\ \psi_R \hat{j} + \sin\ \Phi_R \sin\ \psi_R \hat{k}$$

$$\hat{j}_2 = -\sin \Phi_R \cos\ \theta_R\, \hat{i} + (\cos\ \Phi_R \cos \psi_R - \sin\ \Phi_R \sin\theta_R \sin\psi_R)\hat{j}$$

$$+\ (\cos \Phi_R \sin\ \psi_R + \sin \Phi_R \sin\ \theta_R \cos\ \psi_R)\hat{k}$$

$$\hat{k}_2 = \sin\ \theta_R \hat{i} - \cos\ \theta_R \sin\ \psi_R\, \hat{j} + \cos\ \theta_R \cos\ \psi_R\, \hat{k}$$

These relations can be recast in the following matrix format:

$$\begin{bmatrix} \hat{i}_2 \\ \hat{j}_2 \\ \hat{k}_2 \end{bmatrix} = [T_{R\to R2}] \begin{bmatrix} \hat{i} \\ \hat{j} \\ \hat{k} \end{bmatrix} \qquad \text{(III.6)}$$

in which the transformation matrix from the body frame, R, to the frame connected to the reflector, R_2, has the following form:

$$T_{R\to R2} = \begin{bmatrix} \cos\Phi_R \cos\theta_R & \sin\Phi_R \cos\psi_R & \sin\Phi_R \sin\psi_R \\ -\sin\Phi_R \cos\theta_R & \cos\Phi_R \cos\psi_R - \sin\Phi_R \sin\theta_R \sin\psi_R & C\Phi_R S\psi_R + \sin\Phi_R \sin\theta_R \cos\psi_R \\ \sin\theta_R & -\cos\theta_R \sin\psi_R & \cos\theta_R \cos\psi_R \end{bmatrix}$$

Next, the rotational equations of motion for the system will be derived by taking the time derivative of the angular momentum of the system at G, the center of mass of the Shuttle, and by equating it to the external torques applied to the system.

III.2. Angular Momentum of the SCOLE System

III.A. Angular Momentum of the Shuttle About its Mass Center, G.

The angular momentum of the Shuttle, taken as a rigid body, about its center of mass, G is

$$\vec{H}_{S/G} = \bar{\bar{I}}_{S/G}\ \vec{\Omega}_{S/RO} \qquad \text{(III.7)}$$

(See Appendix C for the inertia tensors of the different components of the SCOLE system).

III.2.B. Angular Momentum of the Beam About G

Consider an element of mass, dm, of the beam located at some point, P, such that (Figure III. 1)

$$\vec{GP} = \bar{r} = \bar{r}_0 + \bar{q} \qquad \text{(III.8)}$$

where $\bar{r}_0 = -z\hat{k}$ is the position vector of P in the undeformed state; $\bar{q}\ (z,t) = u(z,t)\ \hat{i} + v(z,t)\hat{j}$ in which, u

and v are the x and y components of the mode shape vector (Appendix A).

The angular momentum of dm about G, $d\vec{H}_{M/G}$ is given by:

$$d\vec{H}_{M/G} = \bar{r} \times \frac{d}{dt}(\bar{r})\Big|_{R_0} dm \qquad \text{(III.9)}$$

where

$$\bar{r} = -z\hat{k} + u\hat{i} + v\hat{j} \qquad \text{(III.10)}$$

Equation (III.9) is expressed explicitly as:

$$d\vec{H}_{M/G} = \{ (-z\hat{k}+u\hat{i}+v\hat{j}) \times \frac{d}{dt} (-z\hat{k}+u\hat{i}+v\hat{j})\Big|_{R_0} \} dm$$

$$\frac{d\bar{r}}{dt}\Big|_{R_0} = \frac{d\bar{r}}{dt}\Big|_{R} + \Omega_{S/R_0} \times \bar{r} = (\dot{u}-\Omega_z v - z\Omega_y)\hat{i} + (\dot{v}+\Omega_z u + z\Omega_x)\hat{j} + (\Omega_x v - u\Omega_y)\hat{k}$$

After substituting the different terms into Equation (III.10) the following expression results:

$$d\vec{H}_{M/G} = \{[z(\dot{v}+\Omega_z u) + v(\Omega_x v - \Omega_y u) - z^2 \Omega_x]\hat{i}$$

$$+[- z(\dot{u}-\Omega_z v) + u(\Omega_y u - \Omega_x v) + z^2\Omega_y]\hat{j}$$

$$+[\dot{u}(v+ \Omega_z u) - v(\dot{u}-\Omega_z v) + z(u\Omega_x + v\Omega_y)]\hat{k}\}dm \qquad \text{(III.11)}$$

where

$$u(z,t) = \sum_n p^n(t)\, S_x^n(z) \text{ and } v(z,t) = \sum_n p^n(t)\, S_y^n(z)$$

Considering only a single mode in the open loop situation, to show the form of various volume integrations,

$\dot{u} = -\omega \sin(\omega t+\alpha)\, S_x(z)$ and $\dot{v} = -\omega \sin(\omega t+\gamma)\, S_y(z)$.

Assuming small elastic displacements such that $S_i\, S_j/L^2 << 1$ and dividing $\vec{dH}_{M/G}$ by $\omega_0 L^2$, where ω_0 is the Shuttle orbital angular velocity and L a reference length, then,

$$\vec{dH}_{M/G}/\omega_0 L^2 \simeq \frac{1}{\omega_0 L^2}\{(z\dot{v}+z\Omega_z u+ \Omega_x z^2)\hat{i} + (-z\dot{u}$$

$$+\Omega_z zv+z^2\ \Omega_y)\hat{j} + (\Omega_x\ uz +\ \Omega_y zv)\hat{k}\}\rho\ dz$$

where ρ is the mass per unit length of the beam. After multiplying both sides of this equation by $\omega_0\ L^2$, there results:

$$\vec{dH}_{M/G} \simeq \{(z\dot{v}+zu\ \Omega_z+z^2\Omega_x)\hat{i} + (z\dot{u}+zv\Omega_z+z^2\Omega_y)\hat{j}$$

$$+(zu\Omega_x+zv\Omega_y)\hat{k}\}\ \rho\ dz \qquad \text{(III.12)}$$

The total angular momentum of the mast about G is obtained by integrating Equation (III.12) over the total length of the mast.

$$\vec{H}_{M/G} = \int_0^{-L} \vec{dH}_{m/G} \qquad \text{(III.13)}$$

The eight terms appearing in $\vec{dH}_{M/G}$ are integrated using integral tables - e.g.

$$\int_0^{-L} \rho z\dot{v}\, dz = -\rho\omega \sin(\omega t+\gamma) \int_0^{-L} z(A_2 \sin\beta z + B_2 \cos\beta z + C_2 \sinh\beta z + D_2 \cosh\beta z)\, dz$$

$$= \rho\omega \sin(\omega t+\gamma)\left[A_2\left(\frac{-\sin\beta L}{\beta^2} + L\,\frac{\cos\beta L}{\beta}\right) + B_2\left(L\,\frac{\sin\beta L}{\beta} + \frac{\cos\beta L}{\beta^2} - \frac{1}{\beta^2}\right)\right.$$

$$+ C_2\left(-L\,\frac{\cosh\beta L}{\beta} + \frac{\sinh\beta L}{\beta^2}\right) + D_2\left(L\,\frac{\sinh\beta L}{\beta} - \frac{\cosh\beta L}{\beta^2} - \frac{1}{\beta^2}\right)$$

To simplify the notations, let

$$f_i(\beta) = \left\{A_i\left(L\,\frac{\cos\beta L}{\beta} - \frac{\sin\beta L}{\beta^2}\right) + B_i\left(L\,\frac{\sin\beta L}{\beta} + \frac{\cos\beta L}{\beta^2} - \frac{1}{\beta^2}\right)\right.$$

$$\left. + C_i\left(\frac{\sinh\beta L}{\beta^2} - L\,\frac{\cosh\beta L}{\beta}\right) + D_i\left(L\,\frac{\sinh\beta L}{\beta} - \frac{\cosh\beta L}{\beta^2} + \frac{1}{\beta^2}\right)\right\}$$

After substitution of f_i and $\frac{M}{L}$ for ρ, where M = mass of the mast, in the expression of $\vec{H}_{M/G}$, one arrives at:

$$\vec{H}_{M/G} = \frac{M}{L} \{[\Omega_z \cos(\omega t+\alpha) f_1 - \omega \sin(\omega t+\gamma) f_2 - \Omega_x L^3/3]\hat{i}$$

$$+[\omega \sin(\omega t+\alpha) f_1 + \Omega_z \cos(\omega t+\gamma) f_2 - \Omega_y L^3]\hat{j}$$

$$+[\Omega_x \cos(\omega t+\alpha) f_1 + \Omega_y \cos(\omega t+\gamma) f_2]\hat{k}\} \quad \text{(III.14)}$$

III.2.C. Angular Momentum of the Reflector About, G

Since small deflections are assumed for the beam, the reflector can be assumed to be located at a constant distance from G, the Shuttle mass center.

Using the transfer theorem for the angular momentum (See Appendix B), the angular momentum, $\vec{H}_{R/G}$, of the reflector, assumed rigid, about G can be expressed as:

$$\vec{H}_{R/G} = \bar{\bar{I}}_{R/G_1} \vec{\Omega}_{R/R_0} + M_R \vec{GG_1} \times \frac{d}{dt}(\vec{GG_1})\Big|_{R_0} \quad \text{(III.15)}$$

where $\bar{\bar{I}}_{R/G1}$, the inertia tensor of the reflector expressed at G_1, its center of mass, and $\vec{\Omega}_{R/R_0} = \vec{\Omega}_{R/S} + \vec{\Omega}_{S/R_0}$ (respectively, the inertial angular velocity of the reflector, its relative angular velocity with respect to the Shuttle and the inertial angular velocity of the

Orbiter) are both expressed in the same coordinate system, R_2, moving with the reflector.

The inertial angular velocity of the reflector is expressed in R_2 using the transformation matrix $[Tij]_{R \to R_2}$ as:

$$\vec{\Omega}_{R/R_0} = \{\Omega_x + \dot{\psi}_R) T_{11} + \Omega_y T_{12} + \Omega_z T_{13} + \dot{\theta}_R \sin \Phi_R\}\hat{i}_2$$

$$+ \{(\Omega_x + \psi_R) T_{21} + \Omega_y T_{22} + \Omega_z T_{23} + \dot{\theta}_R \cos \Phi_R\}\hat{j}_2$$

$$+ \{(\Omega_x + \psi_R) T_{31} + \Omega_y T_{32} + \Omega_z T_{33} + \Phi_R\}\hat{k}_2$$

$$= \Omega_1 \hat{i}_2 + \Omega_2 \hat{j}_2 + \Omega_3 \hat{k}_2 \qquad \text{(III.16)}$$

Now, after rewriting the second term in Equation (III.15),

$$M_R \vec{GG}_1 \times \frac{d}{dt}(\vec{GO}_1 + \vec{O_1G_1})\Big|_{R_0} = M_R(\vec{GO}_1 + \vec{O_1G_1}) \times \frac{d}{dt}(\vec{GO}_1 + \vec{O_1G_1})\Big|_R$$

where O_1 is the reflector attachment point to the mast,

$$\frac{d}{dt}\vec{GO}_1\Big|_{R_0} = \frac{d}{dt}(-L\hat{k} + u(-L,t)\hat{i} + v(-L,t)\hat{j}) + \vec{\Omega}_{S/R} \times (-L\hat{k} + u\hat{i} + v\hat{j})\Big|_{z=-L}$$

$$= (\dot{u} - \Omega_y L - \Omega_z v)\hat{i}\Big|_{z=-L} + (\dot{v} + \Omega_x L + \Omega_z u)\hat{j}\Big|_{z=-L} + (\Omega_x v - \Omega_y u)\hat{k}\Big|_{z=-L}$$

$$\frac{d}{dt}\vec{O_1G_1}|_{R_0} = \vec{\Omega}_{R|R} \times \vec{O_1G_1} = (\Omega_1 \hat{i}_2+\Omega_2\hat{j}_2+\Omega_3\hat{k}_2) \times (X \hat{i}_2 + Y \hat{j}_2)$$

$$= (\Omega_1 Y-\Omega_2 X)\hat{i}_2 - \Omega_3 X \hat{j}_2 - \Omega_3 Y \hat{i}_2$$

X, and Y are the "x" and "y" offset coordinates, respectively.

After subsitution of the terms into Equation (III.15), one arrives at:

$$\vec{H}_{R/G} = \Omega_1 I_{R1} \hat{i}_2 + \Omega_2 I_{R2} \hat{j}_2 + \Omega_3 I_{R3} \hat{k}_2$$

$$+ M_R \{ (bL + c(v+Y))\hat{i}-(aL+c(u+X))\hat{j} + (b(u+X)-a(v+Y))\hat{k}\} \quad \text{(III.17)}$$

I_{R1}, I_{R2}, and I_{R3} are the principal moments of inertia of the reflector.

$$a = \{\dot{u} - \Omega_y L - \Omega_z v - \Omega_3 Y T_{11} + X\Omega_3 T_{21} + (\Omega_1 Y-\Omega_2 X)T_{31}\}$$

$$b = \{\dot{v}+\Omega_x L + \Omega_z u - \Omega_3 Y T_{12} + \Omega_3 X T_{22} + (\Omega_1 Y-\Omega_2 X)T_{32}\}$$

and

$$c = \{\Omega_x v - \Omega_y u - \Omega_3 Y T_{13} + \Omega_3 X T_{23} + (\Omega_1 Y - \Omega_2 X)T_{33}\}$$

III.2.D. Angular Momentum of the System About G

The angular momentum of the system about G, $\vec{H}_{syst/G}$, is given by the sum of the angular momentum of each of the three components evaluated about the same point, G.

$$\vec{H}_{syst/G} = \vec{H}_{S/G} + \vec{H}_{M/G} + \vec{H}_{R/G}$$

The unit vectors $\hat{i}_2$, $\hat{j}_2$, and $\hat{k}_2$ are transformed into unit vectors along the Shuttle axes as follows:

$$\hat{i}_2 = \cos\phi_R \cos\theta_R \hat{i} + \sin\phi_R \cos\psi_R \hat{j} + \sin\phi_R \sin\psi_R \hat{k}$$

$$\hat{j}_2 = -\sin\phi_R \cos\theta_R \hat{i} + (\cos\phi_R \cos\psi_R - \sin\phi_R \sin\theta_R \sin\psi_R)\hat{j} + (\sin\phi_R \sin\theta_R \cos\psi_R + \cos\phi_R \sin\psi_R)\hat{k}$$

$$\hat{k}_2 = \sin\theta_R \hat{i} - \cos\theta_R \sin\psi_R \hat{j} + \cos\theta_R \cos\psi_R \hat{k}$$

After this substitution into Equation (III.17), the angular momentum of the system is expressed as:

$$\vec{H}_{syst/G} = \{\Omega_x I_{S1} - \dot{\Omega}_z I_{S4} + \frac{M}{L}[\Omega_z \cos(\omega t+\alpha) f_1 - \sin(\omega t+\gamma) f_2 + \Omega_x L^3/3\ ] + M_R(bL + c(v+y)) + \Omega_1 I_{R1} \cos\phi_R \cos\theta_R - \Omega_2 I_{R2} \sin\phi_R \cos\theta_R + \Omega_3 I_{R3} \sin\theta_R\}\hat{i} + \{\Omega_y I_{S2} + \frac{M}{L}[\omega \sin(\omega t+\alpha) f_1$$

$$+ \Omega_z \cos(\omega t+\gamma) f_2 - \Omega_y L^3/3 \,] - M_R\,(aL + c(u+X)) + \Omega_1 I_{R1} \sin\Phi_R \cos\psi_R$$

$$+ \Omega_2 I_{R2} (\cos\Phi_R \cos\psi_R - \sin\Phi_R \sin\theta_R \sin\psi_R) - \Omega_3 I_{R3} \cos\theta_R \sin\psi_R \}\hat{j}$$

$$+ \{-\Omega_x I_{S4} + \Omega_z I_{S3} + \frac{M}{L}[\Omega_x \cos(\omega t+\alpha) f_1 + \Omega_y \cos(\omega t+\gamma) f_2]$$

$$+ M_R\,(b(u+X) - a(v+Y)) + \Omega_1 I_{R1} \sin\Phi_R \sin\psi_R$$

$$+ \Omega_2 I_{R2} (\sin\Phi_R \sin\theta_R \cos\psi_R + \cos\Phi_R \sin\psi_R) + \Omega_3 I_{R3} \cos\theta_R \cos\psi_R \}\hat{k} \quad \text{(III.18)}$$

or

$$\vec{H}_{syst/G} = H_x\hat{i} + H_y\hat{j} + H_z\hat{k} \qquad \text{(III.19)}$$

III.3. Rotational Equations of Motion (Torque free).

The rotational equations of motion for the system, when free of all external torques, are obtained as:

$$(\dot{\vec{H}}_{syst/G})|_{R_0} = \dot{\vec{H}}_{syst/G/S} + \vec{\Omega}_{S/R_0} \times \vec{H}_{syst/G} = \vec{0} \quad \text{(III.20)}$$

The vector equation (III.20) itself is equivalent to

$$\begin{aligned} \dot{H}_x + \Omega_y H_z - \Omega_z H_y &= 0 \\ \dot{H}_y + \Omega_z H_x - \Omega_x H_z &= 0 \\ \dot{H}_z + \Omega_x H_y - \Omega_y H_x &= 0 \end{aligned} \qquad \text{(III.21)}$$

Under the small angle approximation assumption, on

ψ, θ, and ϕ ($\sin\sigma \sim \sigma$; $\cos\sigma \sim 1$) the torque free rotational equations of motion (III.21) for the SCOLE system, after linearization are rewritten as:

i) **The Roll Equation**: $\dot{H}_x + \Omega_y H_z - \Omega_z H_y = 0$

$$(\ddot{\psi}-\omega_0\dot{\phi})I_{S1} - (\ddot{\phi}+\omega_0\dot{\psi})I_{S4} + \frac{M}{L}[(\ddot{\phi}+\omega_0\dot{\psi})\cos(\omega t+\alpha)f_1$$

$$-\omega(\dot{\phi}+\omega_0\psi)\sin(\omega t+\alpha)\,f_1 - \omega^2\cos(\omega t+\gamma)f_2 + (\ddot{\psi}-\omega_0\dot{\phi})L^3/3]$$

$$+ (\ddot{\psi}-\omega_0\dot{\phi}+\ddot{\psi}_R-\omega_0\dot{\phi}_R)I_{R1} + \omega_0\dot{\phi}_R I_{R2} - (\omega_0^2\phi-\omega_0\dot{\psi})I_{S4}$$

$$+(\omega_0\dot{\phi}+\omega_0^2\psi)(I_{S2}-I_{S3}+I_{R2}-I_{R3}I_{R1}) + \frac{M}{L}[(\omega_0^2\phi-\omega_0\dot{\psi})\cos(\omega t+\alpha)f_1$$

$$+(\omega_0\dot{\phi}+\omega_0^2\psi)\frac{L^3}{3}+(\omega_0^2-2\omega_0\dot{\theta})\cos(\omega t+\gamma)\,f_2]+\omega_0^2\psi_R I_{R2}$$

$$-(\psi_R\omega_0^2+\omega_0\dot{\phi}_R)I_{R3} + \omega_0^2\psi(M_R L^2-I_{R1}) + M_R(u+X)[(\dot{\theta}-\omega_0)\dot{v}$$

$$+L(\omega_0^2\phi-\omega_0\dot{\psi}) - (\omega_0\dot{\phi}+\omega_0^2\psi)u - X(\omega_0^2\psi_R+\omega_0\dot{\phi}_R)$$

$$+\omega_0^2\psi_R X] - M_R(v+Y)[(\dot{\theta}-\omega_0)\dot{u} + (\omega_0\dot{\theta}-\omega_0^2)L$$

$$+(\omega_0\dot{\phi}+\omega_0^2\psi)v + Y(\omega_0^2\psi_R+\omega_0\dot{\phi}_R-\omega_0\dot{\phi}+\omega_0^2\psi) - \omega_0^2\theta_R X]$$

$$+M_R L[\ddot{v} + (\ddot{\psi}-\omega_0\dot{\phi})L + X(-\ddot{\phi}+\omega_0\ddot{\psi} + \ddot{\phi}_R + \omega_0\dot{\phi}_R)] + M_R\, vX\,\omega_0^2$$

$$+M_R\, Y\{Y(\ddot{\psi}+\ddot{\psi}_R - \omega_0\dot{\phi} - \omega_0\dot{\phi}_R) - X(\ddot{\theta}+\ddot{\theta}_R)\} = 0 \qquad \text{(III.22)}$$

ii) The Pitch Equation: $\dot{H}_y + \Omega_z H_x - \Omega_x H_z = 0$

$$\ddot{\theta}I_{S2} + \frac{M}{L}[-\omega^2 \cos(\omega t+\alpha)f_1 + (\ddot{\phi}+\omega_0\dot{\psi})\cos(\omega t+\gamma)f_2$$

$$-2\omega(\dot{\phi}+\omega_0\psi)\sin(\omega t+\gamma)\, f_2 + \ddot{\theta}L^3/3 + \omega_0(\dot{\psi}-\omega_0\phi)\cos(\omega t+\gamma)(f_2)]$$

$$+ (\ddot{\theta}-\ddot{\theta}_R)\, I_{R2} - M_R L[\ddot{u} - (\ddot{\theta}+\ddot{\theta}_R)L - Y(\ddot{\phi}+\ddot{\phi}_R + \omega_0\dot{\psi} + \omega_0\dot{\psi}_R) +$$

$$\omega_0\dot{\theta}_R X] - 2M_R X\omega_0\dot{u} - M_R XY(\ddot{\psi} - \omega_0\dot{\phi} + \ddot{\psi}_R - \omega_0\dot{\phi}_R)$$

$$+ M_R X^2(\ddot{\theta}+\ddot{\theta}_R) - M_R Y(\dot{\psi}-\omega_0\phi)\,\omega_0 L = 0 \qquad \text{(III.23)}$$

iii) The Yaw Equation: $\dot{H}_z\ \Omega_x H_y - \Omega_y H_x = 0$

$$-(\ddot{\psi}+\omega_0\dot{\phi})\, I_{S4} + (\ddot{\phi}+\omega_0\dot{\psi})(I_{S3} + I_{R3}) + \frac{M}{L}[(\ddot{\psi}-\omega_0\dot{\phi})\cos(\omega t+\alpha)\, f_1$$

$$-\omega(\dot{\psi}-\phi\omega_0)\sin(\omega t+\alpha)f_1 + \ddot{\theta}\cos(\omega t+\gamma)f_2 - \omega(\dot{\theta}-\omega_0)\sin(\omega t+\gamma)f_2\,] + M_R(u+X)[\ddot{v}-\ddot{\psi}L - \omega_0\dot{\phi}L$$

$$+\ddot{\phi}u + \dot{\phi}\dot{u} + \omega_0\dot{\psi}\dot{u} + \omega_0\dot{\psi}u + X(\omega_0\dot{\psi}_R + \ddot{\phi}_R + \omega_0\dot{\psi} + \ddot{\phi})] + M_R\dot{u}[\dot{v} + (\dot{\psi}-\omega_0\phi)L + (\dot{\phi}+\omega_0\psi)\, u$$

$$+ X(\dot{\phi}+\omega_0\psi+\dot{\phi}_R+\omega_0\psi_R)] - M_R(v+Y)[\ddot{u} - \ddot{\theta}L - \ddot{\phi}v - \dot{\phi}\dot{v} - \dot{\psi}\omega_0 v - \omega_0\psi v - \psi\omega_0\dot{v} - Y(\omega_0\dot{\psi}_R +$$

$$+\ddot{\phi}_R+\omega_0\dot{\psi}+\dot{\phi}) + \omega_0 X\dot{\theta}_R] - M_R\dot{v}[\dot{u} - (\theta-\omega_0)L$$

$$-(\dot{\phi}+\omega_0\dot{\psi})v + \omega_0\theta_R X - Y(\dot{\phi}+\omega_0\psi+\omega_0\psi_R+\dot{\phi}_R)]$$

$$-(\dot{\psi}-\omega_0\phi)\omega_0 I_{S2} + \frac{M}{L}(\dot{\psi}-\omega_0\phi)(\omega\sin(\omega t+\alpha)f_1 + \omega_0\frac{L^3}{3})$$

$$-\omega_0(\dot{\psi}-\omega_0\phi) I_{R2} - M_R L(\dot{\psi}-\omega_0\phi)(\dot{u}+\omega_0 L)$$

$$-M_R(u+X)^2_{\omega_0}(\dot{\psi}-\omega_0\phi) + \omega_0(\dot{\psi}-\omega_0\phi) I_{S1} + \omega_0(\dot{\phi}+\omega_0\psi) I_{S4}$$

$$+\frac{M}{L}[\omega_0(\dot{\phi}+\omega_0\psi)\cos(\omega t+\alpha)f_1 + (\dot{\theta}-\omega_0)\omega\sin(\omega t+\gamma)f_2]$$

$$+\omega_0(\dot{\psi}-\omega_0\phi+\dot{\psi}_R-\omega_0\phi_R) I_{R1} + \omega_0^2\phi_R I_{R2}$$

$$+M_R\omega_0\{\dot{v}L + (\dot{\psi}+\omega_0\phi)L^2 + XL(\psi_R\omega_0+\dot{\phi}_R+\omega_0+\dot{\phi}) - \omega_0 XL\psi_R$$

$$+\omega_0 Yu + Y^2(-\dot{\psi}+\dot{\psi}_R-\phi\omega_0-\omega_0\phi_R) + YX(\theta+\dot{\theta}_R)\} = 0 \qquad \text{(III.24)}$$

Equations (III.22 - III. 24) have been developed under the assumption that only a single mast flexible mode is excited.

For multiple mode interaction, terms involving $\cos(\omega t+\alpha)$, $\sin(\omega t + \alpha)$, etc. would be expanded to include the effects of the multiple frequencies. Where u, v and their derivatives appear explicitly, multiple modes can be included by direct substitution.

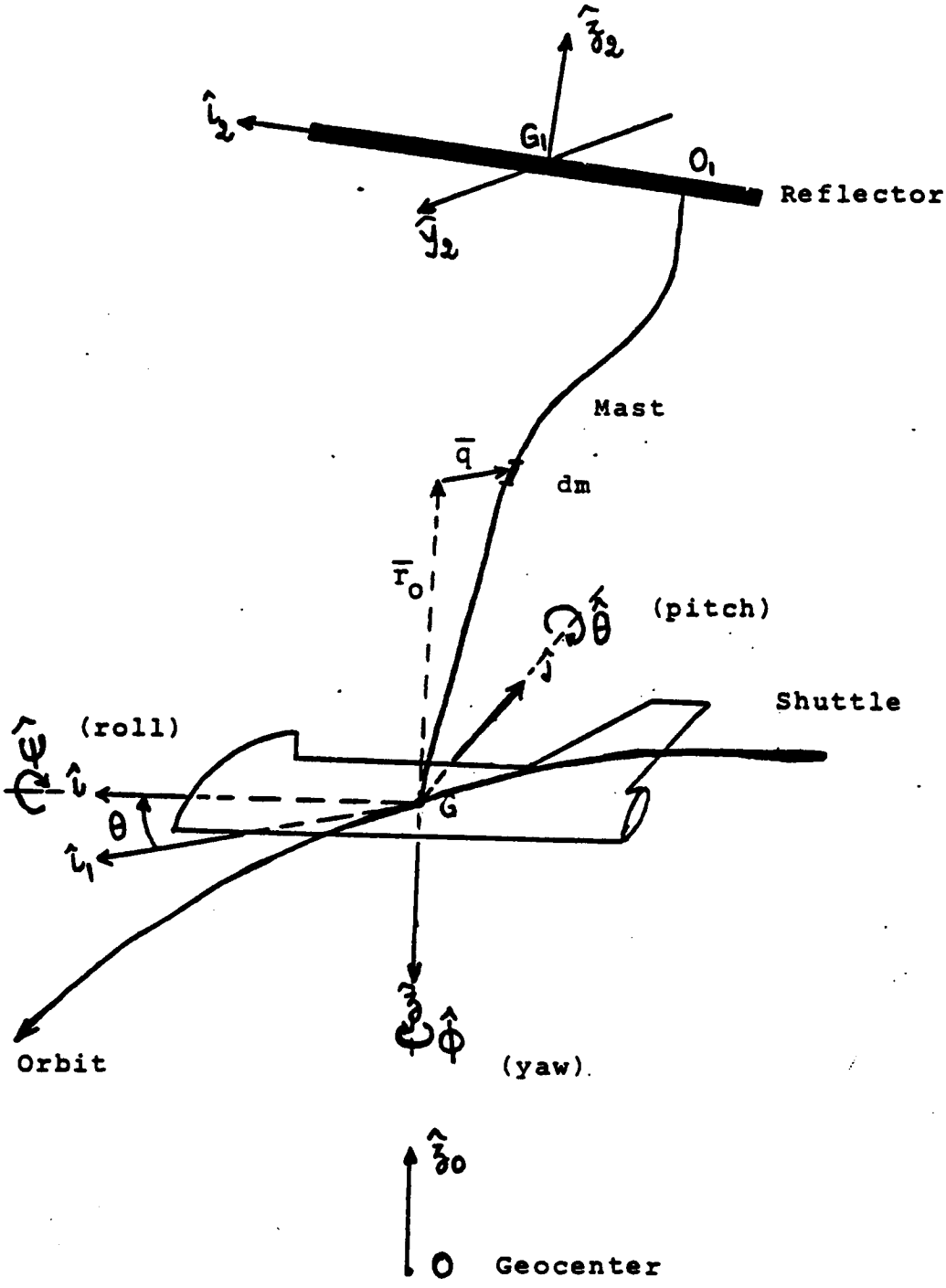

FIGURE III-1: THE 3-D GEOMETRY OF THE SCOLE CONFIGURATION IN ITS DEFORMED STATE

CHAPTER FOUR

STABILITY OF THE SCOLE SYSTEM IN SOME OF ITS CONFIGURATIONS

In Chapter III, Equations (III.22), (III.23), and (III.24) describe the dynamics of the orbiting SCOLE configuration. In what follows, the stability analysis of the SCOLE system will be conducted in three different steps.

First, it will be assumed that the mast is rigid; also that the interface point between the beam and the reflector is the reflector center of mass; second, still assuming, the mast rigid, the interface point will be offset in the "x" direction; finally, a two dimensional offset of the interface point will be introduced. The mast will still be assumed rigid. The system dynamics, in all the aforementioned cases, includes the gravity - gradient torques. (Appendix C)

IV. The SCOLE System Without Offset or Fexibility

In the absence of flexibility ($f_1=f_2=\psi_R=\dot{\psi}_R=\ddot{\psi}_R=\theta_R=\dot{\theta}_R=\ddot{\theta}_R=\phi_R=\dot{\phi}_R=\ddot{\phi}_R=u=\dot{u}=\ddot{u}=v=\dot{v}=\ddot{v}=0$), and in the absence of offset in the location of the interface point ($X=Y=0$),.

equations (III.22), (III.23), and (III.24) respectively, can be rewritten in the presence of gravity gradient torques as: (See Appendix C)

$$\ddot{\psi}[I_{S1} + ML^2/3 + M_R L^2 + I_{R1}] - \ddot{\phi} I_{S4} - \omega_0 \dot{\phi}[I_{S1} - I_{S2} + I_{S3}$$

$$+ I_{R1} - I_{R2} + I_{R3}] - \omega^2_0 \phi I_{S4} - \omega^2_0 \psi [I_{S3} - I_{S2} + I_{R3} - I_{R2} - ML^2/3$$

$$-M_R L^2 + 3(I_3 - I_2)] = 0 \qquad \text{(IV.1)}$$

$$\ddot{\theta}[I_{S2} + I_{R2} + M_R L^2 + ML^2/3] + 3\omega_0^2 \theta (I_1 - I_3) + 3\omega_0 I_4 = 0 \qquad \text{(IV.2)}$$

$$-\ddot{\psi} I_{S4} + \ddot{\phi}(I_{S3} + I_{R3}) + \omega_0 \dot{\psi}[I_{S1} + I_{S3} - I_{S2} + I_{R1} + I_{R3} - I_{R2}] +$$

$$-\omega_0^2 [I_{S1} - I_{S2} + I_{R1} - I_{R2}] \; -\omega_0^2 \psi [I_{S4} + 3I_4] = 0 \qquad \text{(IV.3)}$$

It is seen that in such configuration, in the linear range, the equation describing the pitch motion (Equation IV.2) of the system decouples from the equations describing the motion in the two remaining degrees of freedom (Equations. (IV.1)and (IV.3)).

IV.I.A. Stability Analysis

Equation (IV.2) can be recast in the following form:

$$\ddot{\theta}h_1 - \theta h_2 + h_3 = 0 \qquad \text{(IV.4)}$$

in which,

$$h_1 = I_{S2} + I_{R2} + M_R L^2 + \frac{ML^2}{3}$$

$$h_2 = 3\omega_0^2(I_3 - I_1) \text{ and } h_3 = -3\omega_0^2 I_4$$

The homogeneous part of Equation (IV.4) yields the following solution:

$$\theta_h = C_1 e^{\delta t} + C_2 e^{-\delta t} \qquad \text{(IV.5)}$$

where $\delta = \sqrt{h_2/h_1} = 0.00176$ based on nominal SCOLE parameters [1,6]

since for this configuration, $h_2/h_1 > .0$, $\theta_h(t)$ is unstable. A particular solution to (IV.4) is obtained as:

$$\theta_p = h_3/h_2 = 0.0012 \text{ (based on nominal SCOLE parameters)} \qquad \text{(IV.6)}$$

The constants of integration, C_1 and C_2, are determined from the initial conditions as:

$$C_1 = \frac{\theta_0}{2} + \frac{\dot{\theta}_0}{2\delta} \quad \text{and}$$

$$C_2 = \frac{\theta_0}{2} - \frac{\dot{\theta}_0}{2\delta}$$

giving

$$\theta(t) = \theta_h + \theta_p = \theta_0 \cosh\frac{\delta t}{\delta} + \frac{\dot{\theta}_0}{\delta}\sinh\delta t + h_3/h_2(1-\cosh\delta t) \quad \text{(IV.7)}$$

In the absence of control, the system is seen to be unstable in its pitch degree of freedom.

Equations (IV.1) and (IV.3) which have the following forms, respectively.

$$\ddot{\psi} k_1 + \ddot{\phi} k_2 - \dot{\phi} k_3 + \theta k_4 - \psi k_5 = 0 \quad \text{(IV.8)}$$

$$\ddot{\psi} n_1 + \ddot{\phi} n_2 + \dot{\psi} n_3 - \phi n_4 + \psi n_5 = 0 \quad \text{(IV.9)}$$

where; $k_1 = [I_{S1} + ML^2/3 + M_R L^2 + I_{R1}]$; $k_2 = -I_{S4}$;

$k_3 = \omega_0[I_{S1} - I_{S2} + I_{S3} + I_{R1} - I_{R2} + I_{R3}]$; $k_4 = -\omega_0^2 I_{S4}$;

$k_5 = \omega_0^2[I_{S3} - I_{S2} + I_{R3} - I_{R2} - (ML^2/3) + 3(I_3 - I_2) - M_R L^2]$;

$n_1 = -I_{S4}$; $n_2 = I_{S3} + I_{R3}$; $n_3 = \omega_0[I_{S1} + I_{S3} - I_{S2} + I_{R1} + I_{R3} - I_{R2}]$

$n_4=\omega_0^2[I_{S1}-I_{S2}+I_{R1}-I_{R2}]$; and $n_5=-\omega_0^2(I_{S4}+3I_4)$

can be recast in the following state matrix format:

$$\dot{X} = A\,X \text{ or}$$

$$\begin{bmatrix} \dot{\psi} \\ \dot{\phi} \\ \ddot{\psi} \\ \ddot{\phi} \end{bmatrix} = \begin{bmatrix} 0 & 0 & 1 & 0 \\ 0 & 0 & 0 & 1 \\ p_2 & p_4 & p_1 & p_3 \\ -p_6 & p_8 & -p_5 & -p_7 \end{bmatrix} \begin{bmatrix} \psi \\ \phi \\ \dot{\psi} \\ \dot{\phi} \end{bmatrix} \qquad \text{(IV.10)}$$

where, $p_1 = \dfrac{k_2\, n_3}{k_1 n_2 - k_2 n_1}$; $p_2 = \dfrac{n_5 k_2 + k_5 n_2}{k_1 n_2 - k_2 n_1}$; $p_3 \dfrac{k_3 n_2}{k_1 n_2 - k_2 n_1}$

$p_4 = \dfrac{-(k_2 n_4 + k_4 n_2)}{k_1 n_2 - k_2 n_1}$; $p_5 = \dfrac{n_1 p_1 + n_3}{n_2}$; $p_6 = \dfrac{n_1 p_2 n_5}{n_2}$; $p_7 = \dfrac{n_1 p_3}{n_2}$

and $p_8 = -\dfrac{(n_1 p_4 - n_4)}{n_2}$

Some of the eigenvalues of the state matrix, in this subcase have positive real parts, based on the actual SCOLE system parameters indicating instability in the open loop dynamics of the roll and yaw degrees of freedom.

IV. 2. The SCOLE System Without Flexibility but With Offset in the "X" Direction

The configuration analyzed in section (IV.1) is upgraded to the one considered here by letting X be non-zero in the equations of motion (III.22) - (III.24) and by setting all the flexibility terms and the "Y offset" equal to zero.

The equations of motion then become:

$$\ddot{\psi}[I_{S1}+(ML^2/3)+M_RL^2+I_{R1}] - \ddot{\phi}(I_{S4}+M_RXL) - \dot{\phi}\omega_0[I_{S1}+I_{S3}-I_{S2}$$

$$+I_{R1}+I_{R3}-I_{R2}] - \omega_0^2\phi(I_{S4}+M_RXL) - \omega_0^2\psi[I_{S3}-I_{S2}-\frac{ML^2}{3}+I_{R3}$$

$$-I_{R2}-M_RL^2+3(I_3'-I_2')] = 0 \qquad \text{(IV.11)}$$

$$\ddot{\theta}[I_{S2}+I_{R2}+M_R(X^2+L^2)+\frac{ML^2}{3}] + 3\omega_0^2\theta(I_1'-I') + 3\omega_0^2(I_{S4}+M_RXL) = 0 \qquad \text{(IV.12)}$$

$$-\ddot{\psi}[I_{S4}+M_RXL] + \ddot{\phi}[I_{S3}+I_{R3}+M_RX^2] + \omega_0\dot{\psi}[I_{S1}-I_{S2}+I_{S3}+I_{R1}$$

$$+I_{R3}-I_{R2}]- \omega_0^2\phi[I_{S1}-I_{S2}+I_{R1}-I_{R2}-M_R X^2]$$

$$- \omega_0^2 \psi\{3(I_{S4}+M_R XL)\} = 0 \qquad \text{(IV.13)}$$

Again, it is seen that in this configuration, the pitch equation, (Equation IV.12), decouples from the roll, (Equation (IV.II)) and yaw (Equation (IV. 13)) equations and can be rewritten as:

$$\ddot{\theta} h_1' - \theta h_2' + h_3' = 0 \qquad \text{(IV.14)}$$

where, $h_1' = I_{S2}+I_{R2}+M_R(X^2+ L^2)+ML^2/3$

$h_2' = 3\omega_0^2(I_3' - I_1')$; and $h_3' = 3\omega_0^2(I_{S4}+M_R X\ L)$

Here again, h_2'/h_1' is a positive quantity. By analogy with the previous configuration,

$$\theta(t) = \theta_0 \cosh \delta' t + \frac{\dot{\theta}_0}{\delta'} \sinh \delta' t + h_3'/h_2'(1-\cosh \delta' t) \qquad \text{(IV.15)}$$

$$\text{with } \delta' = \sqrt{h_2'/h_1'} = 0.00176 \text{ (based on SCOLE}_{1,6}\text{ nominal parameters)}$$

In the absence of control, it is seen that the pitch angle is unbounded indicating an instability in that degree of freedom.

A reasoning similar to the one previously done for the case without offset, enables one to recast Equations (IV.11) and (IV.13) in the following state matrix format:

$$X = A' X \quad \text{or}$$

$$\begin{bmatrix} \dot{\psi} \\ \dot{\phi} \\ \ddot{\psi} \\ \ddot{\phi} \end{bmatrix} = \begin{bmatrix} 0 & 0 & 1 & 0 \\ 0 & 0 & 0 & 1 \\ p'_2 & p'_4 & p'_1 & p'_3 \\ -p'_6 & p'_8 & -p'_5 & -p'_7 \end{bmatrix} \begin{bmatrix} \psi \\ \phi \\ \dot{\psi} \\ \dot{\phi} \end{bmatrix} \qquad \text{(IV.16)}$$

where, $p'_1 = \dfrac{k'_2 n'_3}{k'_1 n'_2 - n'_1 k'_2}$; $p'_2 = \dfrac{n'_5 k'_2 + k'_5 n'_2}{k'_1 n'_2 - n'_1 k'_2}$; $p'_3 = \dfrac{k'_3 n'_2}{k'_1 n'_2 - n'_1 k'_2}$;

$p'_4 = \dfrac{-(n'_4 k'_2 - k'_4 n'_2}{k'_1 n'_2 - n'_1 k'_2}$; $p'_5 = \dfrac{n'_1 p'_2 + n'_3}{n'_2}$; $p'_6 = \dfrac{n'_1 p'_2 + n'_5}{n'_2}$

$p'_7 = \dfrac{n'_1 p'_3}{n'_2}$; $p'_8 = \dfrac{-n'_1 p'_4 + n'_4}{n'_2}$

$k'_1 = I_{S1} + \dfrac{ML^2}{3} + M_R L^2 + I_{R1}$; $k'_2 = -(I_{S4} + M_R XL)$

$k'_3 = \omega_0 [I_{S1} + I_{S3} - I_{S2} + I_{R1} + I_{R3} - I_{R2}]$; $k'_4 = \omega_0^2 (I_{S4} + M_R XL)$;

$$k_5' = \omega_0^2[I_{S3}-I_{S2}+I_{R3}-I_{R2}-M_R L^2 - \frac{ML^2}{3} +3(I_3'-I_2')];$$

$$n_1' = -(I_{S4}+M_R XL);\ n_2' = I_{S3}+I_{R3}+M_R X^2 ;$$

$$n_3' = \omega_0[I_{S1}+I_{S3}-I_{S2}+I_{R1}+I_{R3}-I_{R2}]$$

$$n_4' = \omega_0^2[I_{S1}-I_{S2}+I_{R1}-I_{R2}-M_R(X^2)] \text{ and}$$

$n_5' = -\omega_0^2\{3(I_{S4}+M_R XL)\}$. Here again, some of the eigenvalues of the state matrix have positive real parts. Therefore, the open loop dynamics of the system are seen to be unstable in its roll and yaw degrees of freedom.

IV. 3. The SCOLE System with Offset in Both the "X" and "Y" Directions but Without Flexibility

If once more the description of the system dynamics is upgraded by introducing the "Y offset", the rotational equations of motion become:

$$\ddot{\psi}[I_{S1}+I_{R1}+\frac{ML^2}{3}+M(L^2+Y^2)] - \ddot{\phi} I_{xz} - \ddot{\theta} M_R XY - \dot{\phi}\omega_0[I_{S1}+I_{S3}$$

$$+2M_R Y^2-I_{S2}+I_{R1}+I_{R3}-I_{R2}] - \omega_0\dot{\theta} M_R YL - \omega_0^2\psi[I_{S3}-I_{S2}+I_{R3}-I_{R2}$$

$$+M_R(Y^2-L^2)-\frac{ML^2}{3}+3(I_{zz}-I_{yy})]-\omega_0^2\phi I_{xz}-3\omega_0^2\theta I_{xy}$$

$$+\omega_0^2[M_R Y\ L + 3I_{yz}] = 0 \qquad \text{(IV.17)}$$

$$\ddot{\theta}[I_{S2}+\frac{ML^2}{3}+I_{R2}+M_R(L^2+X^2)] + \ddot{\phi}M_R YL + \ddot{\psi}M_R XY+\omega_0\dot{\phi}M_R XY$$

$$-\omega_0\dot{\psi}M_R YL+\omega^2\phi M_R YL - 3\omega_0^2\psi I_{xy}+3\omega_0^2\theta(I_{xx}-I_{zz})$$

$$+3\omega_0^2 I_{xz} = 0 \qquad \text{(IV.18)}$$

$$\ddot{\phi}[I_{S3}+I_{R3}+M_R(X^2+Y^2)] - \ddot{\psi}I_{zx}+\omega_0\dot{\psi}[I_{S1}+I_{S3}-I_{S2}+I_{R1}+I_{R3}-I_{R2}$$

$$+2M_R Y^2] - \ddot{\theta}M_R YL - \omega_0\dot{\theta}M_R XY+3\omega_0^2\theta I_{yz}-\omega_0^2\psi(4I_{xz})$$

$$-\omega_0^2\phi[I_{S1}-I_{S2}+I_{R1}-I_{R2}+M_R(Y^2-X^2)] - \omega_0^2 M_R XY=0 \qquad \text{(IV.19)}$$

It should be noted here that the pitch equation no longer decouples from the roll and yaw equations. Equations (IV.17), (IV.18), and (IV.19) can be recast in the following state matrix format

$$\dot{X} = A'' X + C \quad \text{or}$$

$$\begin{bmatrix} \dot{\psi} \\ \dot{\theta} \\ \dot{\phi} \\ \ddot{\psi} \\ \ddot{\theta} \\ \ddot{\phi} \end{bmatrix} = \begin{bmatrix} 0 & 0 & 0 & 1 & 0 & 0 \\ 0 & 0 & 0 & 0 & 1 & 0 \\ 0 & 0 & 0 & 0 & 0 & 1 \\ a_1 & a_2 & a_3 & a_4 & a_5 & a_6 \\ a_7 & a_8 & a_9 & a_{10} & a_{11} & a_{12} \\ a_{13} & a_{14} & a_{15} & a_{16} & a_{17} & a_{18} \end{bmatrix} \begin{bmatrix} \psi \\ \theta \\ \phi \\ \dot{\psi} \\ \dot{\theta} \\ \dot{\phi} \end{bmatrix} + \begin{bmatrix} 0 \\ 0 \\ 0 \\ a_{19} \\ a_{20} \\ a_{21} \end{bmatrix} \qquad \text{(IV.20)}$$

where, given

$$I_{xx}=I_{S1}+I_{R1}+\frac{ML^2}{3}+M_R(L^2+Y^2); \quad I_{xy}=M_R XY$$

$$I_{yy}=I_{S2}+I_{R2}+\frac{ML^2}{3}+M_R(L^2+X^2); \quad I_{xz}=I_{S4}+M_R XL$$

$$I_{zz}=I_{S3}+I_{R3}+M_R(X^2+Y^2); \quad I_{yz}=+M_R YL$$

$$A_1' = I_{xz}/I_{xx}, \quad A_2' = \frac{M_R XY}{I_{xx}}; \quad A_3' = \omega_0(I_{xx}+I_{zz}-I_{yy})/I_{xx}$$

$$A_4 = \omega_0 M_R YL/I_{xx}; \quad A_5 = 4\omega_0^2(I_{zz}-I_{yy})/I_{xx};$$

$$A_6 = \omega_0^2 I_{xz}/I_{xx}; \quad A_7 = 3\omega_0^2 I_{xy}/Ixx; \quad A_8 = \omega_0^2(M_R YL+3I_{yz})/I_{xx}$$

Here A_1-A_3, B_1-B_3 have been identified with primes in order to avoid confusion with coefficients appearing in the spatially dependent functions $s_x(z)$, $s_y(z)$ and $\theta(z)$ appearing in the solutions to the partial differential equations describing the vibrations of the mast, Appendix A) .

$$A_9 = \frac{M_R YL}{I_{yy}} \; ; \quad A_{10} = \frac{M_R XY}{I_{yy}} \; ; \quad A_{11} = \omega_0 \frac{M_R XY}{I_{yy}} \; ; \quad A_{12} = 0;$$

$$A_{13} = \omega_0^2 \frac{M_R YL}{I_{yy}} \; ; \quad A_{14} = 3\omega_0^2 \, I_{xy}/I_{yy}; \quad A_{15} = 3\omega_0^2 (I_{xx} - I_{zz})/I_{yy};$$

$$A_{16} = 3\omega_0^2 \, I_{xz}/I_{yy}; \quad A_{17} = I_{zx}/I_{zz}; \quad A_{18} = \frac{M_R YL}{I_{zz}};$$

$$A_{19} = \omega_0 \, (I_{xx} + I_{zz} - I_{yy})/I_{zz} \; ; \quad A_{20} = \omega_0 \frac{M_R XY}{I_{zz}};$$

$$A_{21} = 3\omega^2 \, I_{yz}/I_{zz} \; ; \quad A_{22} = 4\omega^2 \, I_{xz}/I_{zz}$$

$$A_{23} = \omega_0^2 (I_{xx} - I_{yy} - + I_{zz})/I_{zz}; \quad A_{24} = \omega_0^2 M_R XY/I_{zz}$$

$$B_1' = (A_2' + A_1' \, A_{18})/(1 - A_1' \, A_{17}'); \quad B_2' = -A_1' \, A_{19}/(1 - A_1' \, A_{17});$$

$B_3^{'}=A_3/(1-A_1^{'}\ A_{17})$; $B_4=(A_4-A_1^{'}\ A_{20})/(1-A_1^{'}\ A_{17})$;

$B_5=(A_5+A_1^{'}A_{22})/(1-A_1^{'}\ A_{17})$; $B_6 = (A_6+A_1^{'}\ A_{23})/(1-A_1^{'}\ A_{17})$;

$B_7=(A_7-A_1\ A_{21}^{'})/(1-A_1\ A_{17}^{'})$;$B_8 = (A_1\ A_{24}-A_8)/(1-A_1^{'}\ A_{17})$;

$B_9=(1+A_9\ A_{18})/(A_{10}+A_9\ A_{17})$; $B_{10}=(A_{12}+A_9\ A_{19})/(A_{10}+A_9\ A_{17})$;

$B_{11}=-A_{11}/(A_{10}+A_9\ A_{17})$; $B_{12}=A_9\ A_{20}/(A_{10}+A_9\ A_{17})$;

$B_{13}=(A_{14}-A_9\ A_{22})/(A_{10}+A_9\ A_{17})$; $B_{14}=-(A_{13}+A_9\ A_{23}/(A_{10}+A_9\ A_{17})$

$B_{15}=(A_9\ A_{21}-A_{15})/(A_{10}+A_9\ A_{17})$; $B_{16}=-(A_{16}+A_9\ A_{24})/(A_{10}+A_9\ A_{17})$;

$a_{20}= \dfrac{B_{16} - B_8}{B_1^{'} - B^9}$; $a_1 = B_{13} + B_9\ a_7$; $a_2 = B_9\ a_8 + B_{15}$;

$a_3=B_9\ a_9 + B_{14}$; $a_4 = B_9\ a_{20} + B_{10}$; $a_5 = B_9\ a_{11} + B_{12}$;

$$a_6 = B_9\, a_{12} + B_{11};\quad a_{19} = B_9\, a_{20} + B_{16};$$

$$a_7 = \frac{B_{13} - B_5}{B_1' - B_9};\quad a_8 = \frac{B_{15} - B_7}{B_1' - B_9};\quad a_9 = \frac{B_{14} - B_6}{B_2' - B_9}$$

$$a_{10} = \frac{B_{10} + B_2'}{B_1' - B_9};\quad a_{11} = \frac{B_{12} - B_4}{B_1' - B_9};\quad a_{12} = \frac{B_{11} - B_3'}{B_1' - B_9}$$

$$a_{13} = A_{17}\, a_1 + A_{18}\, a_7 + A_{22};\quad a_{14} = A_{17}\, a_2 + A_{18} a_8 - A_{21};$$

$$a_{15} = A_{17}\, a_3 + A_{18}\, a_9 - A_{23};\quad A_{16} = A_{17}\, a_4 + A_{18}\, a_{10} - A_{19};$$

$$a_{17} = A_{17}\, a_5 + A_{18}\, a_{11} - A_{20};\quad a_{18} = A_{17}\, a_6 + A_{18}\, a_{12};$$

and $a_{21} = (A_{17}\, a_{19} + A_{18}\, a_{20} + A_{24})$

Since the Shuttle axes do not correspond to the principal axes of the system, the system dynamics appear in the following state form:

$$\dot{X} = AX + C \qquad \text{(IV.21)}$$

indicating that the system equilibrium position is no longer $\psi_0 = \theta_0 = \phi_0 = 0$.

Let ψ_e, θ_e, and ϕ_e be the equilibrium position for this configuration of the system. Then,

$$\psi = \psi_e + \eta_1 \quad \text{and} \quad \dot{\psi} = \eta_1$$
$$\theta = \theta_e + \eta_2 \quad \text{and} \quad \dot{\theta} = \dot{\eta}_2$$
$$\phi = \phi_e + \eta_3 \quad \text{and} \quad \dot{\phi} = \eta_3$$

The new state vector is $[\eta_1, \eta_2, \eta_3, \dot{\eta}_1, \dot{\eta}_2, \dot{\eta}_3]^T$. Also ψ_e, θ_e, and ϕ_e satisfy

$$a_1 \psi_e + a_2 \theta_e + a_3 \phi_e = -a_{19}$$
$$a_7 \psi_e + a_{8\theta} \theta_e + a_9 \phi_e = -a_{20}$$
$$a_{13} \psi_e + a_{14} \theta_e + a_{15} \phi_e = -a_{21}$$

this simultaneous system is solved using

$$[a] = [A] [\psi_e, \theta_e, \phi_e]^T \Longrightarrow [\psi_e, \theta_e, \phi_e]^T = [A^{-1}] [a]$$

ψ_e = - . 548552 rad.

θ_e = - . 019345 rad. based on nominal SCOLE parameters

ϕ_e = . 207672 rad.

For the open-loop dynamics of the non-linear model of the SCOLE system, the envelopes of the Euler angles are depicted in Figure IV.1, as a function of time.

After substituting the new state vector in the equations describing the system dynamics, linearizing them about the new equilibrium position, recasting them into a state format, one arrives at a system which can be cast in the following form (where $a'_1 \rightarrow a'_{18}$ are constants)

$$A = \begin{bmatrix} 0 & 0 & 0 & 1 & 0 & 0 \\ 0 & 0 & 0 & 0 & 1 & 0 \\ 0 & 0 & 0 & 0 & 0 & 1 \\ a'_1 & a'_2 & a'_3 & a'_4 & a'_5 & a'_6 \\ a'_7 & a'_8 & a'_9 & a'_{10} & a'_{11} & a'_{12} \\ a'_{13} & a'_{14} & a'_{15} & a'_{16} & a'_{17} & a'_{18} \end{bmatrix} \qquad \text{(IV.22)}$$

The open loop system in this configuration is also unstable due to the unfavorable intertia distribution.

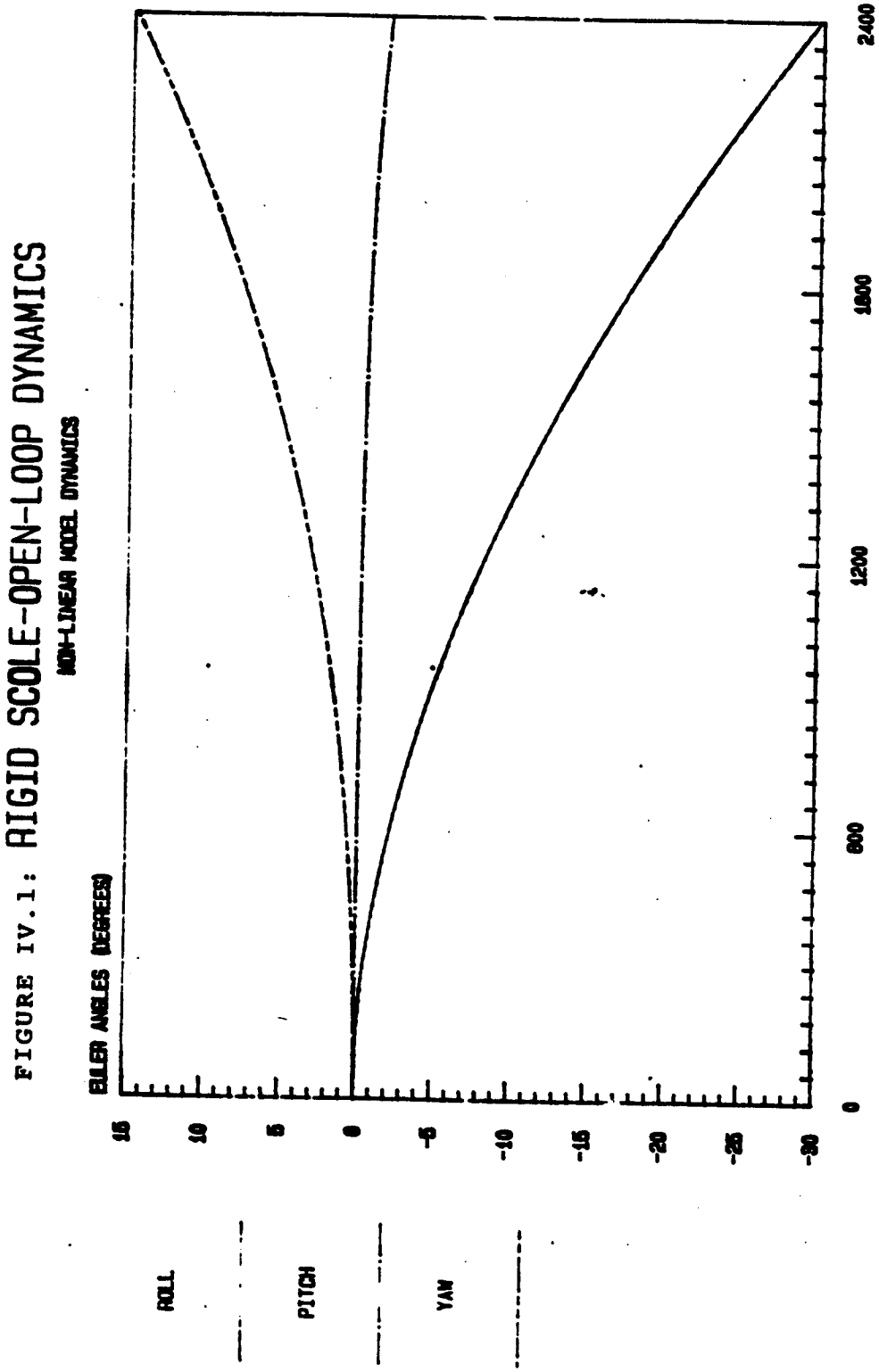
RIGID SCOLE-OPEN-LOOP DYNAMICS
NON-LINEAR MODEL DYNAMICS
EULER ANGLES (DEGREES)
15
10
5
0
-5
-10
-15
-20
-25
-30
0
800
1200
1600
2400
TIME (SECONDS)
ROLL
PITCH
YAW

FIGURE IV.1:

CHAPTER FIVE

CONTROL SYNTHESIS

In this chapter, the different components for the two-stage control strategy which would slew the system as if rigid and then damp out the mast vibration will be analyzed in the following manner:

first, within the linear range, the motion of the rigidized SCOLE is controlled using a strategy, based on the linear regulator problem when the system is subjected to some small perturbations in its degrees of freedom;

second, still within the linear range, the motion of the actual SCOLE system, including its first four vibrational modes, is controlled using a control law based again on the linear regulator theory when the system is subjected to initial perturbations in its different degrees of freedom.

third, the control strategy derived for the linear model of the rigidized SCOLE is applied to the non-linear model of the same configuration. Preliminary slew maneuvers are tested by assuming single axis initial perturbations of 20^{o} in the roll, pitch, and yaw degrees of freedom, respectively. The three Shuttle torquers and the two actuators on the reflector are then assumed to be

the only sources of control moments. The controllers are seen not to reach saturation.

V.1. Control of the Rigidized SCOLE

During the control of this model, it is assumed that the actuators located on the mast (proof masses) are not activated. As a result, the system is controlled by means of the Orbiter torquers and the actuators located on the reflector (Figure I.1).

Since the Shuttle is equipped with three torquers acting about the x, y, and z directions, the total control torque available can be written as

$$\vec{T}=\{M_x U_x + 130F v_y)\,\hat{i} + (M U_y - 130 F_x v_x)\hat{j}$$

$$+ (M_z U_z + 32.5 F_x v_x + 18.75 F_y v_y)\,\hat{k}\} \text{ ft.-lb} \quad (V.1)$$

with the limits for M_x, M_y and M_z = 10,000. ft. lb; F_x and F_y = 800 lb.[1] The constraints, therefore, are

$$|U_x| \leq 1;\ |U_y| \leq 1;\ |U_z| \leq 1;\ |v_x| \leq 1;\ \text{and}\ |v_y| \leq 1$$

where U, the control vector is expressed as

$U = [v_1, v_2, U_1, U_2, U_3]^T$, while the control influence matrix can then be written as:

$$B = \begin{bmatrix} 0 & 0 & 0 & 0 & 0 \\ 0 & 0 & 0 & 0 & 0 \\ 0 & 0 & 0 & 0 & 0 \\ 0 & 130F_y & M_x & 0 & 0 \\ -130F_x & 0 & 0 & M_y & 0 \\ 32.5F_x & 18.75F_y & 0 & 0 & M_z \end{bmatrix} \qquad (V.2)$$

The optimal control U which minimizes a performance index

$$J = \int_0^\infty (X^TQX+U^TRU)\, dt$$

is given by

$$U = -KX = -(R^{-1}B^TP)X \qquad (V.3)$$

where P is the positive definite solution of the steady state Ricatti matrix equation[9].

The equations describing the closed loop system can be recast in the following matrix format:

$$\dot{X} = AX + BU$$

After substitution of -KX for U, the closed loop equation can be rewritten as

$$\dot{X} = (A-BK)X \qquad (V.4)$$

A parametric study was conducted by first examining the variation of the real part of the least damped mode as a function of different values for the (assumed) diagonal Q and R weighting elements (Figures V.1 and V.2). In this initial study, each of the diagonal Q elements were assumed equal i.e. Q=diag. [SQ] and also each of the diagonal R elements were assumed equal R = diag. [SR]. Figure V.1 corresponds to a model of the rigidized SCOLE system where the dimensionality of the state vector is 6 x 1 and 3 Shuttle torquers plus 2 reflector actuators describe the control inputs. On the other hand, Figure V.2 corresponds to the model of SCOLE including the first four flexible mast modes. For this case the state vector has dimensionality 14 x 1, and four additional control actuators are assumed to be placed on the mast - two at 1/3 the total length and the remaining two at 2/3 the total length (see Figure I.1).

It can be seen from both Figures V.1 and V.2 that the best closed-loop transient results are obtained from using larger values of the state penalty along with smaller values of the control penalty elements. However, when the closed loop dynamic responses were simulated using the best combinations of Q and R it was seen that some of the controllers reached saturation levels for responses with initial conditions on pitch, roll, and yaw taken within the slewing angle range (i.e. approx. 0.3 rad.).

As an alternative, the concept of split weighting of both the state and control penalty elements was considered, initially for the rigidized SCOLE model. Since the roll (and to some extent also the pitch) are easier motions to excite than the yaw, due to the SCOLE moment of inertia distribution, it seems intuitively correct to relax the penalty of these control inputs as contrasted with the remaining control penalty elements. Also since both position and rate feedback of the Shuttle rotational motion will be utilized, it appears logical to place a far greater penalty on the (angular) position displacements. Based on this philosophy and by trial and error, the set of Q and R which produced the largest absolute value of the real part of the least damped mode

(while at the same time avoiding saturation during 20^{o} single axis slewing maneuvers) was selected as

$$Q = \text{diag.}[5\text{x}10^{12},\ 5\text{x}10^{12},\ 5\text{x}10^{12},\ 1,\ 1,\ 1]$$

and $R = \text{diag.}[1,\ 1,\ .1,\ .2,\ 1]$

For this set of Q and R thee closed log eigenvalues for the rigidized SCOLE model are calculated

$R(\lambda_i)$	$Im(\lambda_i)$
-0.431436E+02	0.431436E+02
-0.431436E+02	-0.431436E+02
-0.132023E+03	0.132023E+03
-0.132023E+03	-0.132023E+03
-0.328320E+03	0.328320E+03
-0.328320E+03	-0.328320E+03

It has been assumed here that all the state variables are available at each instant (observability matrix = I_6)

The closed loop dynamics has been simulated and Figures (V.3), (V.4) and (V.5) show the transient responses to a 6^{o} initial perturbation in roll, pitch and yaw, respectively. Figu-e V.3 shows that a 6^{o} perturbation in roll is damped out in approximately 13 seconds. During that single axis maneuver, it should also be noticed that the coupling disturbs the yaw degree of

freedom, which reaches a maximum amplitude of 0.25° degree. Figure V.3a, V.3b, and V.3c show, for the 6° maneuver about the roll axis, the forces required from the reflector actuators, the efforts produced by the Shuttle's torquers, and the components of the equivalent total torque acting on the SCOLE system, respectively. The reflector "y" actuator and the Shuttle's "x" torquer are the more active controllers for this maneuvers, as expected.

Figures V.4 and V.5 show the response to 6° initial perturbation in pitch and yaw, respectively. During the maneuver about the pitch axis, the yaw angle is seen to be perturbed and reaches a maximum 1° amplitude. The pitch angle reaches the same amplitude in disturbance when the maneuver about the yaw axis is undertaken. This confirms the strong coupling between the pitch and yaw closed-loop motions of SCOLE. The pitch maneuver takes about 48 seconds to stabilize while it takes the yaw maneuver almost two minutes to do so. This can be attributed to the inertia distribution in this configuration of SCOLE on the one hand, and to the shorter moment arms (offset distances) available to the reflector actuators during a maneuver about the yaw axis on the other. Where the control efforts are as important a factor in the selection

of a control strategy as the response times are, this control law could be chosen over the bang-bang approach.[4] For the cases shown in Figures V.4 and V.5 the maximum control effort from each controller is far below its saturation levels.

V.2. Control of the Orbiting SCOLE with the First Four Modes Included

This model of the SCOLE is controlled through the three torquers on the Shuttle and the six actuators located by pairs at $z = -L/3$; $z = -\frac{2L}{3}$ on the mast; and at G_1, the mass center of the reflector (Figure I.1). The pairs of actuators are arranged in such a manner that one acts along the x direction and the other in the y direction. The actuators, when activated to provide vibration control to the mast, will develop torques about the Orbiter center of mass. Each actuator provides a maximum of 800 lb[1]. force; the resulting torque contributed by all six actuators is computed as

$$\vec{T}_1 = F_y L\,(v_{1y}/3 + 2\,v_{2y}/3 + v_{3y})\,\hat{i} - F_x L\,(v_{1x}/3 + 2v_{2x}/3 + v_{3x})\hat{j} - (YF_x\,v_{3x} - XF\,v_{3y})\hat{k}$$

This is added to the torques provided by the Shuttle's three torquers: $\vec{T}_2 = M_x U_x \hat{i} + M_y U_y \hat{j} + M_z U_z \hat{k}$, to yield the total available control torque for the system as:

$$\vec{T} = [M_x U_x + F_y L (v_{1y}/3 + 2v_{2y}/3 + v_{3y})]\hat{i} [M_y U_y - F_x L(v_{1x}/3 + 2v_{2x}/3 + v_{3x})]\hat{j} + [M_z U_z + X F_y v_{3y} - Y v_{3x} F_x]\hat{k}$$

After the substitution of the new state variables into the generic modal equations, Appendix D, there results:

$$\ddot{A}_n = \omega_n^2 A_n + (a_7 B_n - a_1 C_n - 2\omega_0^2 C_n)\eta_1 + (a_8 B_n - a_2 C_n - 3\omega_0^2 B_n)\eta_2$$

$$+(a_9 B_n - a_3 C_n)\eta_3 + (a_{10} B_n - a_4 C_n)\dot{\eta}_1 + (a_{11} B_n - a_5 C_n - 2\omega_0 D_n)\dot{\eta}_2$$

$$+(a_{12} B_n - a_6 C_n + 2\omega_0 C_n)\dot{\eta}_3 + F_x[v_{3x} s_{nx}(-L) + v_{2x} s_{nx}(-\tfrac{2L}{3}) + v_{1x} s_{nx}(-L/3)]$$

$$+ F_y[v_{3y} s_{ny}(-L) + v_{2y} s_{ny}(-2L/3) + v_{1y} s_{ny}(-L/3)]$$

with the control and global state vectors, respectively, chosen as

$U = [v_{1x}, v_{1y}, v_{2x}, v_{2y}, v_{3x}, v_{3y}, U_1, U_2, U_3]^T$ and

$X = [\eta_1, \eta_2, \eta_3, A_1, A_2, A_3, A_4, \dot{\eta}_1, \dot{\eta}_2, \dot{\eta}_3, \dot{A}_1, \dot{A}_2, \dot{A}_3, \dot{A}_4]^T$

with, $||v_{ix}|| \leq 1$; $||v_{iy}|| \leq 1$; and $||U_i|| \leq 1$.

Let t_{nx}, and t_{ny}, n = 1, 2, 3, 4, be functions such that $t_{nx}(z) = F_x s_{nx}(z)$ and $t_{ny}(z) = F_y s_{ny}(z)$, the control influence matrix can be recast as B =

$$
\begin{bmatrix}
0 & 0 & 0 & 0 & 0 & 0 & 0 & 0 & 0 \\
0 & 0 & 0 & 0 & 0 & 0 & 0 & 0 & 0 \\
0 & 0 & 0 & 0 & 0 & 0 & 0 & 0 & 0 \\
0 & 0 & 0 & 0 & 0 & 0 & 0 & 0 & 0 \\
0 & 0 & 0 & 0 & 0 & 0 & 0 & 0 & 0 \\
0 & 0 & 0 & 0 & 0 & 0 & 0 & 0 & 0 \\
0 & 0 & 0 & 0 & 0 & 0 & 0 & 0 & 0 \\
0 & F_y L/3 & 0 & 2F_y L/3 & 0 & F_y L & Mx & 0 & 0 \\
-F_x L/3 & 0 & -2F_x L/3 & 0 & -F_x L & 0 & 0 & M_y & 0 \\
0 & 0 & 0 & 0 & -YF_x & XF_y & 0 & 0 & M_z \\
t_{1x}(-L/3) & t_{1y}(-L/3) & t_{1x}(-2L/3) & t_{1y}(-2L/3) & t_{1x}(-L) & t_{1y}(-L) & 0 & 0 & 0 \\
t_{2x}(-L/3) & t_{2y}(-L/3) & t_{2x}(-2L/3) & t_{2y}(-2L/3) & t_{2x}(-L) & t_{2x}(-L) & 0 & 0 & 0 \\
t_{3x}(-L/3) & t_{3y}(-L/3) & t_{3x}(-2L/3) & t_{3y}(-2L/3) & t_{3x}(-L) & t_{3x}(-L) & 0 & 0 & 0 \\
t_{4x}(-L/3) & t_{4y}(-L/3) & t_{4x}(-2L/3) & t_{4y}(-2L/3) & t_{4x}(-L) & t_{4x}(-L) & 0 & 0 & 0
\end{bmatrix}
\qquad \text{(V.5)}
$$

The linearized equations of motion describing the rotational open-loop dynamics of the orbiting SCOLE (modified form of Equations III.22 - III.24) are

$$
\ddot{\eta}_1 I_{xx} - \ddot{\eta}_2 M_R XY - \ddot{\eta}_3 I_{xz} - \omega_0 \dot{\eta}_3 (I_{xx} - I_{yy} + I_{zz}) - \omega_0 \dot{\eta}_2 M_R YL
$$

$$-4\omega_0^2\eta_1(I_{zz}-I_{yy})-\omega_0^2\eta_3 I_{xz}-3\omega_0^2\eta_2 I_{xy}+\sum_{n=1}^{4}A_n d_{1n}-\sum_{n=1}^{4}A_n d_{2n}+$$

$$\sum_{n=1}^{4}A_n d_{3n}=0 \qquad (V.6)$$

$$\ddot{\eta}_2 I_{yy}+\ddot{\eta}_1 M_R XY+\ddot{\eta}_3 M_R YL-\dot{\eta}_1\omega_0 M_R YL+\dot{\eta}_3\omega_0 M_R XY-\eta_1 3\omega_0^2 I_{xy}$$

$$+\eta_3\omega_0^2 M_R YL+3\eta_2\omega_0^2(I_{xx}-I_{zz})+\sum_{n=1}^{4}\ddot{A}_n d_{4n}-\sum_{n=1}^{4}\dot{A}_n d_{5n}=0 \qquad (V.7)$$

and

$$\ddot{\eta}_3 I_{zz}-\ddot{\eta}_1 I_{zx}-\ddot{\eta}_2 M_R YL+\omega_0\dot{\eta}_1(I_{xx}-I_{yy}+I_{zz})-\dot{\eta}_2\omega_0 M_R XY$$

$$-4\eta_1\omega_0^2 I_{xz}+3\eta_2\omega_0^2 I_{yz}-\eta_3\omega_0^2(I_{xx}-I_{yy})+\sum_{n=1}^{4}\ddot{A}_n d_{6n}+\sum_{n=1}^{4}\dot{A}_n d_{7n}$$

$$+\sum_{n=1}^{4}A_n d_{8n}=0 \qquad (V.8)$$

where, for the nth mode

$$d_{1n}=M_R(Ls_{ny}(-L)-XY\theta_n(-L)+\frac{M}{L}f_2(\beta_n);$$

$$d_{2n}=M_R\omega_0(Y\,s_{nx}(-L)); \quad d_{3n}=\omega_0^2(\frac{M}{L}\,f_2(\beta_n)-M_R X\theta_n(-L);$$

$$d_{4n} = \frac{M}{L} f_1(\beta_n) + (I_{R2} + M_R[X^2 + L^2])\theta_n(-L)$$

$$- M_R L s_{nx}(-L);$$

$$d_{5n} = \omega_0 M_R X\{L\theta_n(-L) + 2s_{nx}(-L)\}; \quad d_{6n} = M_R(Xs_{ny}(-L) -$$

$$Ys_{nx}(-L)); \; d_{7n} = M_R \omega_0 XY\,\theta_n(-L); \text{ and } d_{8n} = \omega_0{}^2 Ys_{nx}(-L)$$

Equations (V.6), (V.7), and (V.8) can be recast in a matrix format as

$$[A_1]\begin{bmatrix} \ddot{\eta}_1 \\ \ddot{\eta}_2 \\ \ddot{\eta}_3 \end{bmatrix} + [A_2]\begin{bmatrix} \ddot{A}_1 \\ \ddot{A}_2 \\ \ddot{A}_3 \\ \ddot{A}_4 \end{bmatrix} + [B_1]\dot{X}' + [C_1]X' = 0 \qquad (V.9)$$

with $X' = [\eta_1, \; \eta_2, \; \eta_3, \; A_1, \; A_2, \; A_3, \; A_4]^T$

$$[A_1] = \begin{bmatrix} I_{xy} & M_R XY & -I_{xz} \\ M_R XY & I_{yy} & M_R YL \\ I_{zx} & M_R YL & I_{zz} \end{bmatrix}; \quad [A_2] = \begin{bmatrix} d_{11} & d_{12} & d_{13} & d_{14} \\ d_{41} & d_{42} & d_{43} & d_{44} \\ d_{61} & d_{62} & d_{63} & d_{64} \end{bmatrix}$$

$$[B_1] = [B_1' \quad B_2'] \quad ; [C_1] = [C_1' \quad C_2']$$

and

$$[B_1'] = \begin{bmatrix} 0 & -\omega_0 M_R YL & -\omega_0(I_{xx}-I_{yy}+I_{zz}) \\ -\omega_0 M_R Y & 0 & \omega_0 M_R XY \\ \omega_0(I_{xx}-I_{yy}+I_{zz}) & -\omega_0 M_R XY & 0 \end{bmatrix} ; [B_2'] = \begin{bmatrix} d_{21} & d_{22} & d_{23} & -d_{24} \\ d_{51} & -d_{52} & -d_{53} & -d_{54} \\ d_{71} & d_{72} & d_{73} & d_{74} \end{bmatrix}$$

and,

$$[C_1] = \begin{bmatrix} -4\omega_0^2(I_{zz}-I_{yy}) & -3\omega_0^2 I_{xy} & -\omega_0^2 I_{xz} \\ -3\omega^2 I_{xy} & 3\omega_0^2(I_{xx}-I_{zz}) & \omega_0^2 M_R YX \\ -4\omega_0^2 I_{xz} & 3\omega_0^2 I_{yz} & -\omega_0^2(I_{xx}-I_{yy}) \end{bmatrix} [C_2] = \begin{bmatrix} d_{31} & d_{32} & d_{33} & d_{34} \\ 0 & 0 & 0 & 0 \\ d_{81} & d_{82} & d_{83} & d_{84} \end{bmatrix}$$

From the generic modal equations, the expressions for the different $\ddot{A}_i$, (open-loop) can be expressed as follows:

$$\begin{bmatrix} \ddot{A}_1 \\ \ddot{A}_2 \\ \ddot{A}_3 \\ \ddot{A}_4 \end{bmatrix} = [B_2] \begin{bmatrix} A_1 \\ A_2 \\ A_3 \\ A_4 \end{bmatrix} + [C_2] \begin{bmatrix} \eta_1 \\ \eta_2 \\ \eta_3 \end{bmatrix} + [C_2''] \begin{bmatrix} \dot{\eta}_1 \\ \dot{\eta}_2 \\ \eta_3 \end{bmatrix}$$

with

$$[B_2] = \begin{bmatrix} -\omega_1^2 & 0 & 0 & 0 \\ 0 & -\omega_2^2 & 0 & 0 \\ 0 & 0 & -\omega_3^2 & 0 \\ 0 & 0 & 0 & \omega_4^2 \end{bmatrix} \quad \text{and}$$

$$[C_2] = \begin{bmatrix} e_{11} & e_{12} & e_{13} \\ e_{21} & e_{22} & e_{23} \\ e_{31} & e_{32} & e_{33} \\ e_{41} & e_{42} & e_{43} \end{bmatrix} \quad [C''2] = \begin{bmatrix} e_{14} & e_{15} & e_{16} \\ e_{24} & e_{25} & e_{26} \\ e_{34} & e_{35} & e_{36} \\ e_{44} & e_{45} & e_{46} \end{bmatrix}$$

where ω_i is the frequency of vibration of the ith mode, and

$$e_{n1} = (a_7 B_n - a_1 C_n - 2\omega_0^2 C_n)$$

$$e_{n2} = (a_8 B_r - a_2 C_n - 3\omega_0^2 B_n)$$

$$e_{n3} = (a_9 B_n - a_3 C_n)$$

$$e_{n4} = (a_{10} B_n - a_4 C_n)$$

$$e_{n5} = (a_{11} B_n - a_5 C_n - 2 \omega_0^2 D_n) \quad \text{and}$$

$$e_{n6} = (a_{12} B_n - a_6 C_n + 2 \omega_0^2 C_n)$$

C-2

After substitution for the open-loop A (i=1 - 4), Equation (V.9) can be rewritten in the following matrix format:

$$[A_1]\begin{bmatrix}\ddot{\eta}_1\\ \ddot{\eta}_2\\ \ddot{\eta}_3\end{bmatrix} + [A_2B_2]\begin{bmatrix}A_1\\ A_2\\ A_3\\ A_4\end{bmatrix} + [A_2C_2]\begin{bmatrix}\eta_1\\ \eta_2\\ \eta_3\end{bmatrix} + [A_2C_2'']\begin{bmatrix}\dot{\eta}_1\\ \dot{\eta}_2\\ \dot{\eta}_3\end{bmatrix} + [B_1]\begin{bmatrix}\dot{\eta}_1\\ \dot{\eta}_2\\ \dot{\eta}_3\end{bmatrix}$$

$$+[B_2]\begin{bmatrix}\dot{A}_1\\ \dot{A}_2\\ \dot{A}_3\\ \dot{A}_4\end{bmatrix} + [C_1']\begin{bmatrix}\eta_1\\ \eta_2\\ \eta_3\end{bmatrix} + [C'_2]\begin{bmatrix}A_1\\ A_2\\ A_3\\ A_4\end{bmatrix} = 0 \qquad (V.10)$$

which, when the global state vector is taken as: $X^T = [\eta_1, \eta_2, \eta_3, A_1, A_2, A_3, A_4, \dot{\eta}_1, \dot{\eta}_2, \dot{\eta}_3, \dot{A}_1, \dot{A}_2, \dot{A}_3, \dot{A}_4]$, is equivalent to

$$\begin{bmatrix}\ddot{\eta}_1\\ \ddot{\eta}_2\\ \ddot{\eta}_3\end{bmatrix} = [-A_1^{-1}(A_2C_2+C_1') \mid -A^{-1}{}_1(A_2B_2+C_2) \mid -A_1^{-1}(A_2C_2+B'_1) \mid -A_1^{-1}B'_2]\,X$$

The new state matrix A, for the SCOLE system therefore, is

$$
\begin{bmatrix}
[0] & [0] & [I3] & [0] \\
[0] & [0] & [0] & [I4] \\
-A_1^{-1}(A_2C_2+C_1') & -A_1^{-1}(A_2B_2+C_2') & -A_1^{-1}(A_2C''_2+B_1') & -A_1^{-1}B'_2 \\
3 \times 3 & 4 \times 3 & 3 \times 3 & 4 \times 3 \\
[C_2] & [B_2] & [C''_2] & 0 \\
3 \times 4 & 4 \times 4 & 3 \times 4 & 4 \times 4
\end{bmatrix}
$$

Here again, the control U which minimizes the performance index

$J = \int_0^\infty (X^TQX + U^TRU)\, dt$ is obtained after using the ORACLS package to solve the steady state Riccati matrix equation.[9] Figure V.2 shows the same type of parametric study previously conducted for the model of the rigidized SCOLE. Since it is anticipated here that large amplitude slew maneuvers of the flexible SCOLE will be conducted based on the control strategy developed herein, the concept of split weighting of both the state and control penalty elements was considered. The criteria of

selection being based on the control strategy capability to slew the flexible SCOLE through large amplitude angles, i.e. ψ, θ, and ϕ equal to 20^{o} respectively without any of the actuator reaching saturation level.

It should be noted here that the state and control influence matrices have dimensionality of (14 x 14) and (14 x 9), respectively.

The equations describing the closed-loop system,

$\dot{X} = AX + BU$ have been numerically integrated and the corresponding mathematical model simulated for

$Q = diag.[5x10^{6}, 5x10^{6}, 5x10^{6}, 5x10^{4}, 5x10^{4}, 5x10^{4}, 5x10^{4}, 10, 10, 10, 10, 10, 10, 10]$

and R as diag [10,10,10,10,10,10,1,1,1]

The transient responses to some initial perturbations, depicted in Figures (V.6) - (V.17) confirm the controllability of the flexible SCOLE system. During the simulation of this model, the three attitude angles (roll, pitch, and yaw) are each subjected to a 6^{o} single axis maneuver. For each case, the effects of such displacements on the modal amplitudes of the first four modes are shown (Figures (V.6) through (V.11).

The largest disturbance in the flexible modes, caused by the variation of an attitude angle is observed during the roll axis maneuver, the first mode is the most excited; its amplitude doesn't exceed 0.13 ft. (0.1% of L). All the transients are damped out within 25 seconds.

This is due to the contribution of the additional 2 pairs of actuators located on the mast at $z_1 = -L/3$ and $z = -2L/3$. During the 6° maneuver (from equilibrium) about the roll axis, the reflector "y" axis actuator provides a maximum of 210 lb. while the forces in the two "y" actuators located a $z = L/3$ and $z = -L/3$, reach 120 to 80 lb, respectively. The Shuttle "x" torquer provides a maximum of 2800 ft. lb torque bringing to 52,500 ft. lb the maximum value of the x component of the composite control torque required for this maneuver. This, when compared with the total maximum torque of (35,000 ft. lb) required during the same maneuver of the rigidized model of SCOLE (figure V.3c), shows an increase in the total control torque of 50%. However the reflector "y" actuator, when flexibility is included, provides less of a contribution than for the rigidized case.

It should be noted here that because of the additional pairs of actuators located on the mast, one can

now exploit the moment arms provided by the two reflector actuators without the same risks of perturbing the pitch or roll which exists for the rigidized model. The actuators located on the mast would help to prevent such undesired displacements in pitch and roll.

In turn, each of the four flexible modes were given an initial amplitude equal 1.0% of L, to stay within the linear range, Figures (V.13), (V.15), (V.17) and (V.19) show the transient responses to those initial displacements. Also depicted is the result of intra-flexible modal coupling. For this control strategy, the disturbances in each of the flexible modes, for the initial conditions considered herein, are damped in 15 seconds while their effects on the attitude angles take almost 25 seconds to disappear (see Figure (V.12, (V.14), (V.16), and (V.18)). The effects of the coupling between the flexible and rigid rotational modes is best observed in Figure (V. 16) (roll response) when the system is initially excited in its third mode. The control effort required here is similar to that of Figures (V.6-V.11) described above.

V.3. Rigidized SCOLE Preliminary Slew Maneuvers

In this section, the equations governing the motion of the rigidized SCOLE, outside of the linear range, are developed from the most general rotational equations of motion previously derived. The control laws obtained from the application of the linear regulator theory to the linearized model of the rigidized SCOLE are tested for large amplitude manuevers. The closed loop system dynamics are numerically simulated. For single axis slew maneuvers about the roll, pitch, and yaw axes, respectively, the time responses for the Euler angles, the control efforts required of the reflector actuators, control torques demanded from the Shuttle's torquers, and the components of the total control moments, are depicted in the subsequent figures. This enables one to determine the margin left in which to optimize the control strategy without causing saturation of the controllers.

In the absence of flexibility in the system, Equation (III.18) becomes:

$$\vec{H}_{syst/G} = [\Omega_x I_{S1} - \Omega_z I_{S4} + \Omega_x \frac{L^2}{3} M + M_R(bL + cY) + \Omega_1 I_{R1}]\hat{i}$$

$$+ \{\Omega_y I_{S2} + \frac{ML^2}{3}\Omega_y - M_R(aL + cX) + \Omega_2 I_{R2}\}\hat{j}$$

$$+ \{\Omega_z I_{S3} - \Omega_x I_{S4} + M_R(bX - aY) + \Omega_3 I_{R3}\}\hat{k} \qquad (V.11)$$

where Ω_x, Ω_y, and Ω_z have been defined in Equation (III.3). In the absence of flexibility, $[T_{R \to R2}] = [I_3]$ which is equivalent to $T_{11} = T_{22} = T_{33} = 1.0$ and $T_{ij} = 0$, $i \neq j$.

Under these new assumptions

$$\Omega_1 = \Omega_x; \quad \Omega_2 = \Omega_y; \text{ and } \quad \Omega_3 = \Omega_z$$

$$a = -\Omega_y L - \Omega_z Y$$

$$b = \Omega_x L + \Omega_z X \quad \text{and}$$

$$c = \Omega_x Y - \Omega_y X$$

Therefore, Equation (V.11) can be rewritten as

$$\vec{H}_{syst/G} = \{\Omega_x(I_{S1}+I_{R1}+\frac{ML^2}{3} + M_R(L^2 + Y^2)) - \Omega_y M_R XY - \Omega_z(I_{S4}+M_R XL)\}\hat{i}$$

$$+ \{\Omega_y(I_{S2}+\frac{ML^2}{3} + I_{R2} + M_R(L^2+X^2)) - \Omega_x M_R XY + \Omega_z M_R YL\}\hat{j}$$

$$+ \{\Omega_z (I_{S3}+I_{R3}+M_R(X^2+Y^2) + \Omega_x M_R XL + \Omega_y M_R YL\}\hat{k} = 0 \qquad (V.12)$$

which can again be recast as:

$$\vec{H}_{syst/G} = H_x \hat{i} + H_y \hat{j} + H_z \hat{k} \qquad (V.13)$$

The equations governing the motion of the rigidized SCOLE system during large amplitude maneuvers in the presence of gravity gradient and control torques are obtained as:

i) <u>The Roll Equation</u>

$$\dot{H}_x + \Omega_y H_z - \Omega_z H_y = T_x \qquad (V.14)$$

ii) <u>The Pitch Equation</u>

$$\dot{H}_y + \Omega_z H_x - \Omega_x H_z = T_y \qquad (V.15)$$

iii) <u>The Yaw Equation</u>

$$\dot{H}_z + \Omega_x H_y - \Omega_y H_x = T_z \qquad (V.16)$$

where T_x, T_y, and T_z are the components of the external torques acting on the system (including the control torques previously derived for the linear model of the rigidized SCOLE where the feedback now depends on the

original Euler angles and their rates for maneuvers made relative to the Shuttle roll, pitch, and yaw axes).

The closed-loop system dynamics described by Equations (V.14), (V.15), and (V.16) have been numerically simulated and the results are shown in Figures (V.20) to (V.32).

Figures (V.20), (V.25), and (V.29) show the time responses to an initial 20° alignment in roll, pitch, and yaw degrees of freedom, respectively. It is seen that a 20 slew about the roll axis can be achieved in about 30 seconds. The same amplitude maneuver about the pitch and yaw take 45 and 100 seconds, respectively. This is due to:

1. the system inertia distribution
2. with equal amounts of torques available in the Shuttle for each maneuver, the roll and yaw maneuvers benefit more from the actuators located on the reflector for which the length of the beam is then a moment arm.

For this control strategy, each of the single axis slew maneuvers about the roll and pitch axes used 85-90% of the control forces available from the corresponding

actuator located on the reflector, and 80% and 60%, respectively, of the control torque available from the corresponding Shuttle torquer. None of the controllers reach saturation. The control strategy which has been designed so as to avoid an excessive use of the actuator forces, relies mainly on the Shuttle's "z" torquer to slew about the yaw axis. It is seen for this maneuver (Figure V.31), that the corresponding Shuttle torquer is used at 99% of its maximum capacity. Also depicted in the Figures (V.24), (V.28) and (V.32) are the components of the total control moments for each case (moments of the reflector control forces taken about the Shuttle's mass center, plus moments of the Shuttle's torquers). This will make possible a comparison between this strategy and other future control laws which would be based on the two point boundary-value problem, where this or combinations of control inputs may be employed.

In conclusion, it is seen that a control strategy derived from the linearized model of the rigidized SCOLE, based on the linear regulator theory, works well when it is used for single axis slew maneuvers through amplitude angles as large as 20^{o}.

RIGIDIZED SCOLE

FIGURE V.1 REAL PART OF LEAST DAMPED MODE VS. [R]

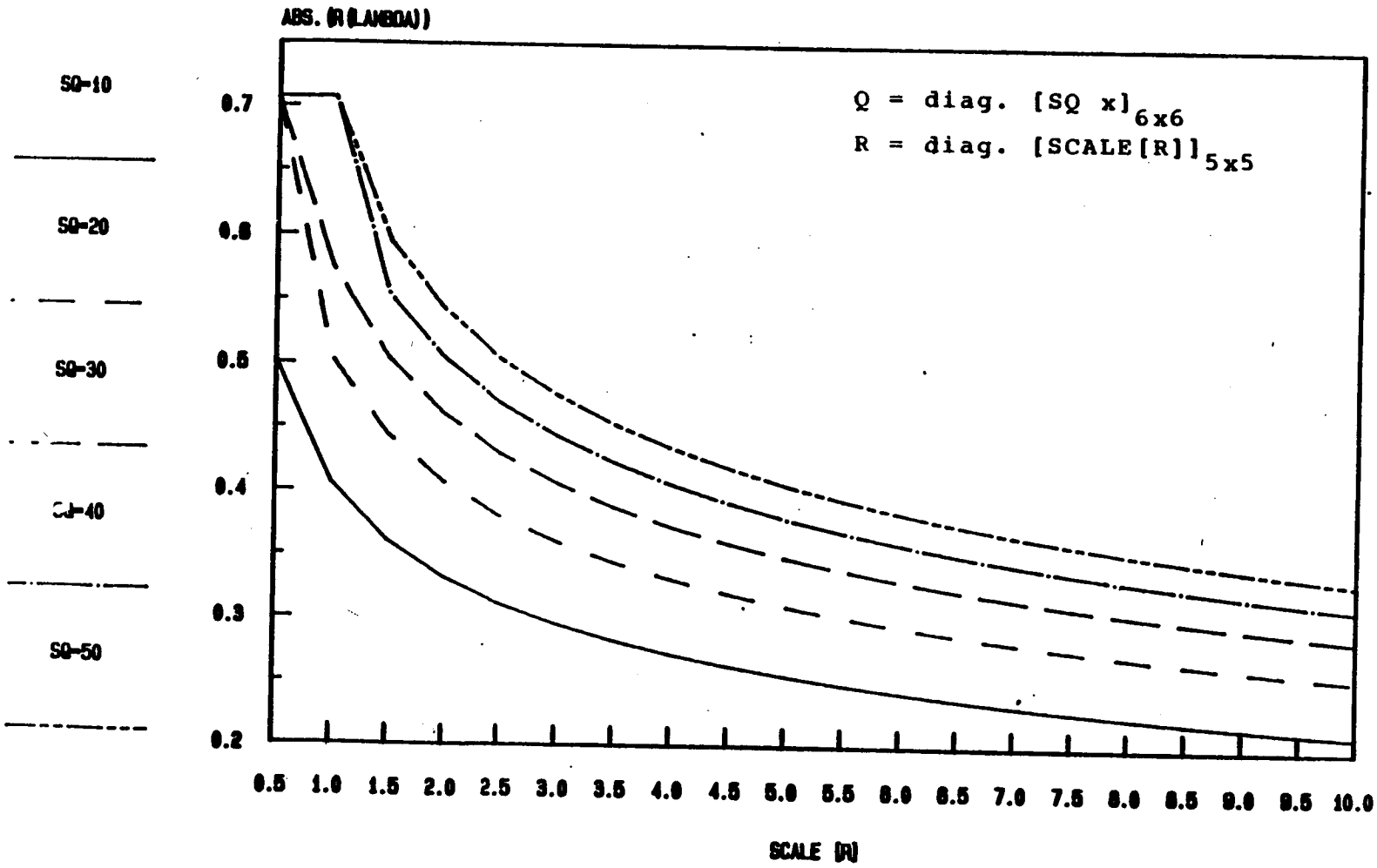

FLEXIBLE SCOLE

FIGURE V.2 REAL PART OF LEAST DAMPED MODE VS. [R]

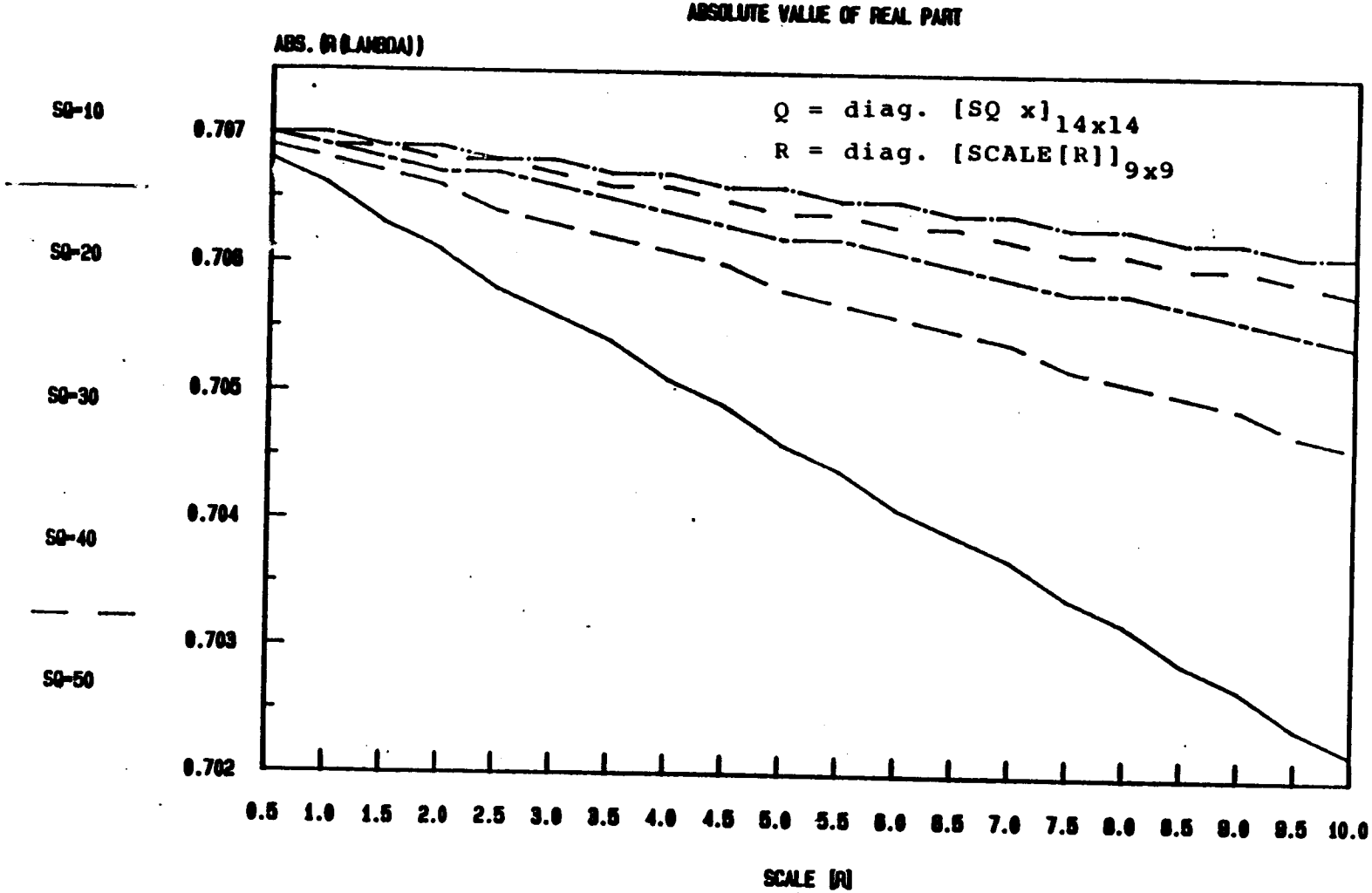

FIGURE V.3 SCOLE: TRANSIENT RESPONSES

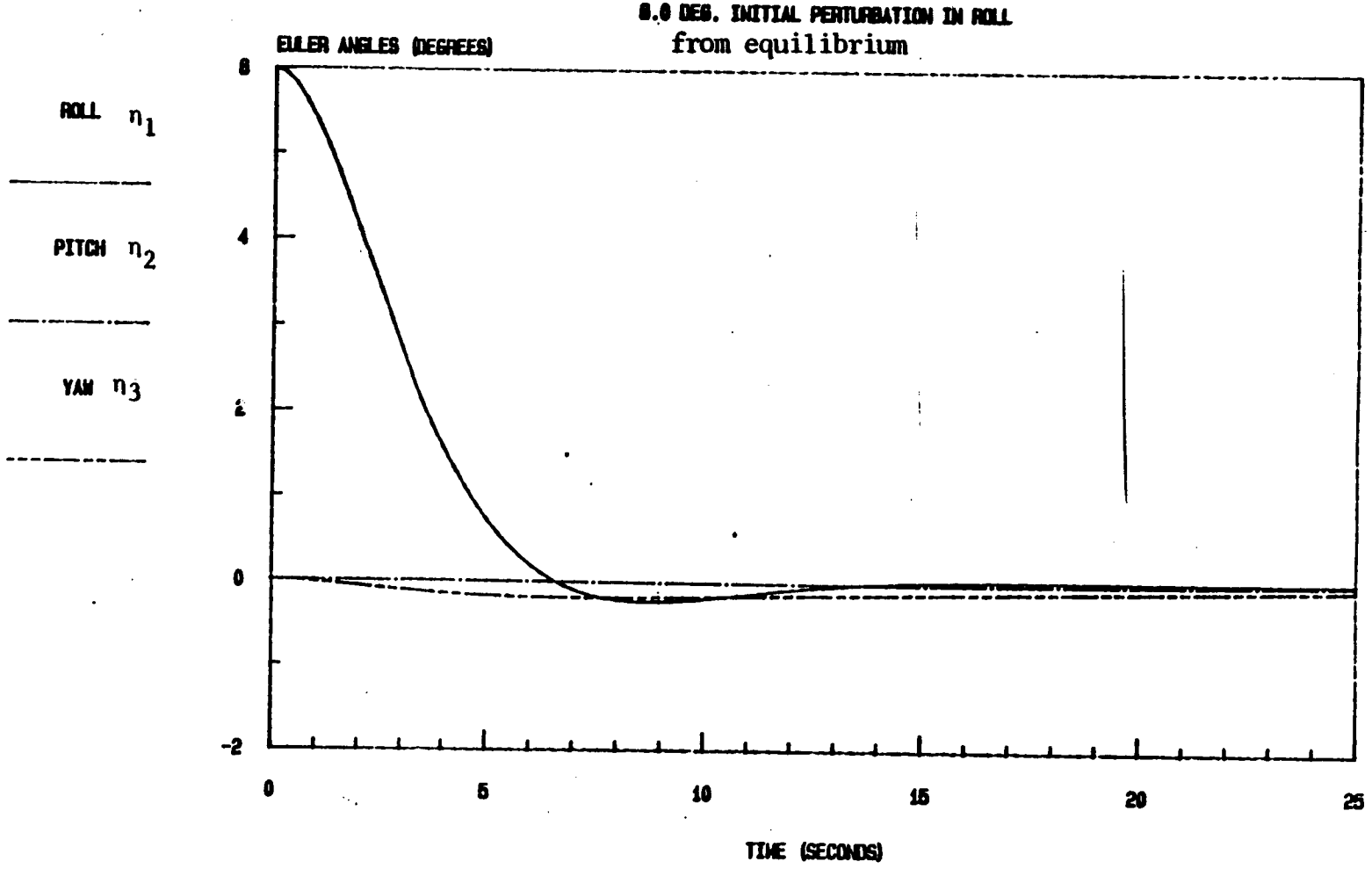

FIGURE V.3a

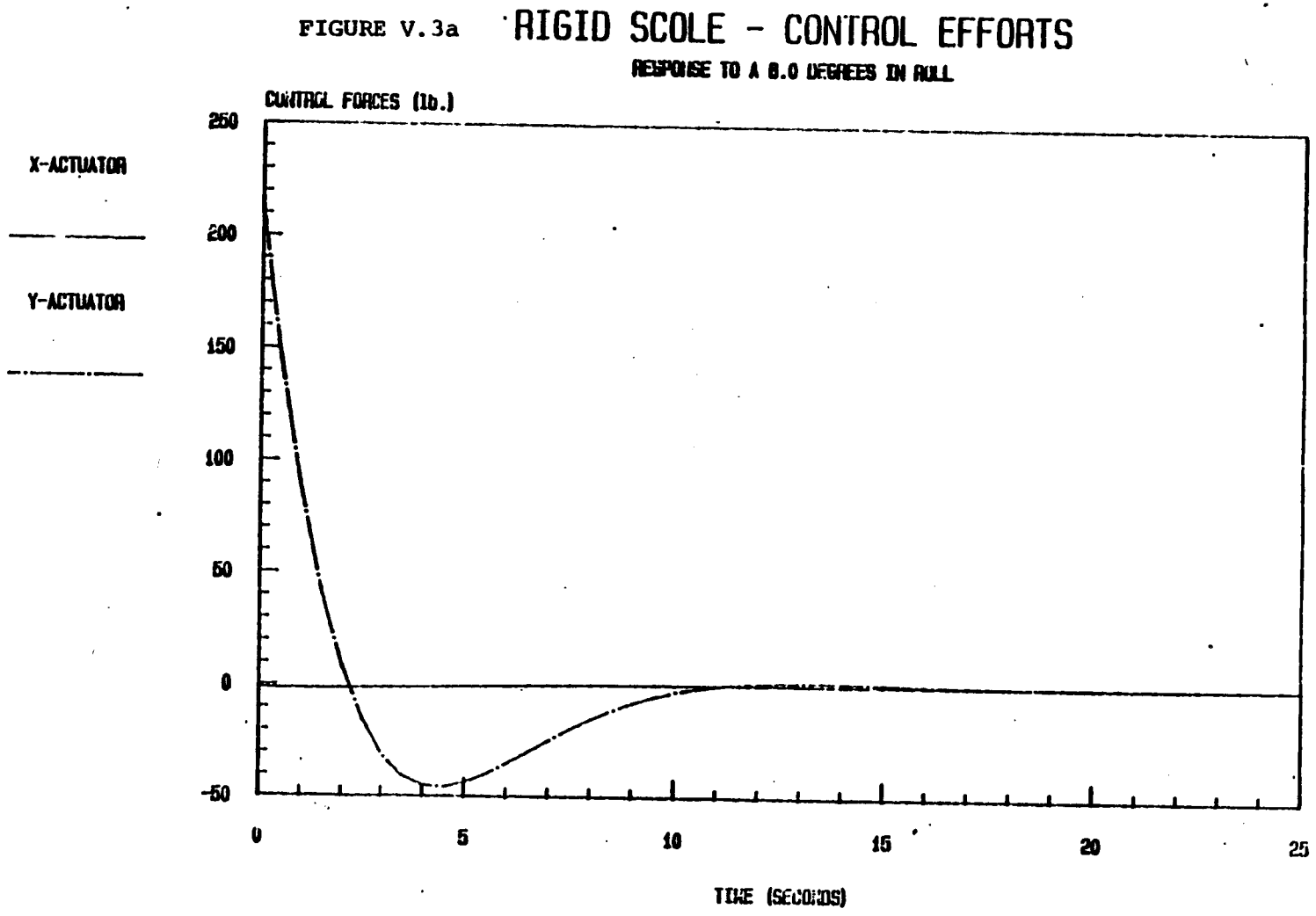
RIGID SCOLE - CONTROL EFFORTS
RESPONSE TO A 8.0 DEGREES IN ROLL
CONTROL FORCES (lb.)
X-ACTUATOR
Y-ACTUATOR
250
200
150
100
50
0
-50
0
5
10
15
20
25
TIME (SECONDS)

FIGURE V.3b

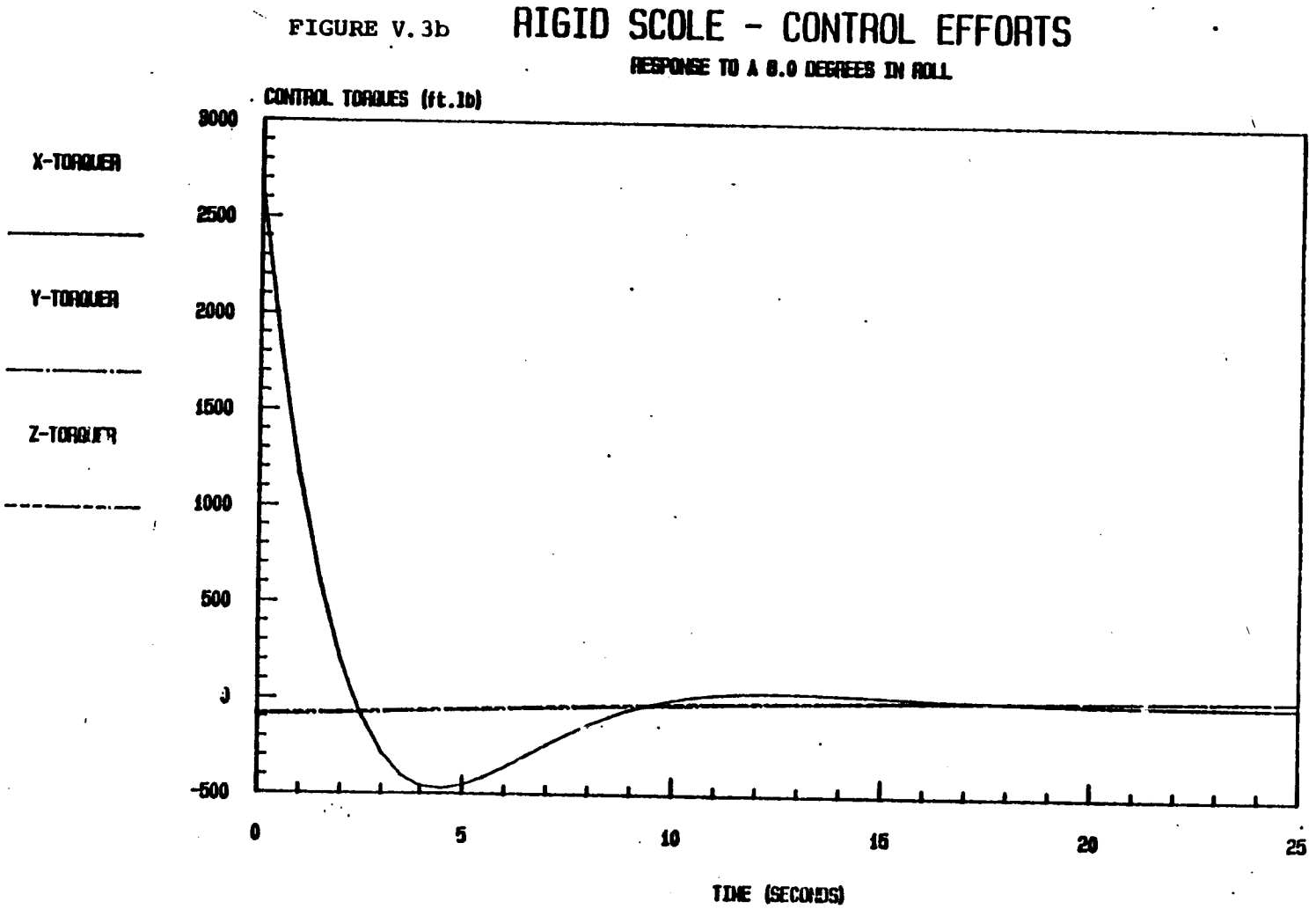
RIGID SCOLE - CONTROL EFFORTS
RESPONSE TO A 8.0 DEGREES IN ROLL
CONTROL TORQUES (ft.lb)
X-TORQUER
Y-TORQUER
Z-TORQUER
3000
2500
2000
1500
1000
500
0
-500
0
5
10
15
20
25
TIME (SECONDS)

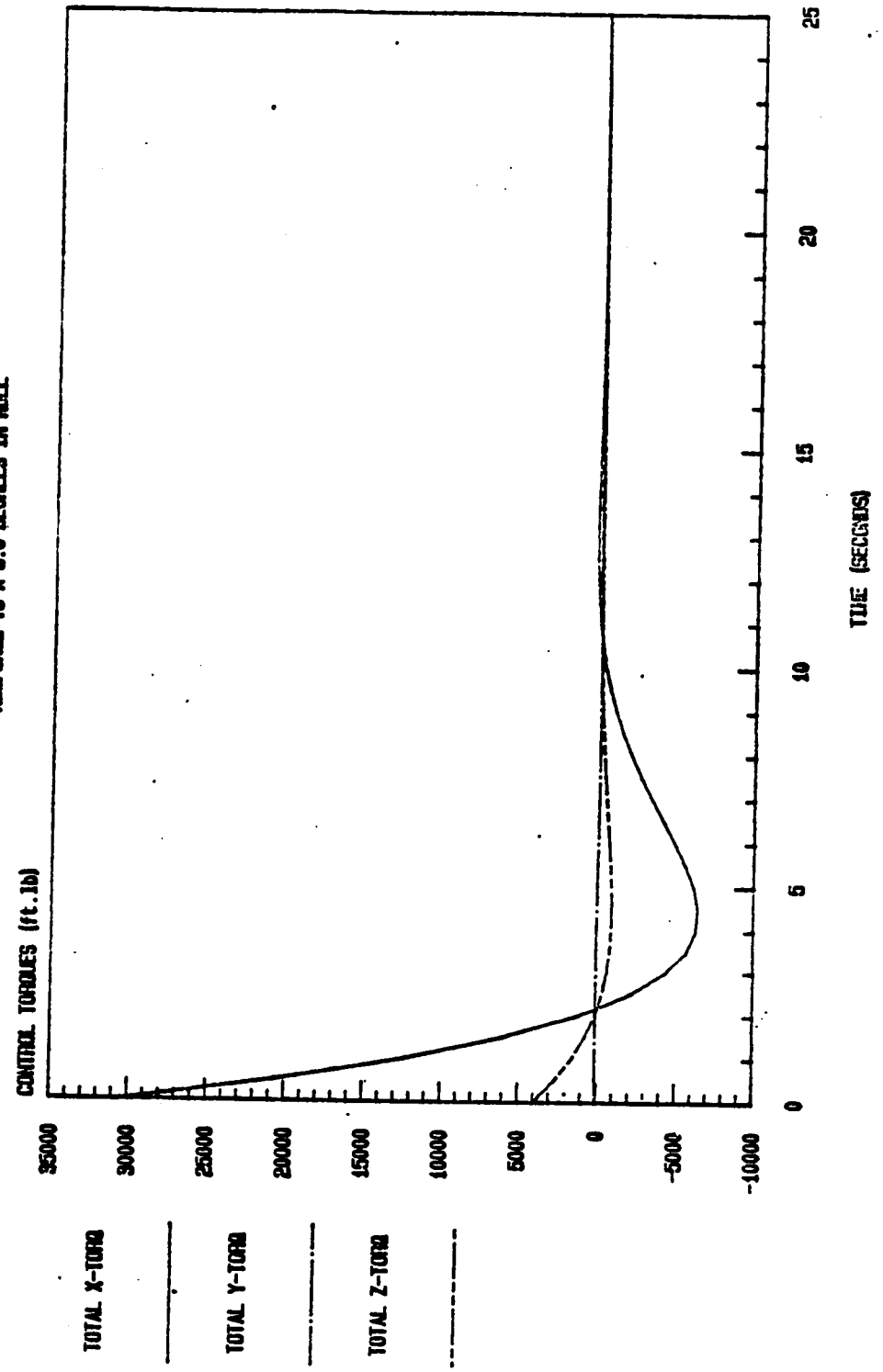
RIGID SCOLE - CONTROL EFFORTS
RESPONSE TO A 6.0 DEGREES IN ROLL
CONTROL TORQUES (ft.lb)
35000
30000
25000
20000
15000
10000
5000
0
-5000
-10000
0
5
10
15
20
25
TIME (SECONDS)
TOTAL X-TORQ
TOTAL Y-TORQ
TOTAL Z-TORQ

FIGURE V.3c

FIGURE V.4 SCOLE: TRANSIENT RESPONSES

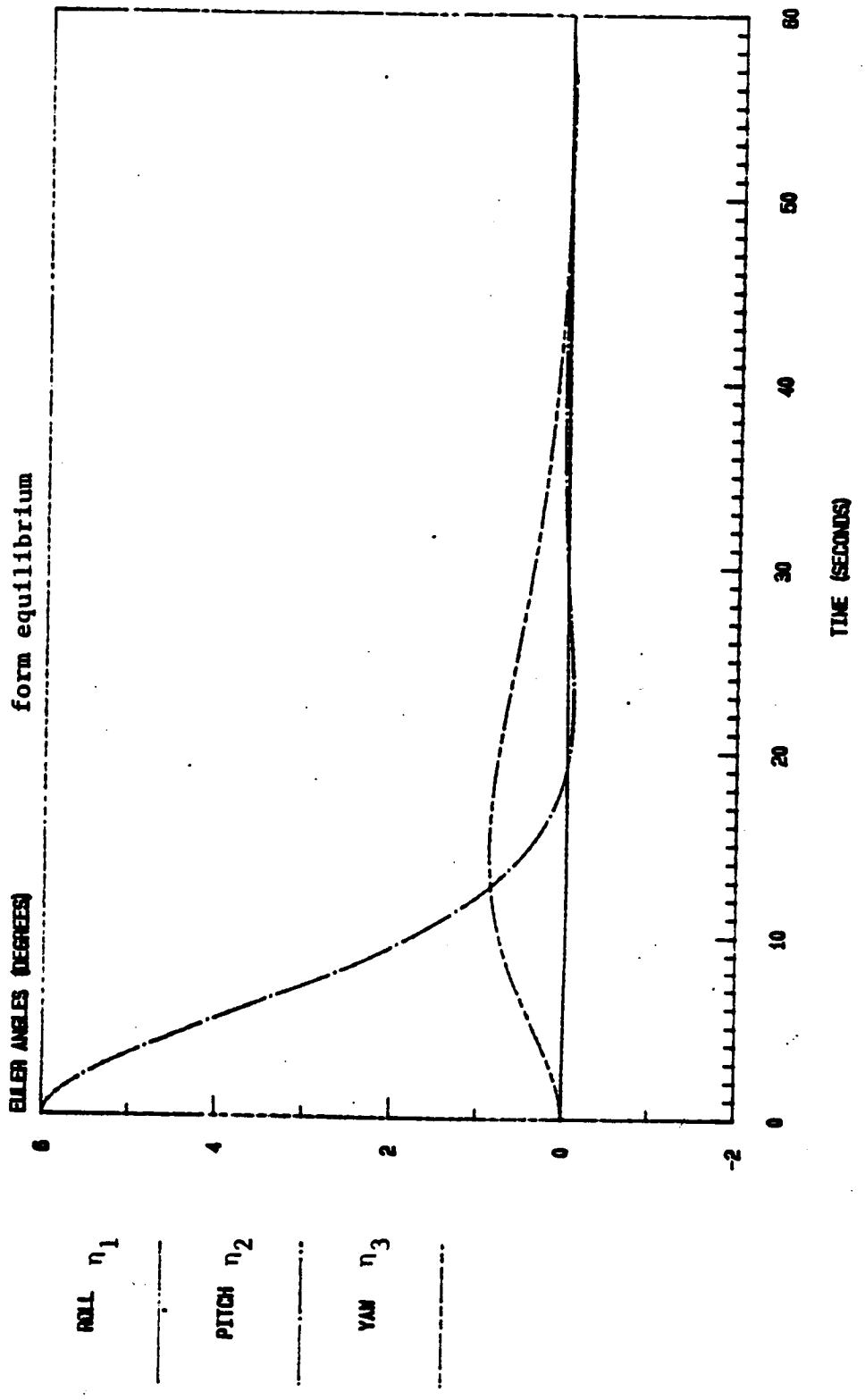

FIGURE V.5 SCOLE: TRANSIENT RESPONSES

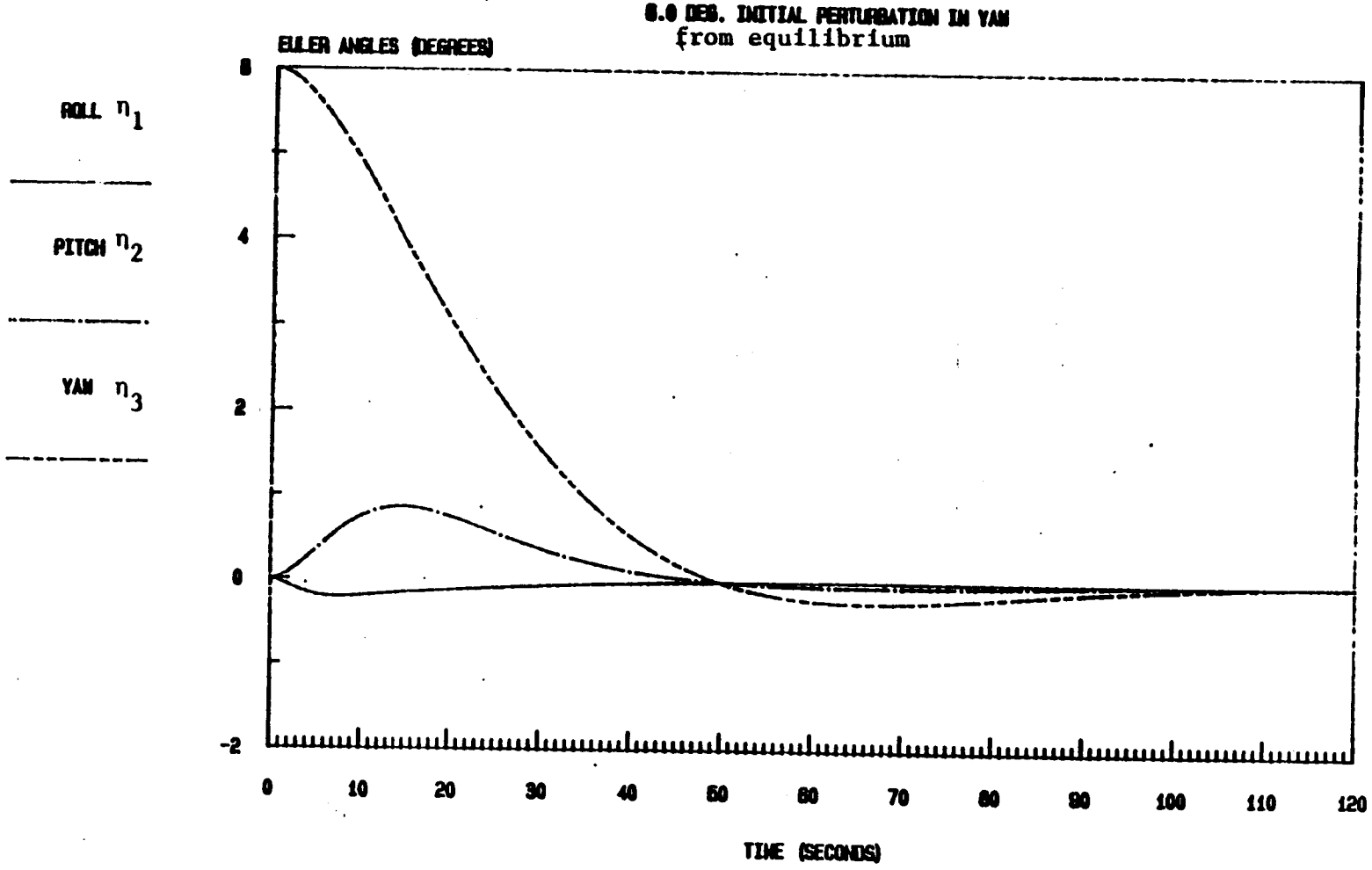

ORIGINAL PAGE IS
OF POOR QUALITY

FIGURE V.6 LINEAR MODEL OF SCOLE WITH FLEXIBILITY

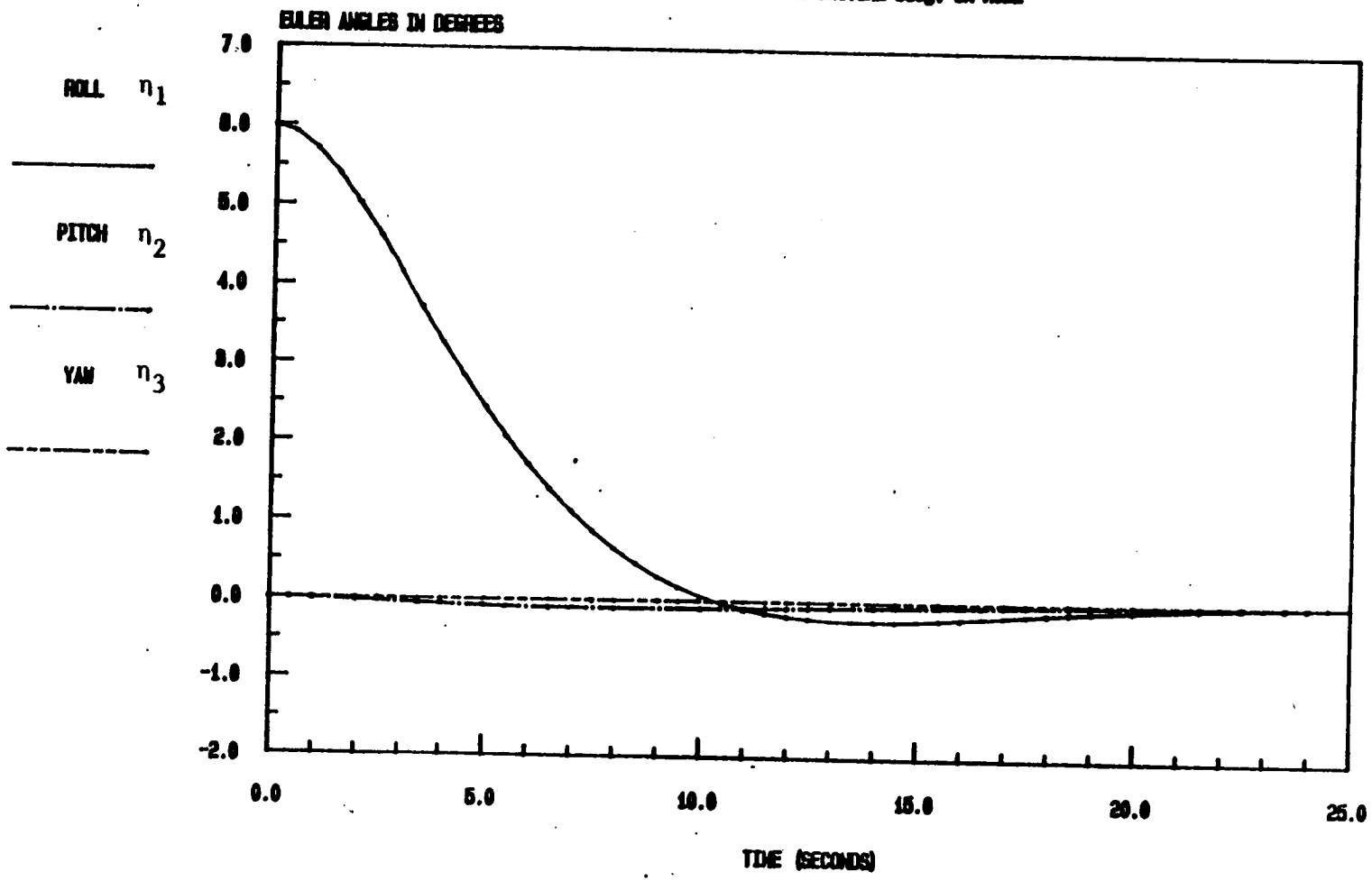

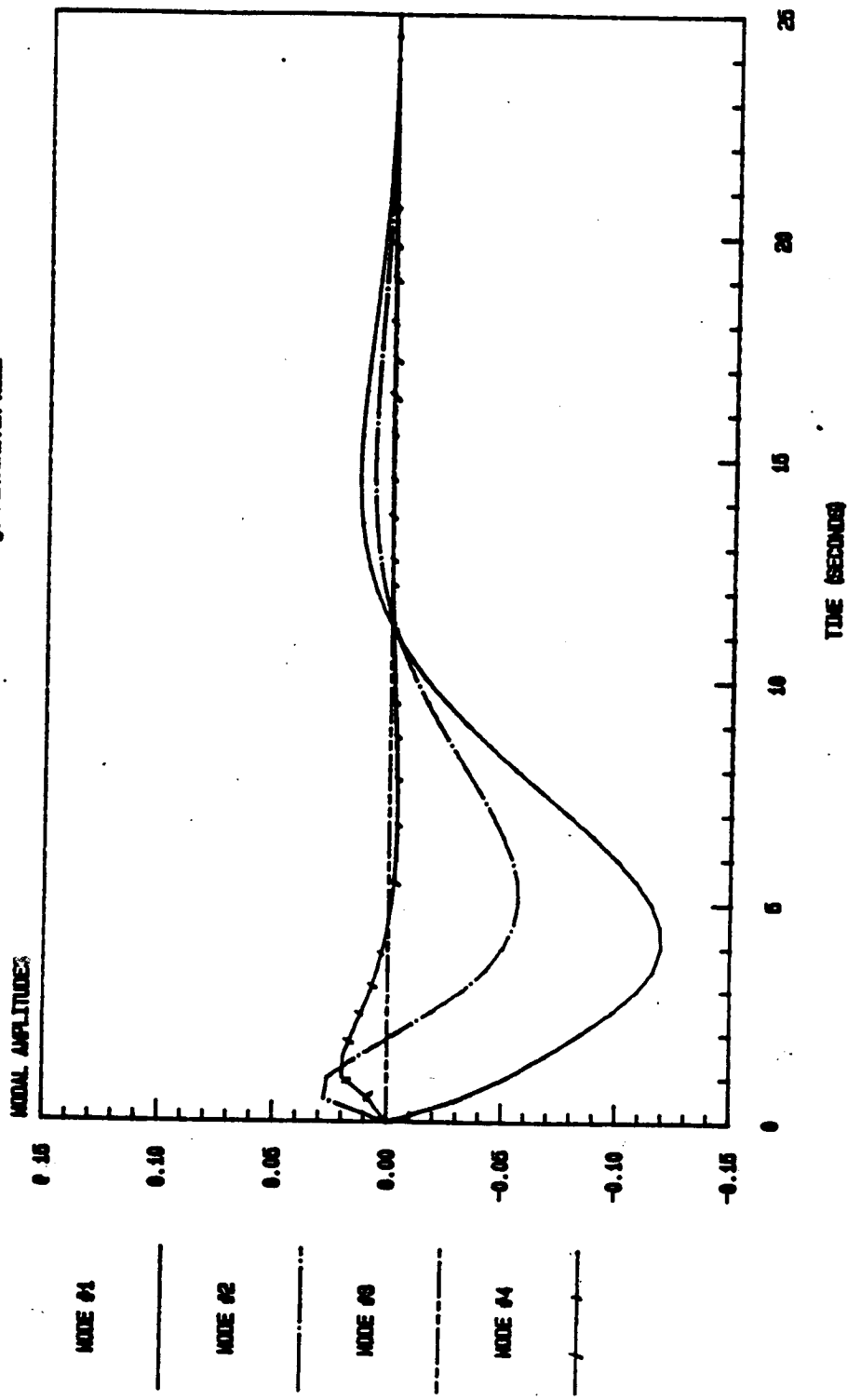
LINEAR MODEL OF SCOLE WITH FLEXIBILITY
TRANS. RESP. TO A 5deg. PERTURB.IN ROLL
MODAL AMPLITUDES
0.15
0.10
0.05
0.00
-0.05
-0.10
-0.15
0
5
10
15
20
25
TIME (SECONDS)
MODE #1
MODE #2
MODE #3
MODE #4

FIGURE V.7

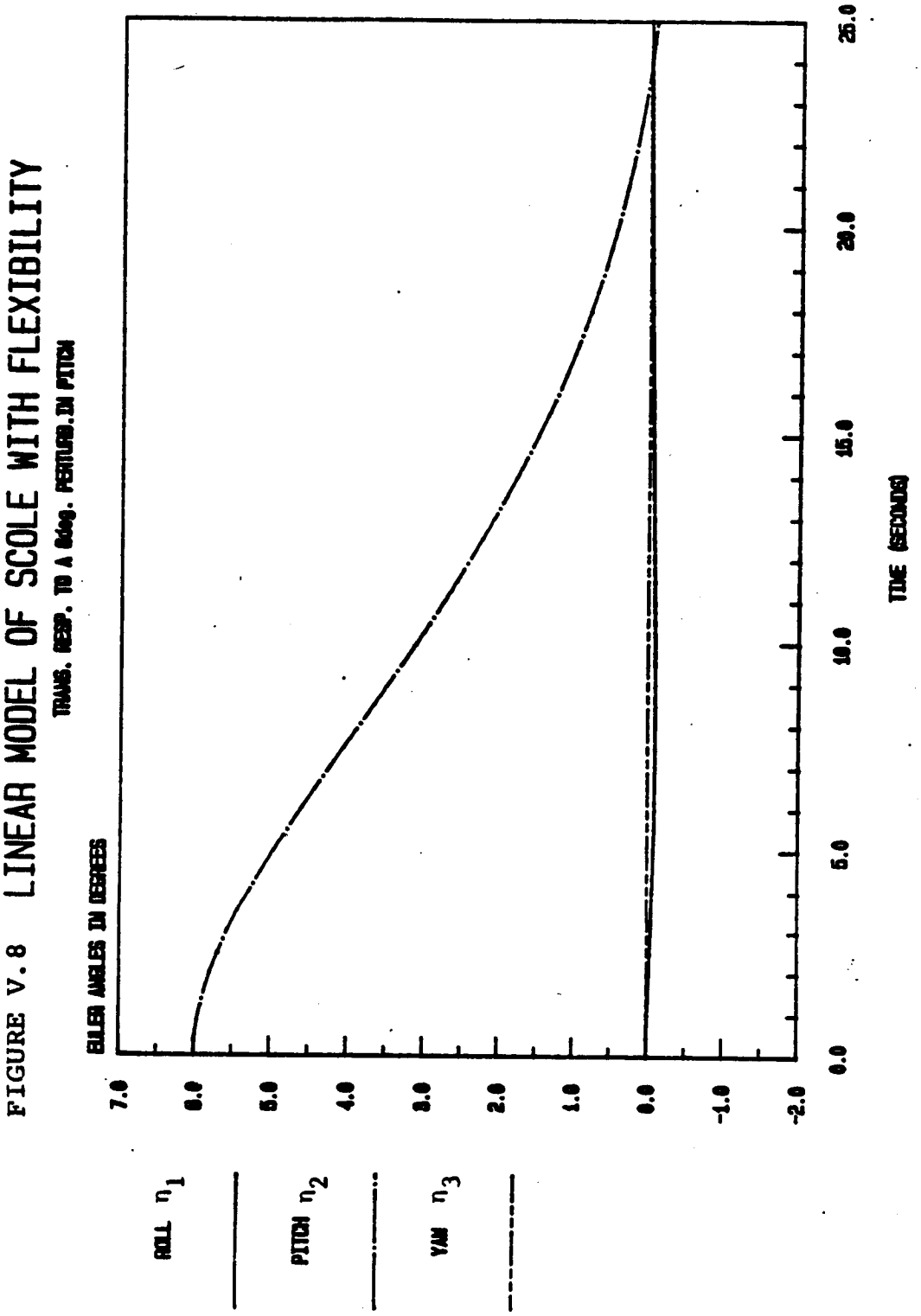
LINEAR MODEL OF SCOLE WITH FLEXIBILITY
TRANS. RESP. TO A 5deg. PERTURB. IN PITCH
EULER ANGLES IN DEGREES
7.0
6.0
5.0
4.0
3.0
2.0
1.0
0.0
-1.0
-2.0
0.0
5.0
10.0
15.0
20.0
25.0
TIME (SECONDS)
ROLL η_1
PITCH η_2
YAW η_3

FIGURE V.8

FIGURE V.9 LINEAR MODEL OF SCOLE WITH FLEXIBILITY

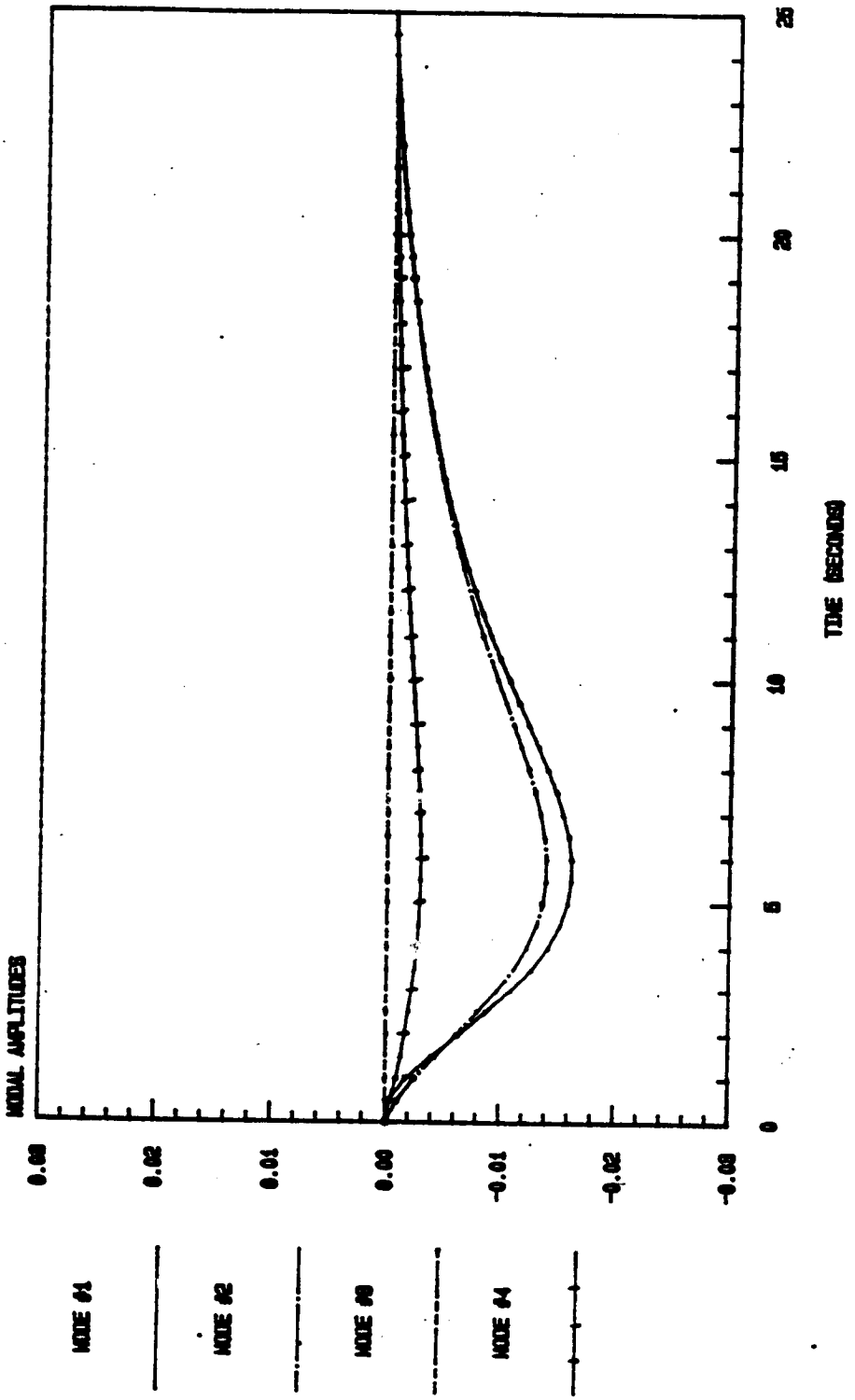

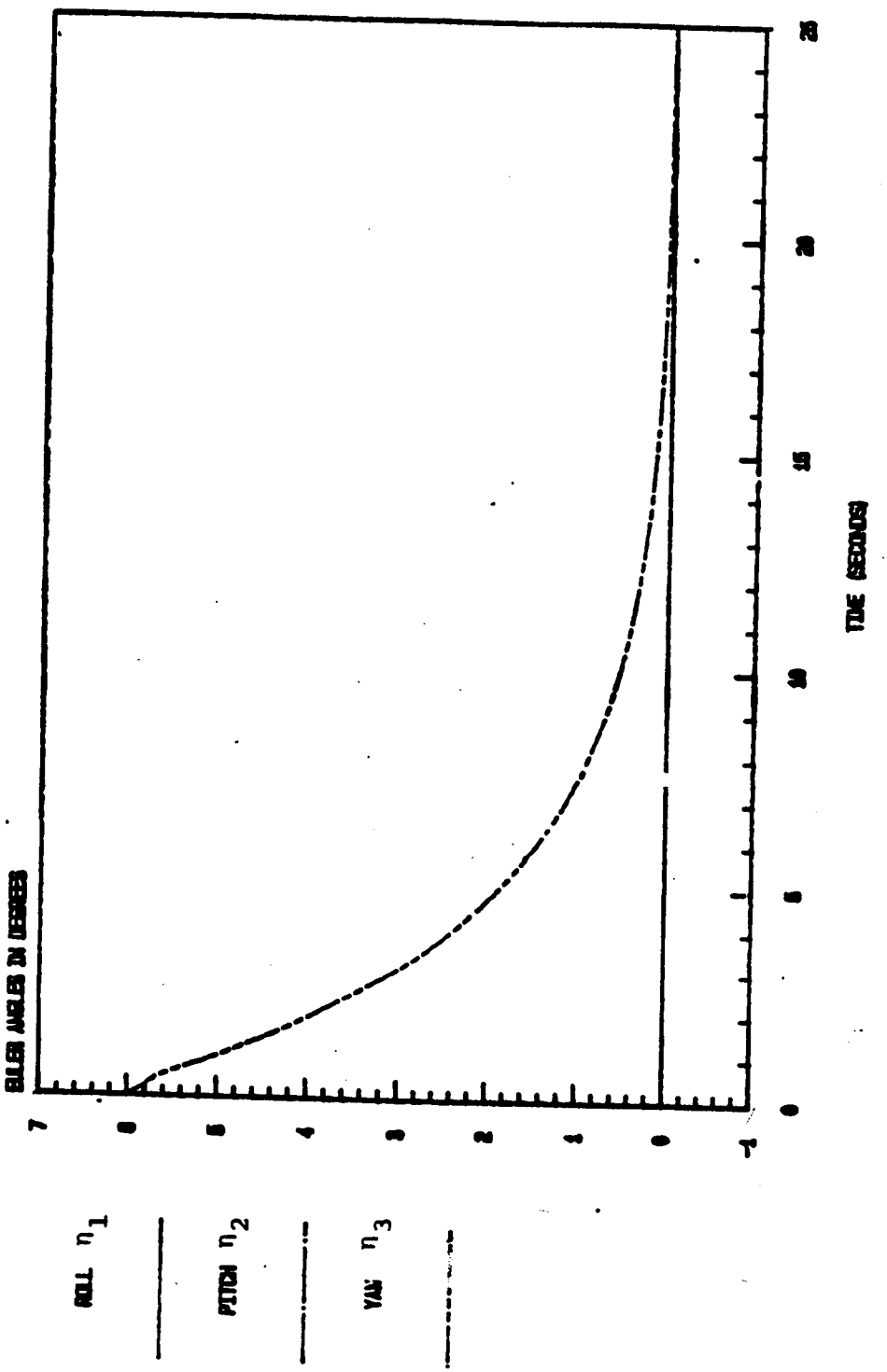

FIGURE V.10:

ORIGINAL PAGE IS
OF POOR QUALITY

ORIGINAL PAGE IS
OF POOR QUALITY

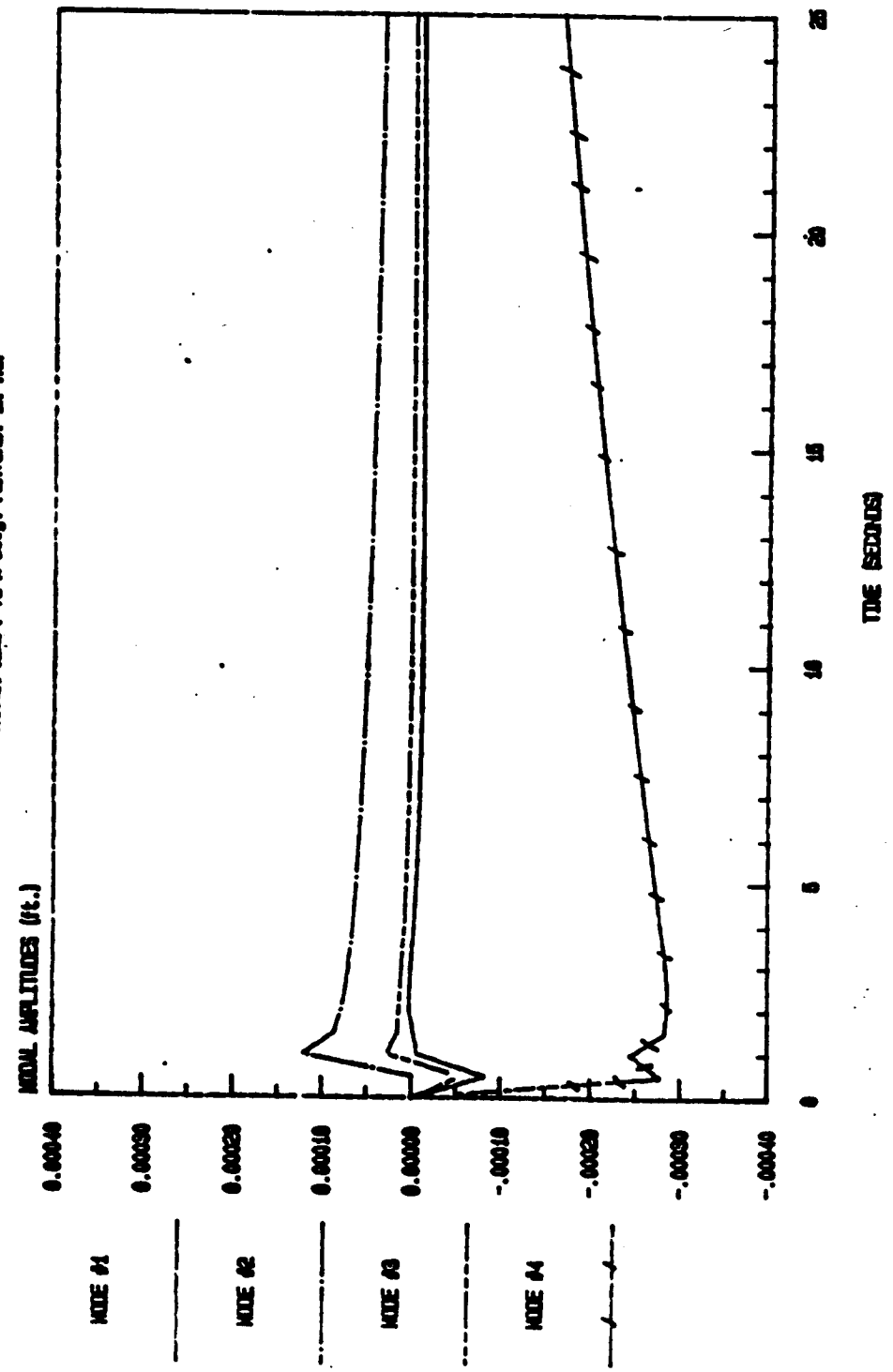

FIGURE V.11:

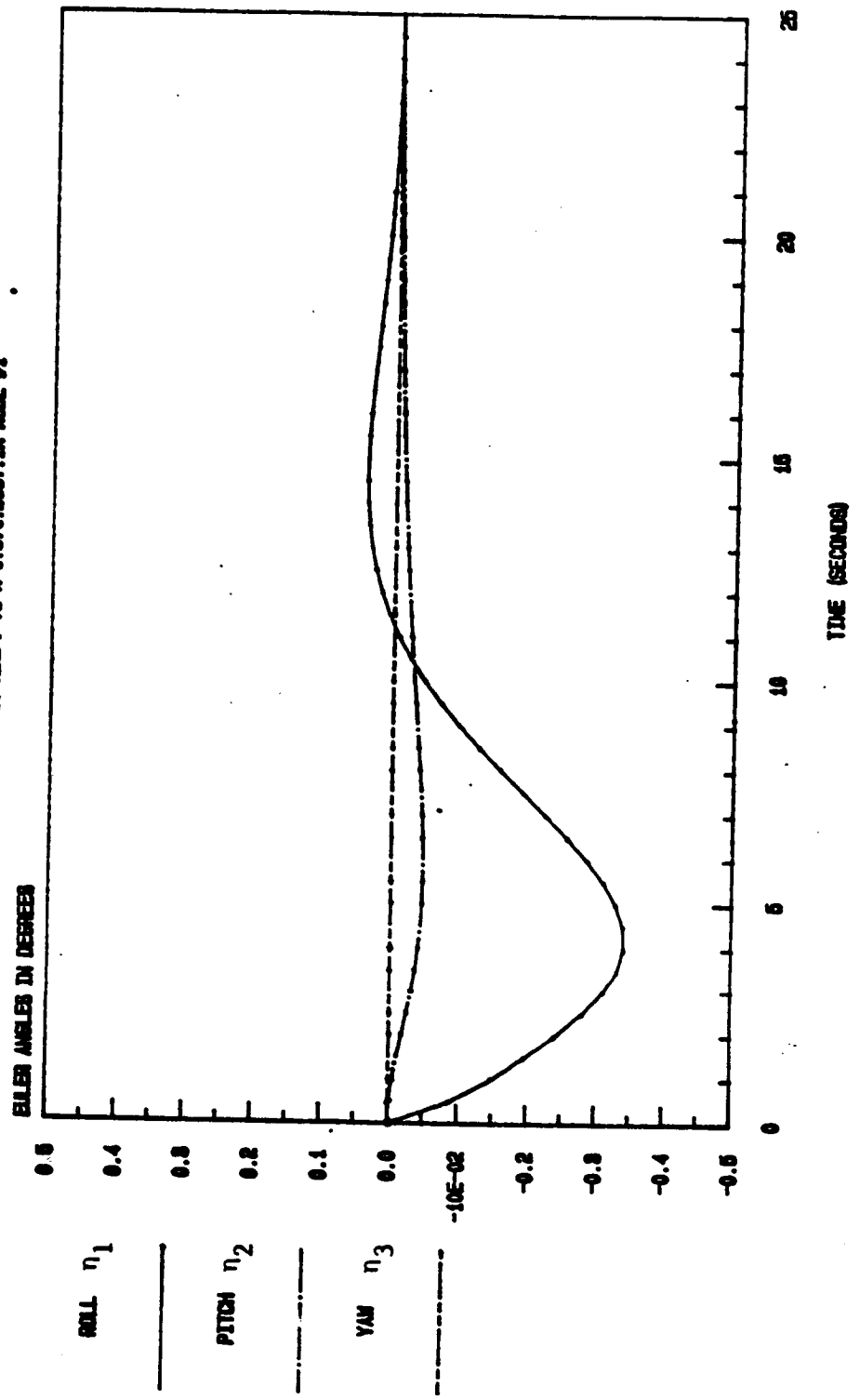

FIGURE V.12:

ORIGINAL PAGE IS
OF POOR QUALITY

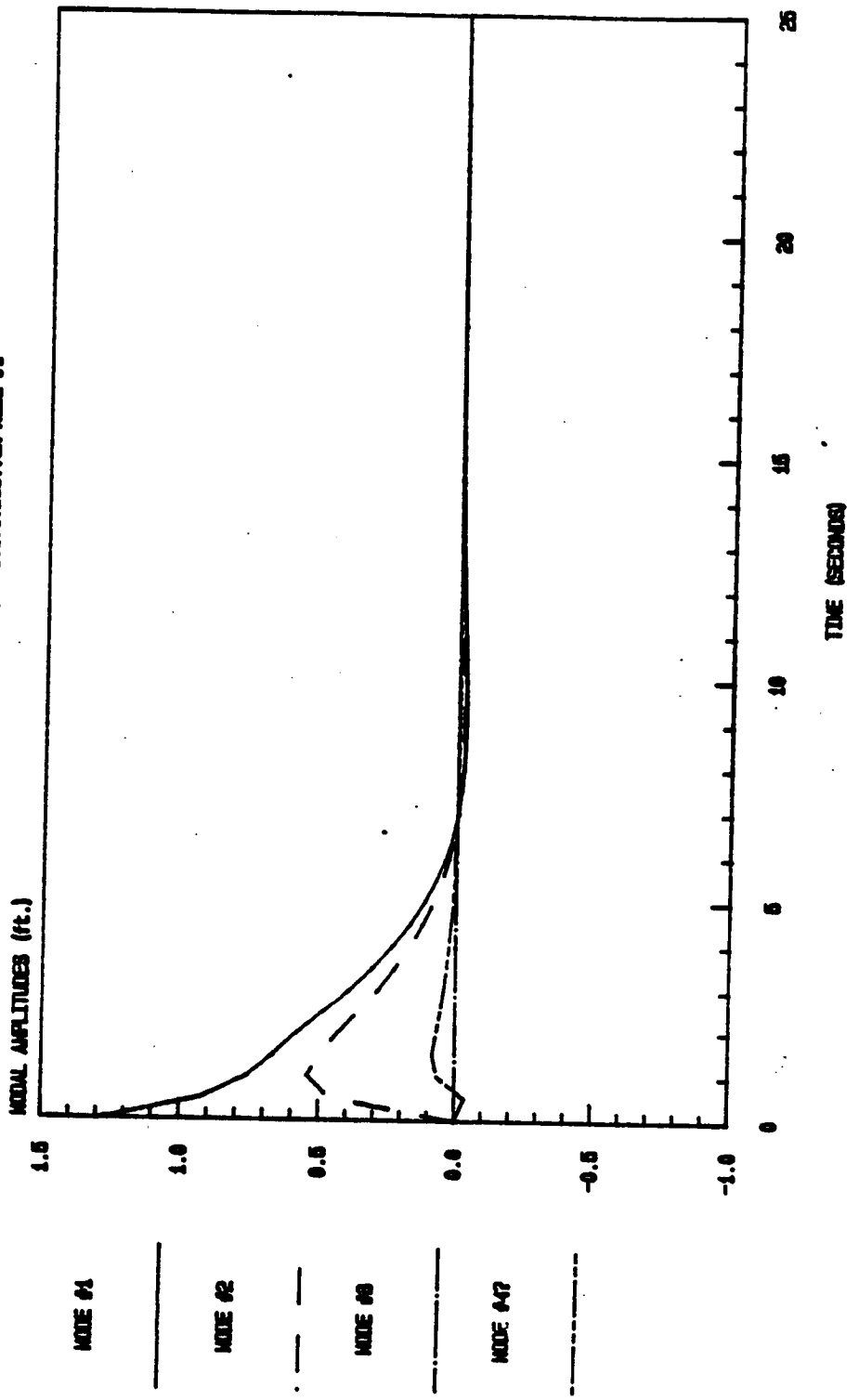
LINEAR MODEL OF SCOLE WITH FLEXIBILITY
TRANS. RESP. TO A 1.0ft. DIST. IN MODE #1
MODAL AMPLITUDES (ft.)
1.5
1.0
0.5
0.0
-0.5
-1.0
0
5
10
15
20
25
TIME (SECONDS)
MODE #1
MODE #2
MODE #3
MODE #47

FIGURE V.13

FIGURE V.14 LINEAR MODEL OF SCOLE WITH FLEXIBILITY

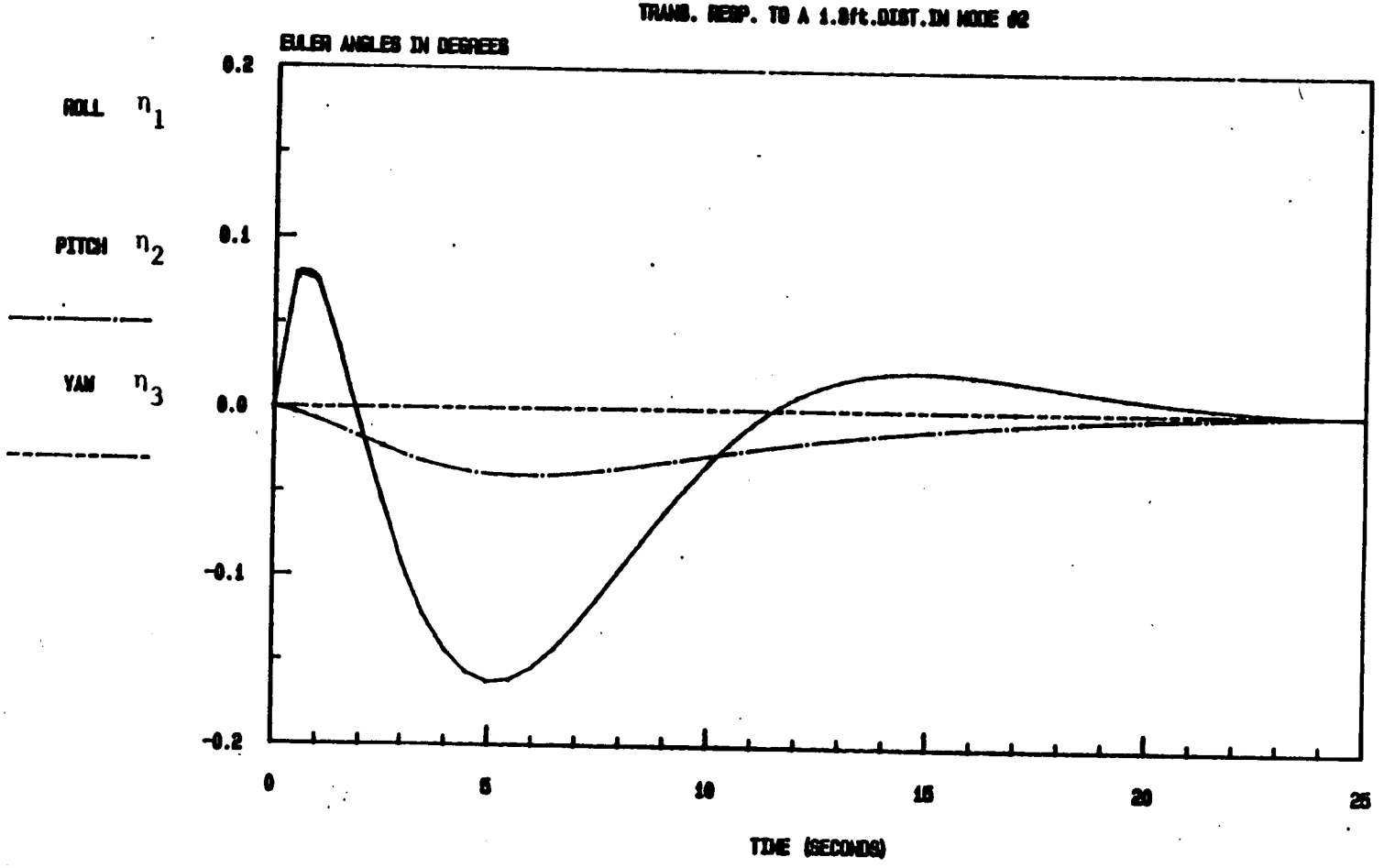

ORIGINAL PAGE IS
OF POOR QUALITY

FIGURE V.15 LINEAR MODEL OF SCOLE WITH FLEXIBILITY

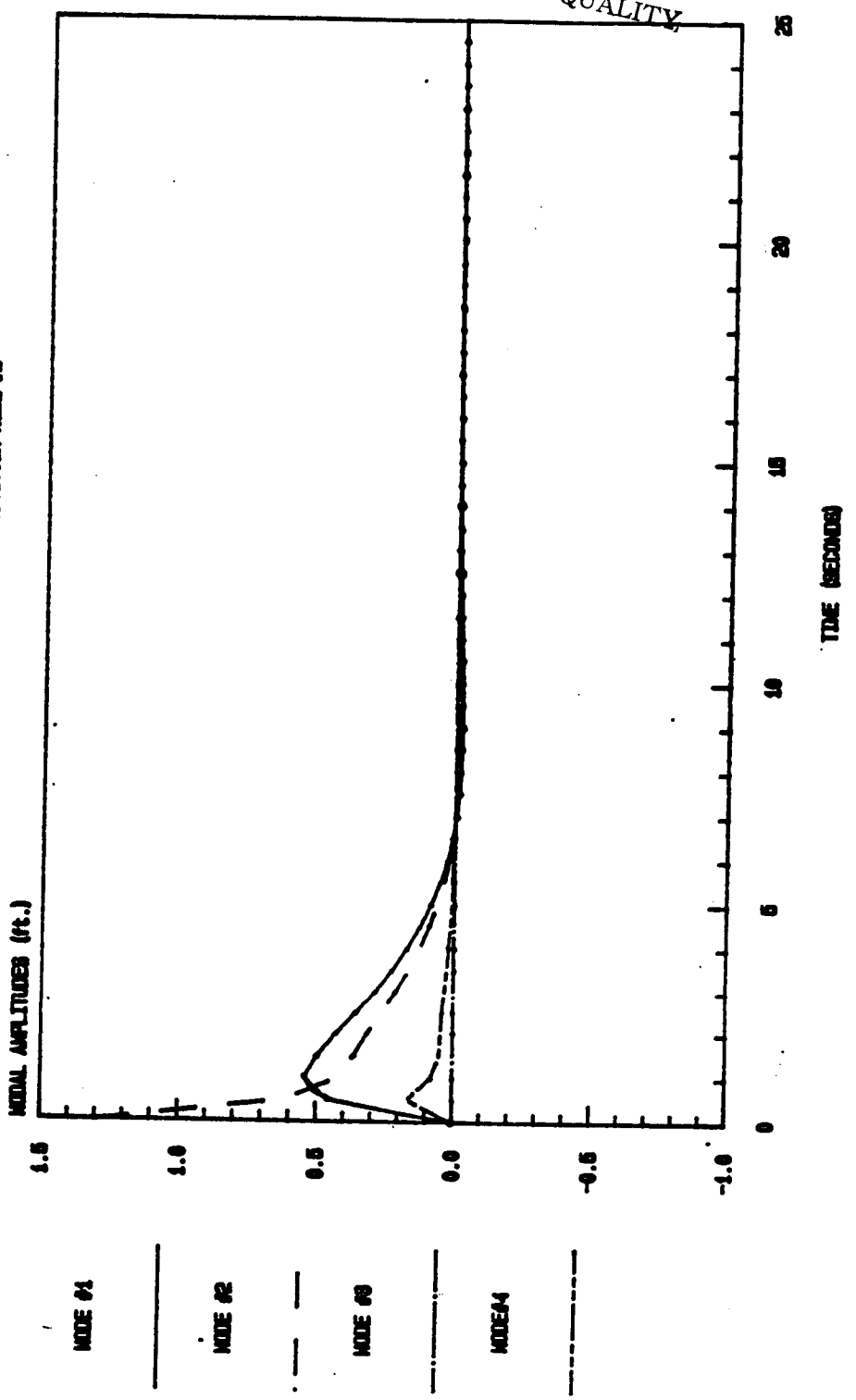

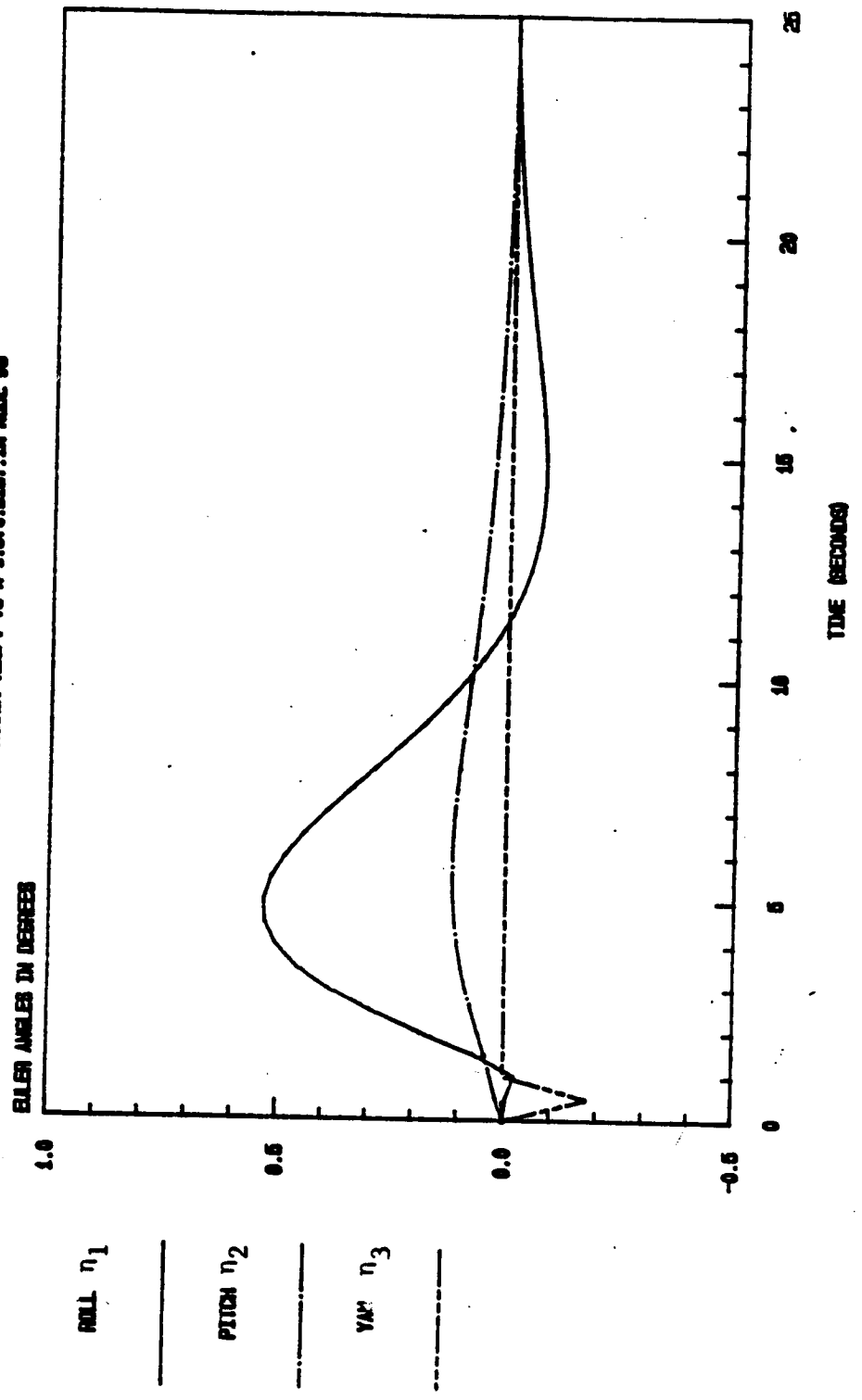
LINEAR MODEL OF SCOLE WITH FLEXIBILITY
TRANS. RESP. TO A 1.0Ft.DIST.IN MODE #8
EULER ANGLES IN DEGREES
1.0
0.5
0.0
-0.5
0
5
10
15
20
25
TIME (SECONDS)
ROLL η_1
PITCH η_2
YAW η_3

FIGURE V.16

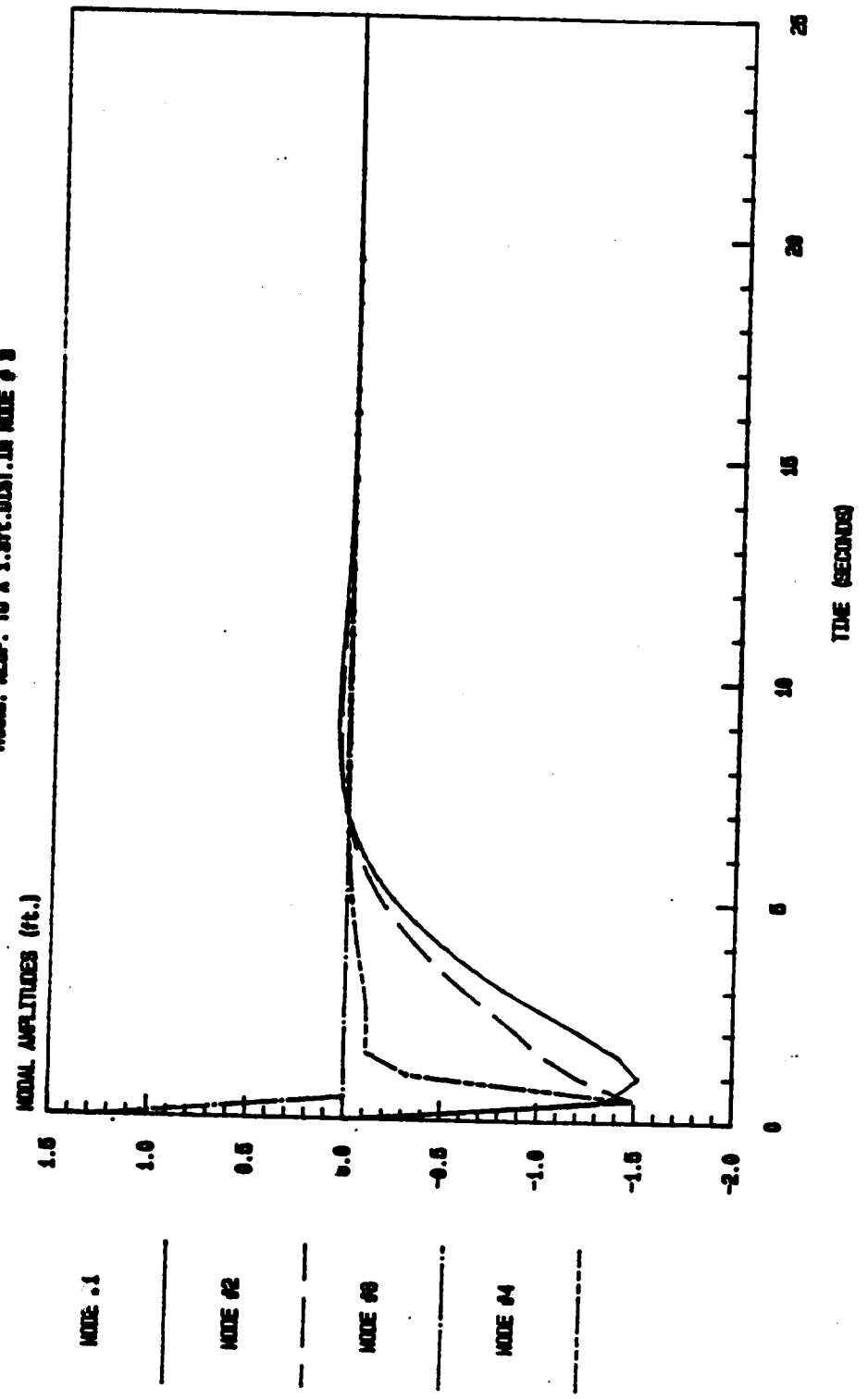
LINEAR MODEL OF SCOLE WITH FLEXIBILITY
TRANS. RESP. TO A 1.0ft. GUST ON MODE # 3
MODAL AMPLITUDES (ft.)
1.5
1.0
0.5
0.0
-0.5
-1.0
-1.5
-2.0
0
5
10
15
20
25
TIME (SECONDS)
MODE #1
MODE #2
MODE #3
MODE #4

FIGURE V.17

FIGURE V.18 LINEAR MODEL OF SCOLE WITH FLEXIBILITY

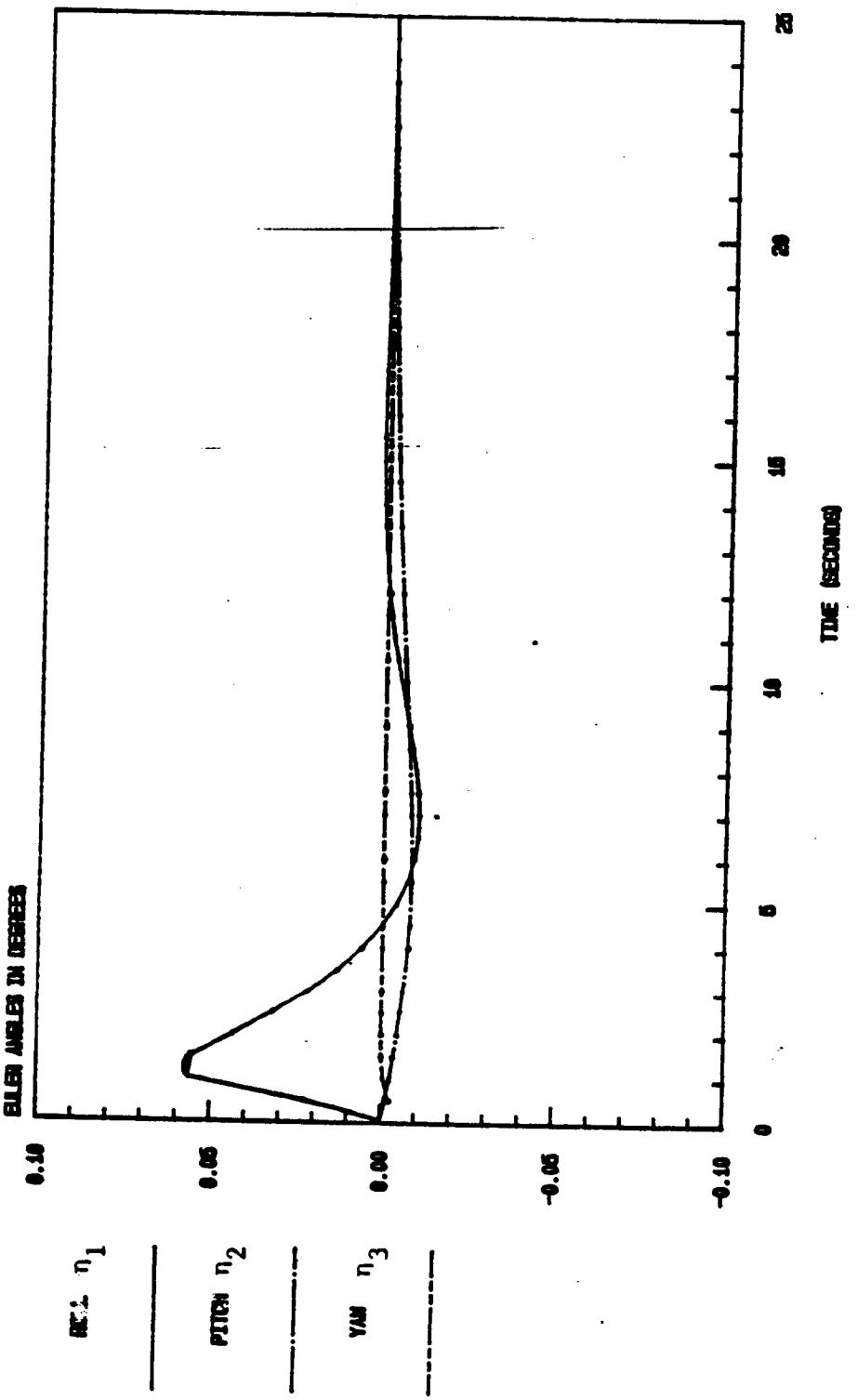

FIGURE V.19 LINEAR MODEL OF SCOLE WITH FLEXIBILITY

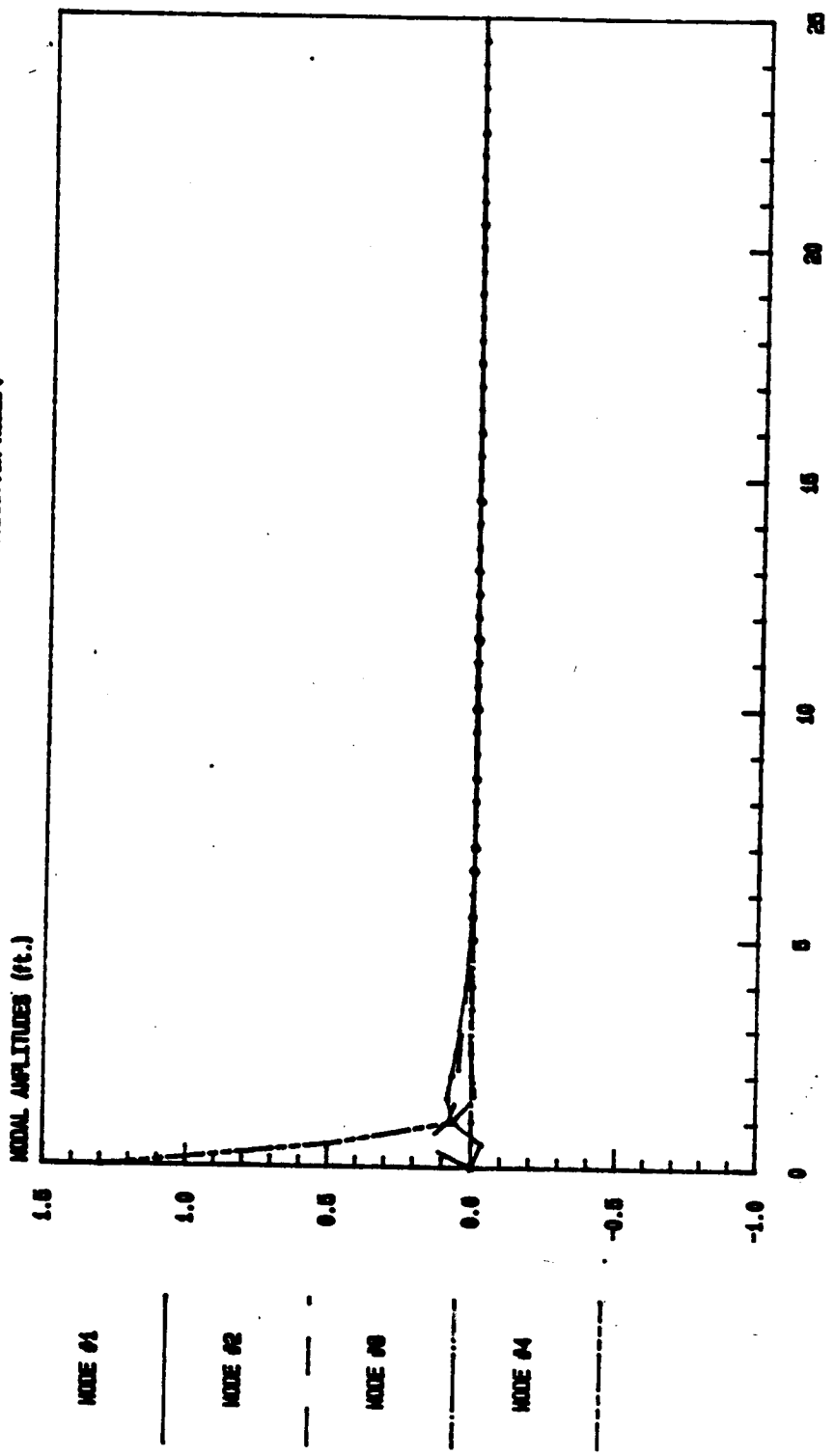

FIGURE V.20 SCOLE: PRELIMINARY SLEW (RIGID SCOLE)

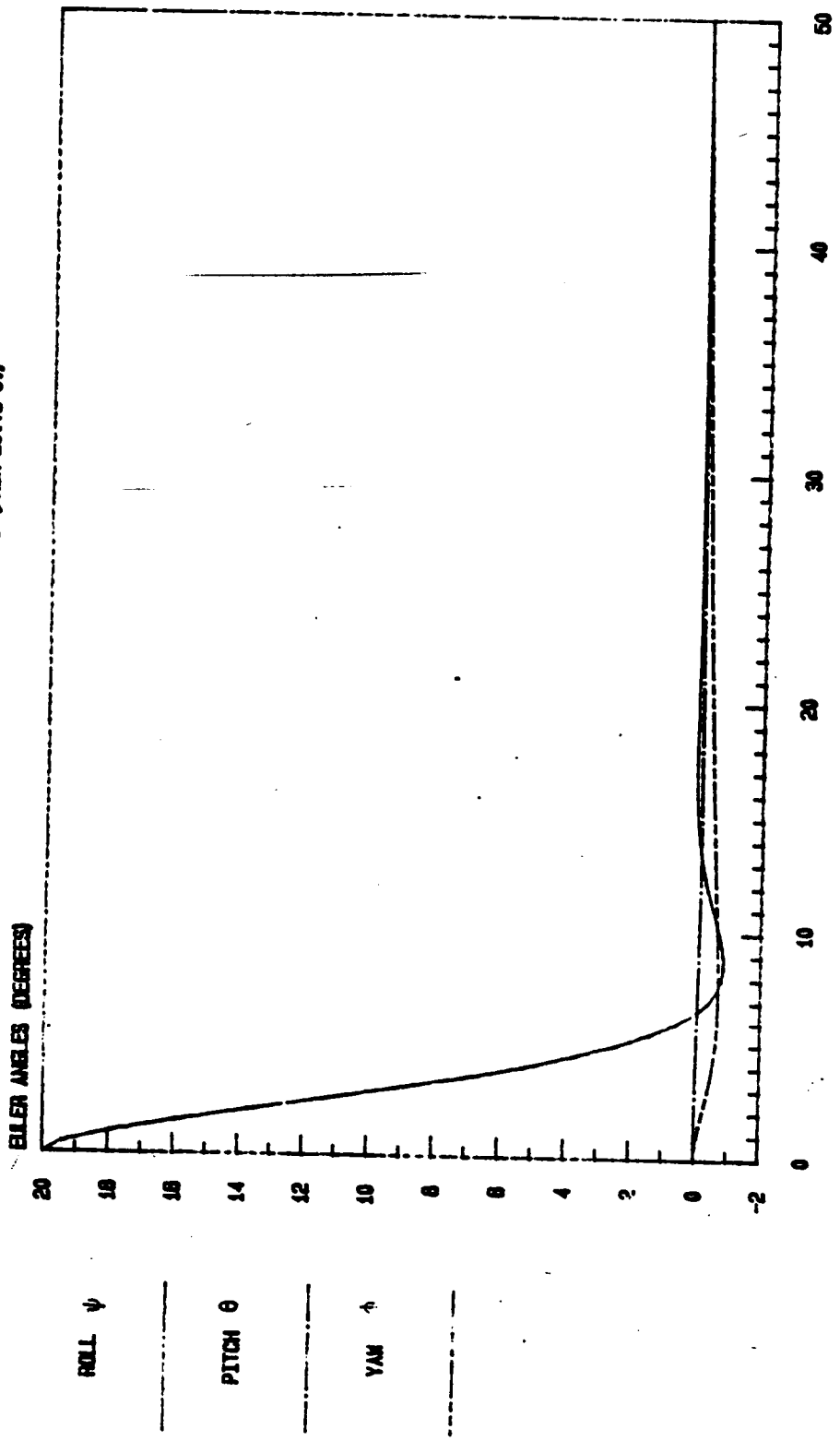

FIGURE V.21 SCOLE: PRELIMINARY SLEW-CONTROL EFFORTS

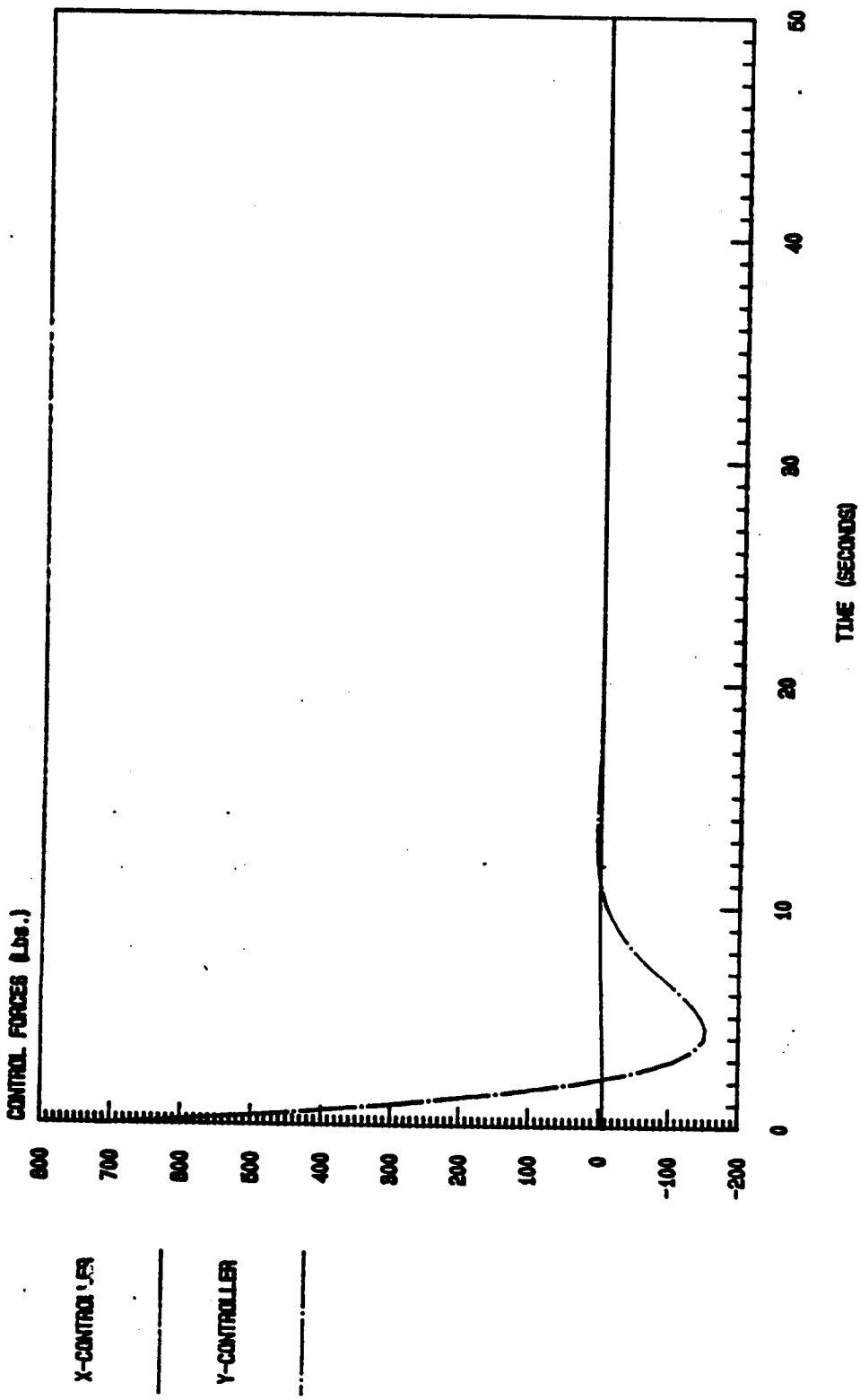

FIGURE V.22 SCOLE: PRELIMINARY SLEW-CONTROL EFFORTS

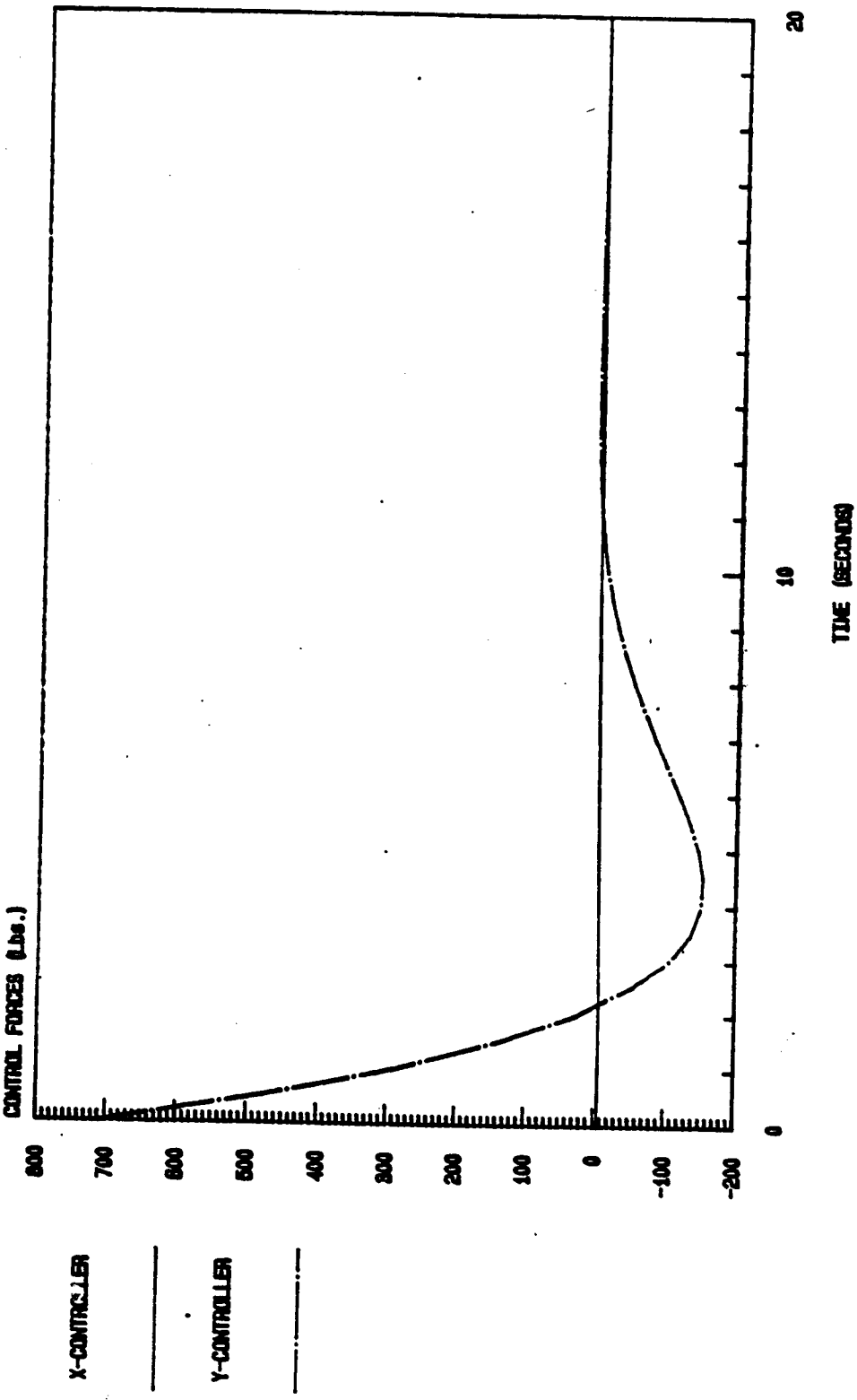

ORIGINAL PAGE IS
OF POOR QUALITY

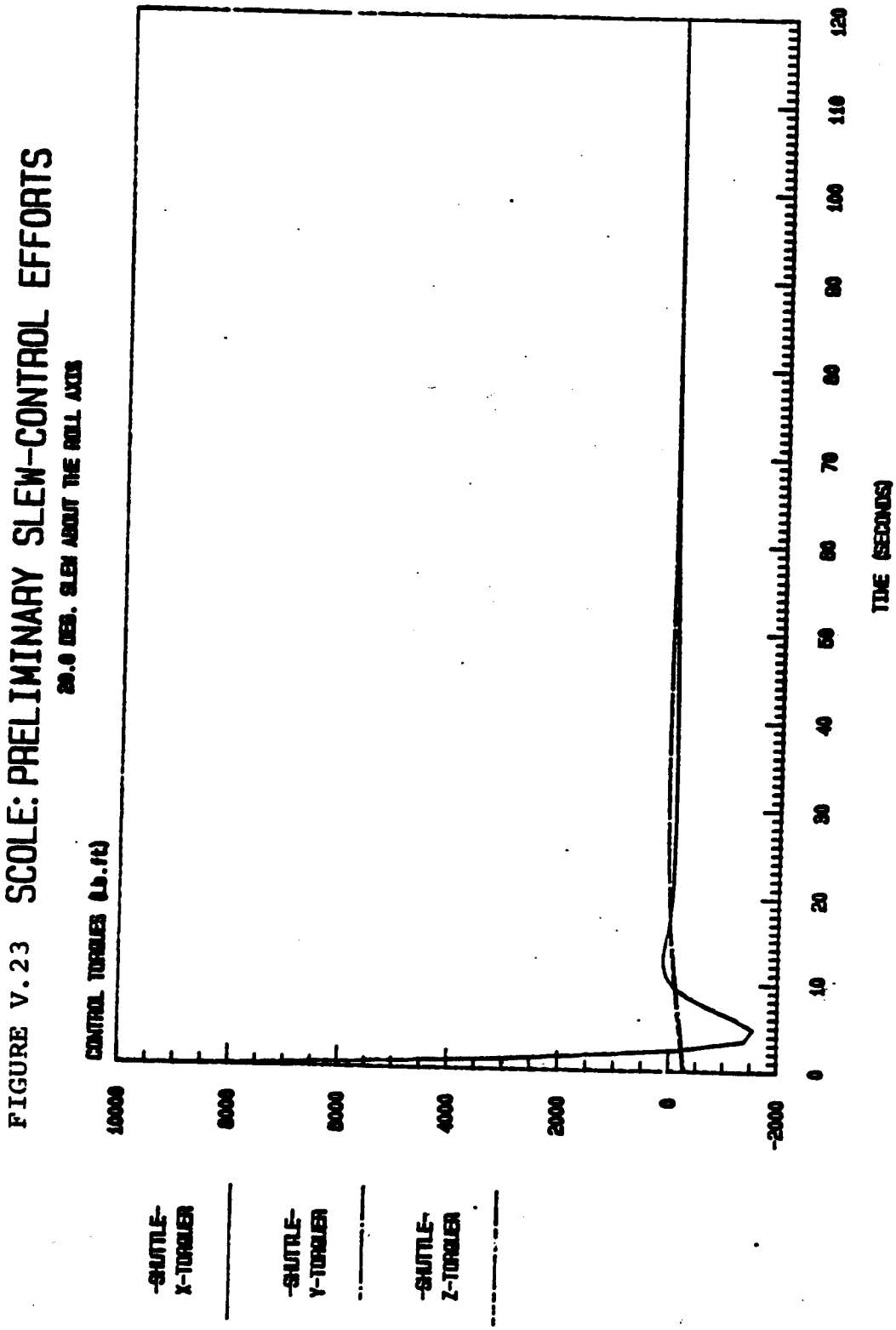

FIGURE V.23

FIGURE V.24 SCOLE: PRELIMINARY SLEW-CONTROL EFFORTS

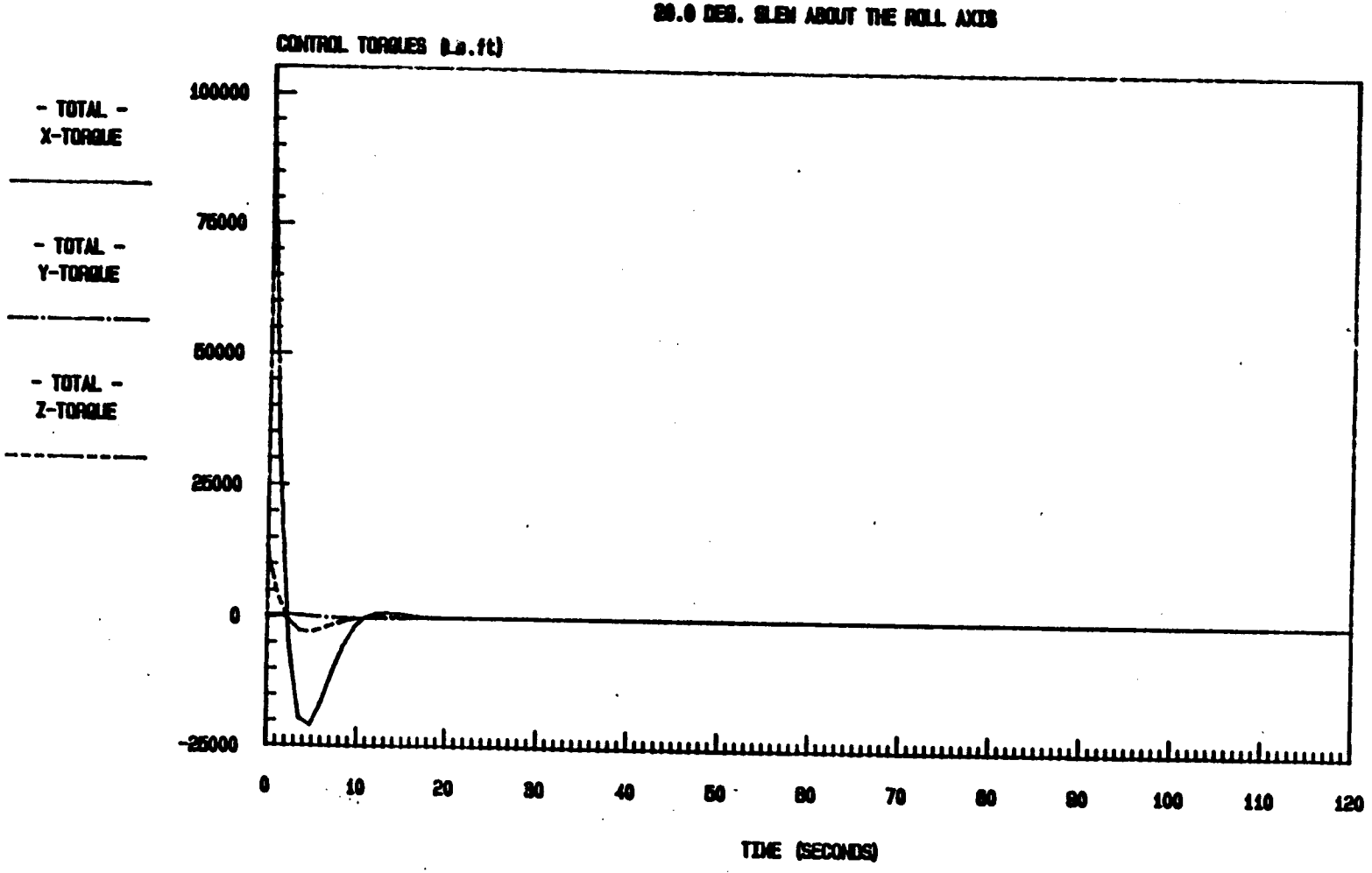

FIGURE V.25 SCOLE: PRELIMINARY SLEW (RIGID SCOLE)

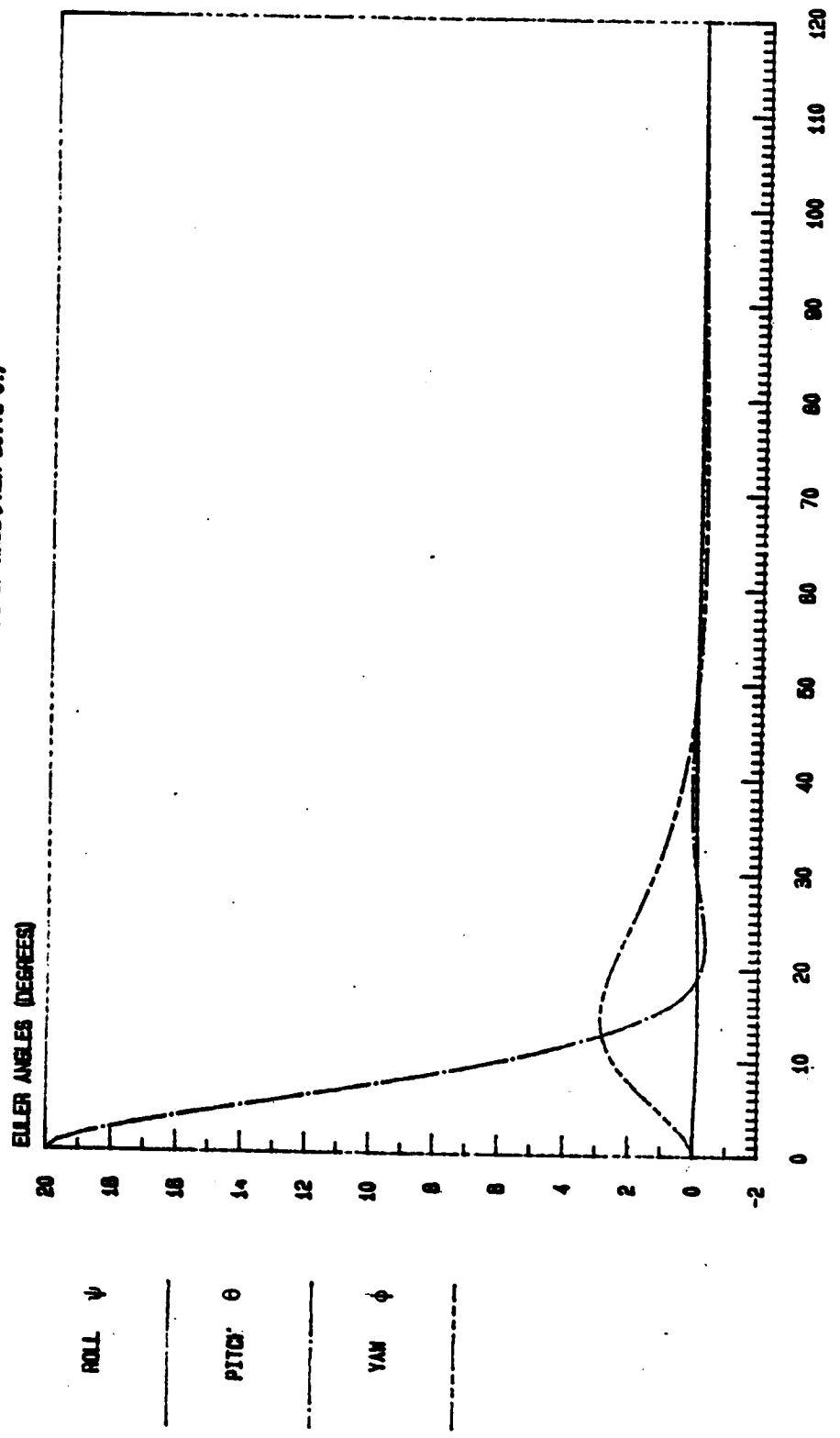

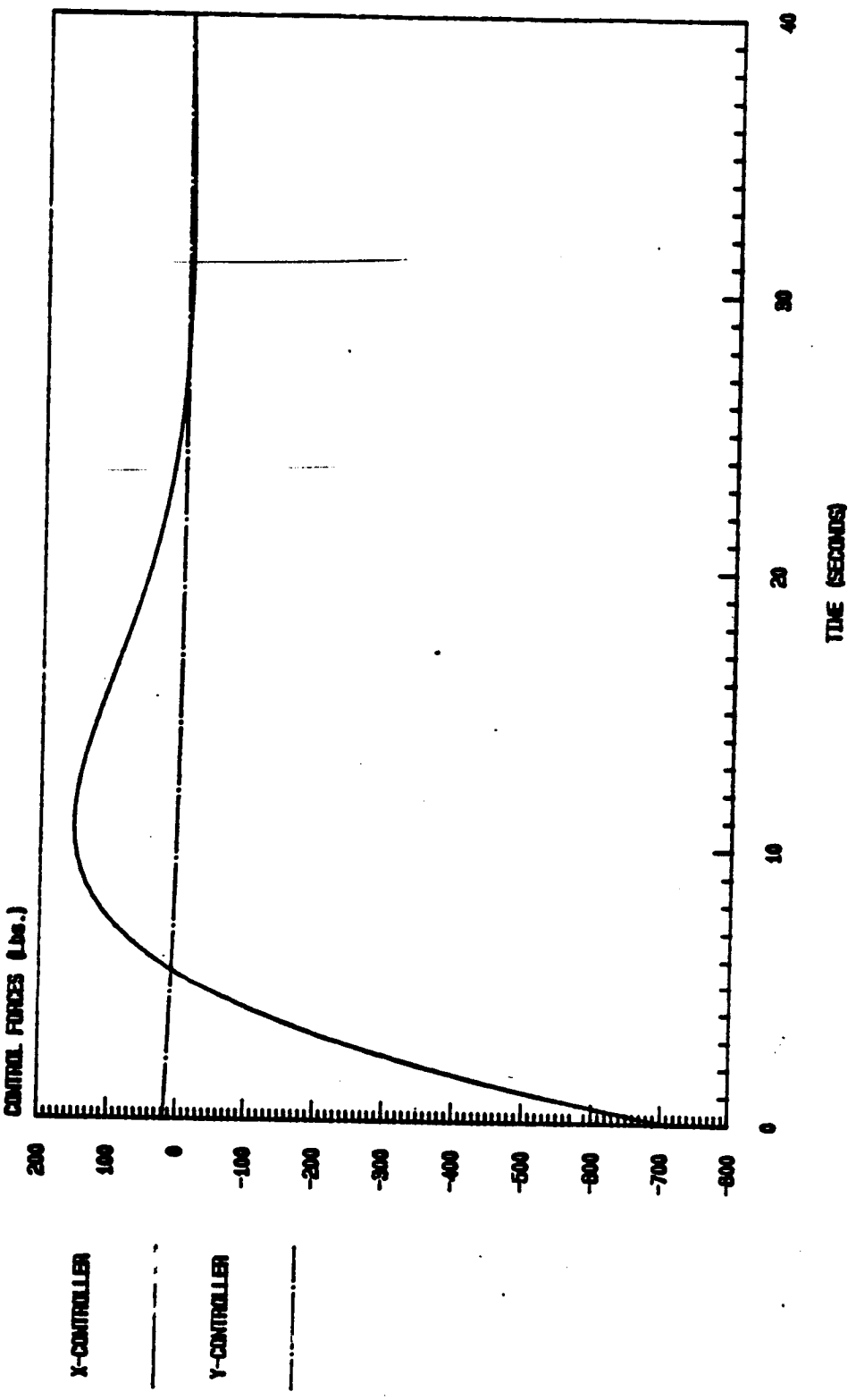
SCOLE: PRELIMINARY SLEW-CONTROL EFFORTS
20.0 DEG. SLEW ABOUT THE PITCH AXIS
CONTROL FORCES (Lbs.)
200
100
0
-100
-200
-300
-400
-500
-600
-700
-800
0
10
20
30
40
TIME (SECONDS)
X-CONTROLLER
Y-CONTROLLER

FIGURE V.26

FIGURE V.27 SCOLE: PRELIMINARY SLEW-CONTROL EFFORTS

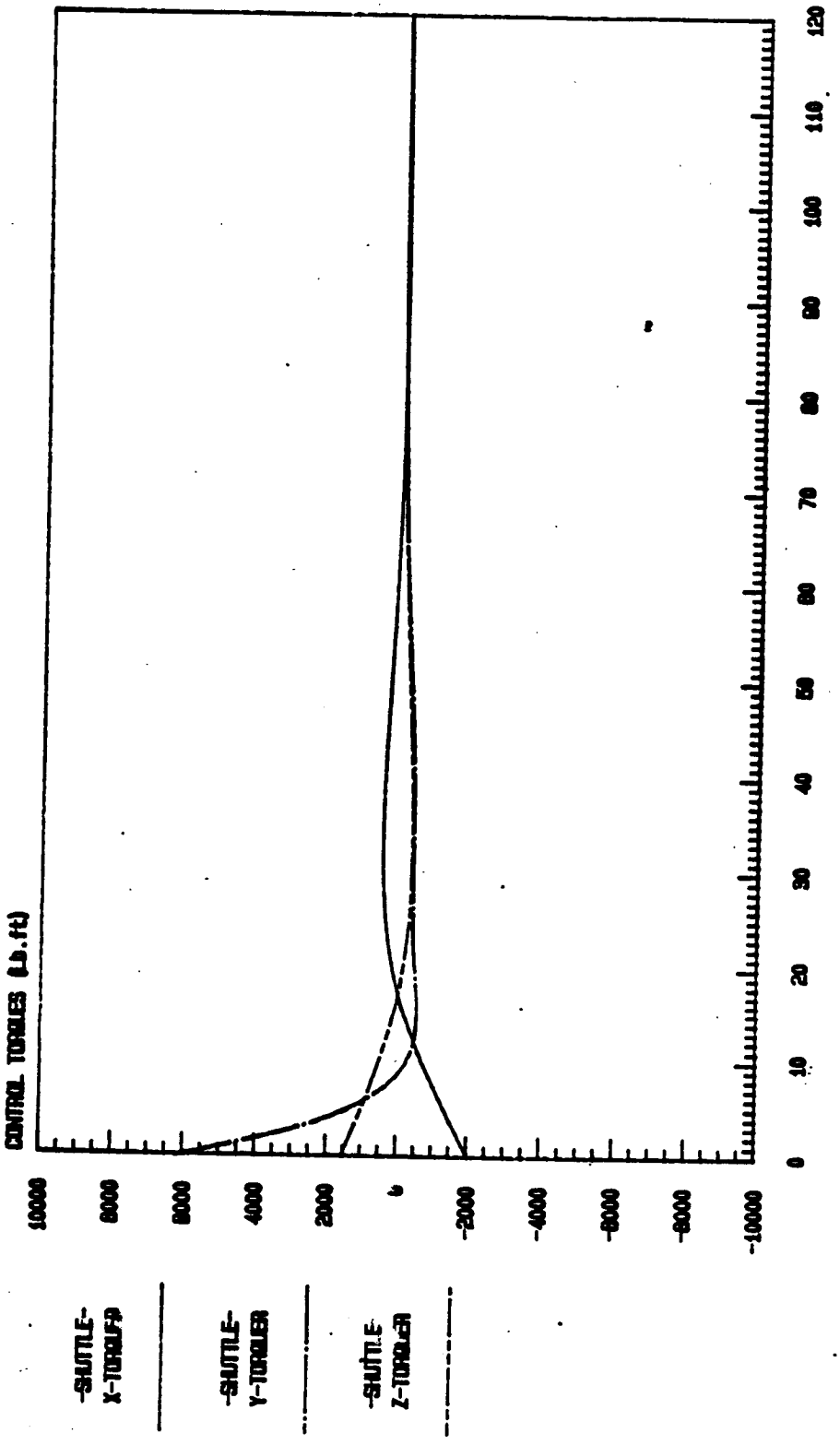

FIGURE V.28 SCOLE: PRELIMINARY SLEW-CONTROL EFFORTS

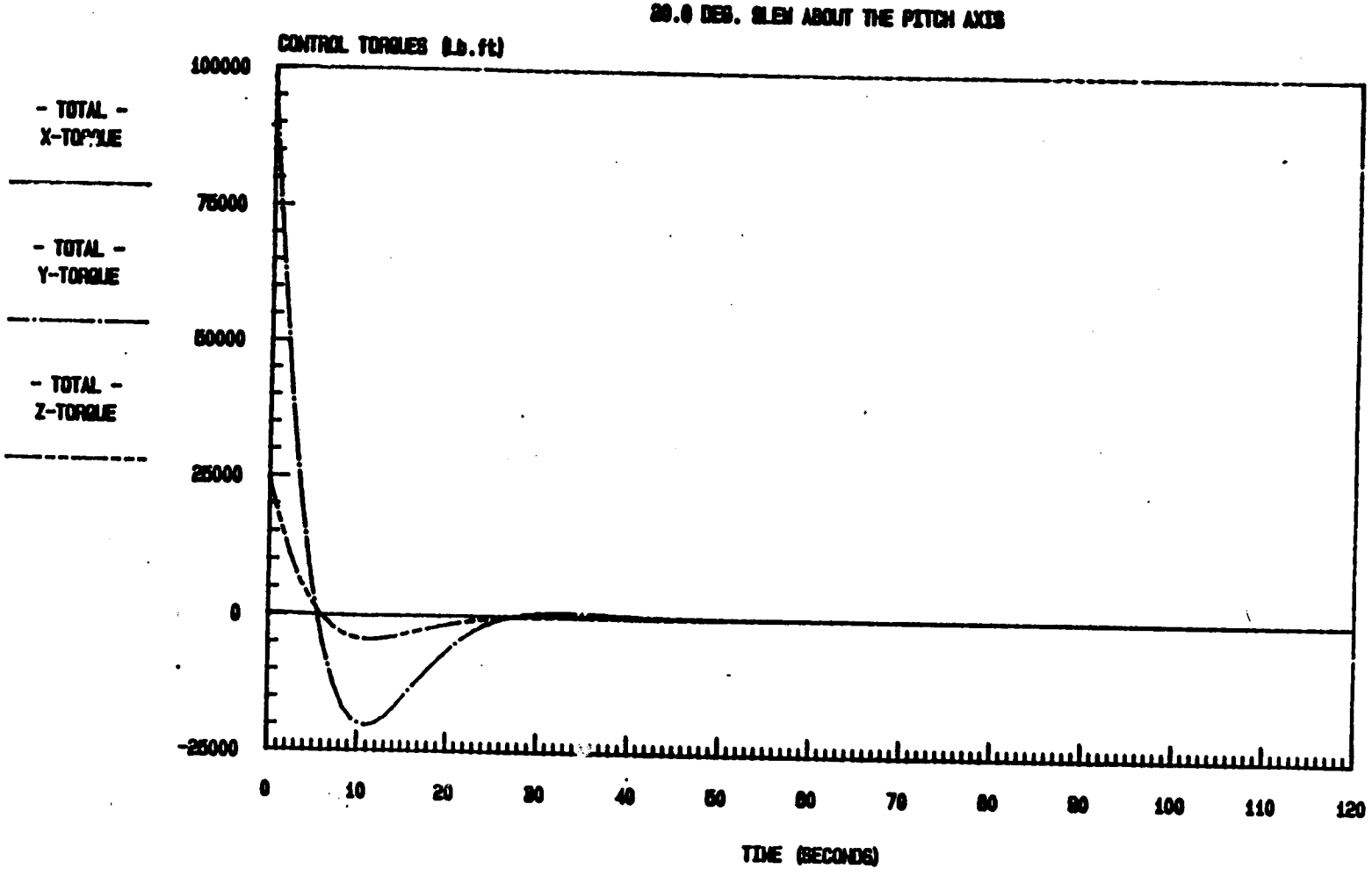

FIGURE V.29 SCOLE: PRELIMINARY SLEW (RIGID SCOLE)

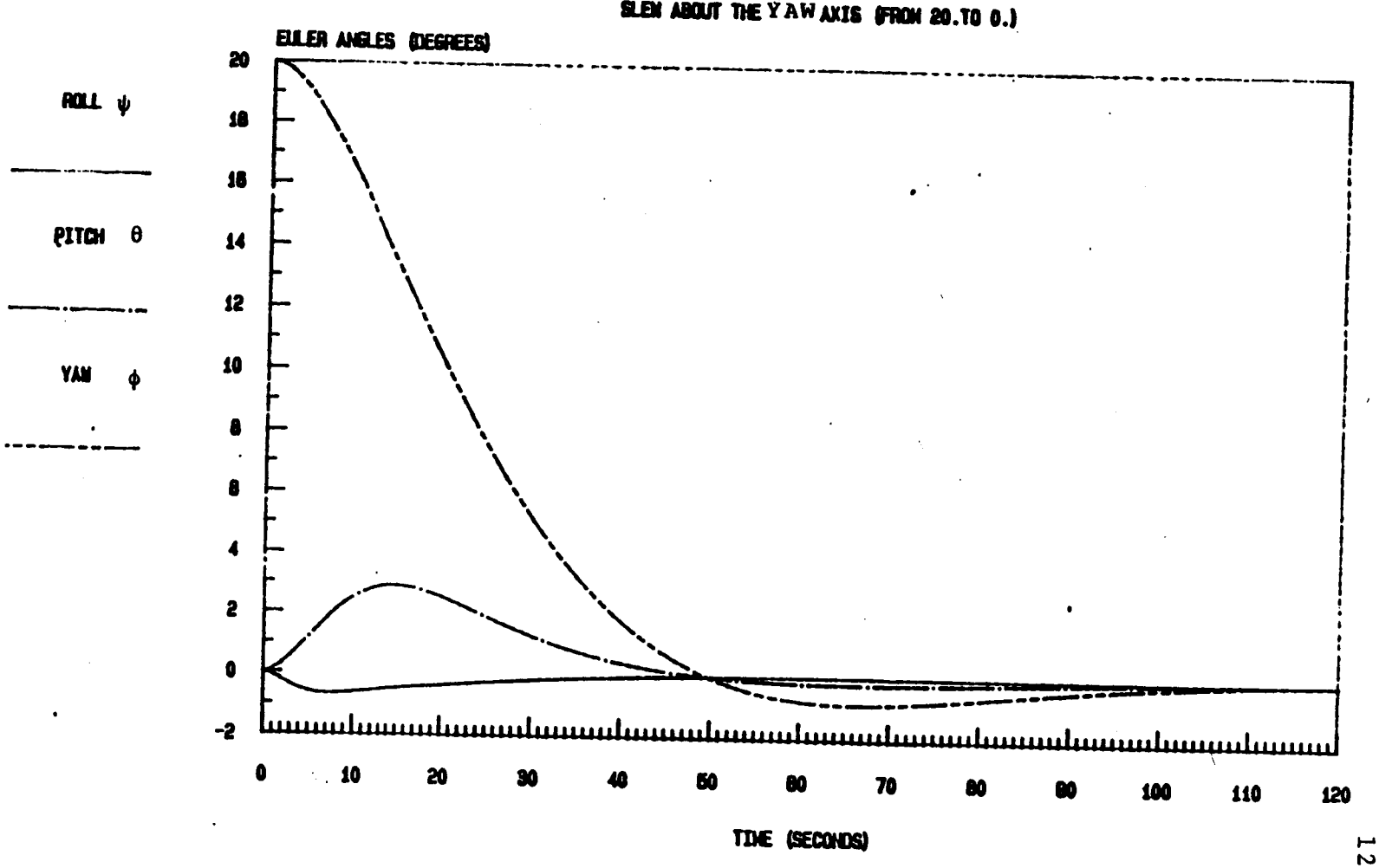

FIGURE V.30 SCOLE: PRELIMINARY SLEW-CONTROL EFFORTS

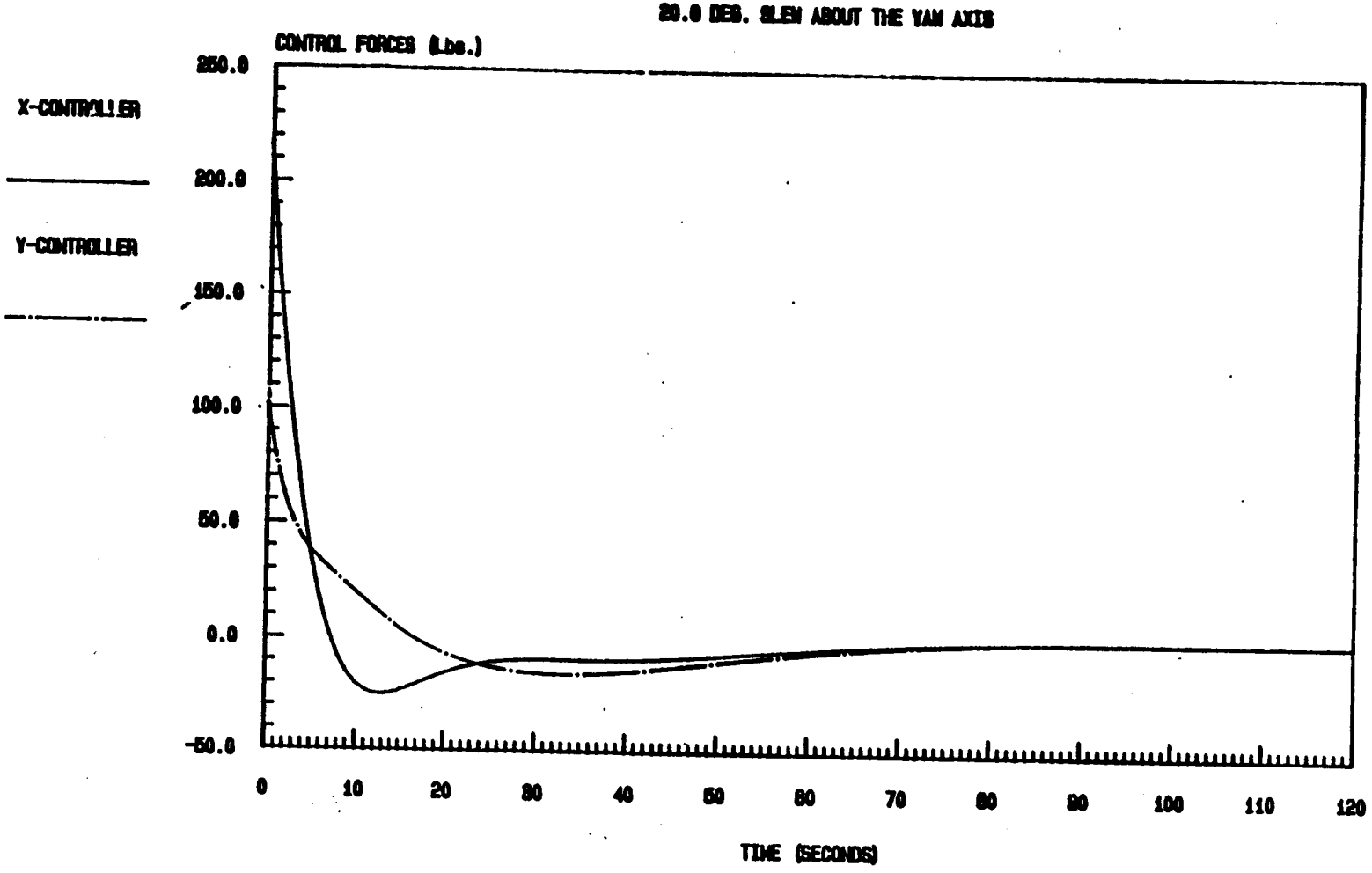

ORIGINAL PAGE IS
OF POOR QUALITY

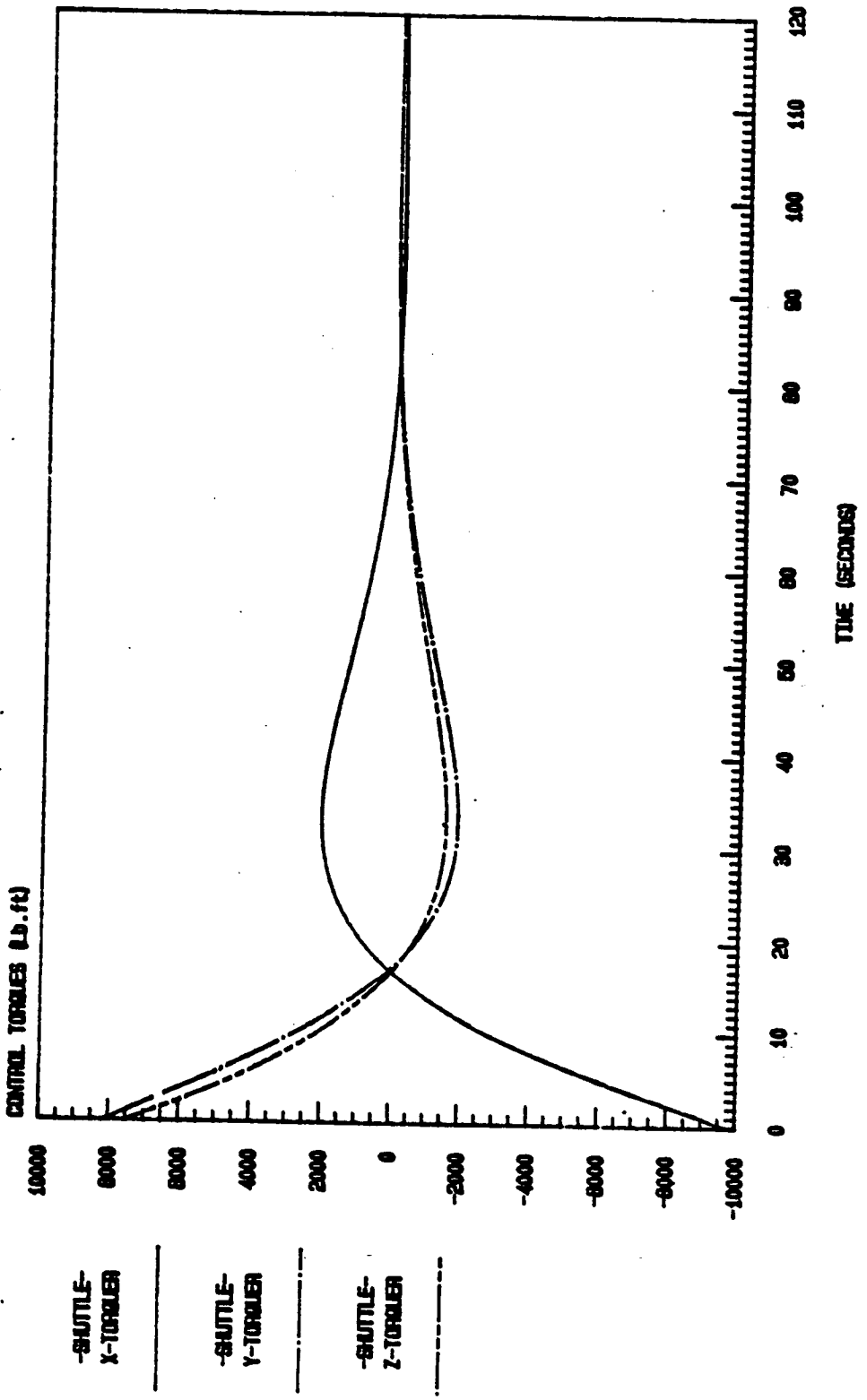

FIGURE V.31

ORIGINAL PAGE IS
OF POOR QUALITY

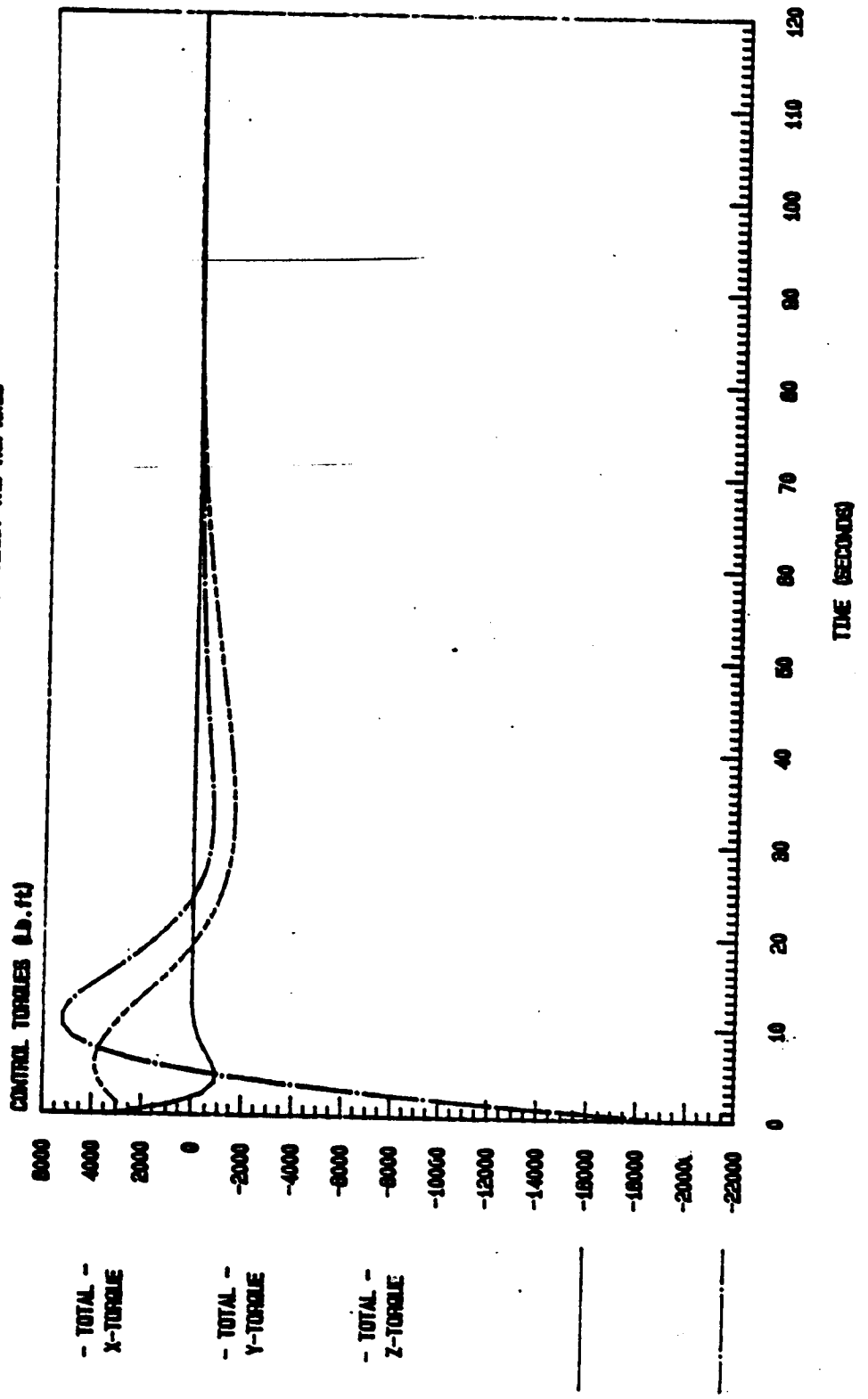

FIGURE V.32

CHAPTER SIX

CONCLUSIONS AND RECOMMENDATIONS FOR FUTURE INVESTIGATIONS

In this thesis, it has been seen that:

1. The SCOLE system, with gravity-gradient torques included in its open-loop dynamics, is unstable. This is due to the inertia distribution of the system in the particular configuration where the Shuttle roll axis nominally follows the orbit.

2. The equations describing the pitch motion decouples, within the linear range, from the roll and yaw equations, when the gravity-gradient torques effects are present in the system dynamics, and when the system is without offset or when the offset is parallel to the roll axis. A result similar to the one depicted here was derived for the tethered platform system.[11]

3. In the absence of control forces and torques, the system will oscillate about a new equilibrium position. The amplitudes of the oscillations

grow with the offset distance and the frequency of oscillation during that motion depends on the frequencies of the modes taken into account in the model.

4. A control law judiciously derived for the linear model of the rigidized SCOLE can be used to slew the system without reaching the saturation level of the controllers. It is anticipated that the trade-off between maneuver time and overall control effort would be in favor of such a control law as compared with the bang-bang strategy or the two point boundary value problem approach.

5. The coupling between the elastic displacements and the rigid modes is strong enough to suggest more accuracy in modeling this class of offseted and large flexible structures.

The author suggests the following topics for future research.

1. In the case of the rigidized SCOLE model for single offset parallel to the roll axis, the

equation describing the pitch motion of the rigid SCOLE, decouples from the roll and yaw motions. In such case, a control law could be derived analytically and compared with the control law derived using the linear regulator theory when a maneuver is done about the pitch axis.

2. Since the SCOLE design challenge consists of slewing the SCOLE configuration in a minimum time through a 20^{o} line of sight angle, it is conceivable that the high rates at which the slewing maneuvers occur would modify the structural configuration of the system, at least for those short periods of time the maneuvers would take. Therefore, a study could be conducted on a model which would include a load equivalent to the effect of such induced centrifugal forces and the subsequent modal shapes and frequencies could be compared with those at hand at the present time. If significant differences in mode shapes/frequencies during slew maneuvers are observed, then the slewing simulations reported here for the

rigidized model should be repeated and compared both with the uncorrected and also with the corrected flexible models.

3. A study could be undertaken which would derive a global control law compatible with the two-stage strategy during which first the system would be slewed as if rigid and second the induced elastic vibrations suppressed.

REFERENCES

1. Taylor, L.W. and A.V. Balakrishnan, "A Laboratory Experiment Used to Evaluate Control Laws for Flexible Spacecraft ... NASA/IEEE Design Challenge," Proceedings of the Fourth VPI&SU Symposium on Dynamics and Control of Large Structures, Blacksburg, VA, June 1983.

2. Montgomery, Raymond C., "COFS II Project Overview and Strawman," Control of Flexible Structures Workshop, NASA Langley Research Center, Hampton, Va., August 27-28, 1985.

3. Robertson, D.K., "Three-Dimensional Vibration Analysis of a Uniform Beam with Offset Inertial Masses at the Ends", NASA TM-86393, September 1985.

4. Lin, J.G., "Rapid Torque Limited Line of Sight Pointing of SCOLE (Spacecraft Control Laboratory Experiment) Configuration", AIAA Guidance, Navigation, and Control Conference, Williamsburg, Va., August 18-20, 1986, Paper No. 86-1991.

5. Meirovitch, L., and Quinn, R.D., "Equations of Motion for Maneuvering Flexible Spacecraft", Journal of Guidance and Control, Vol., 10, No. 5, Sept-Oct, 1987, pp. 453-465.

6. Taylor, L.W. Jr., "Spacecraft Control Laboratory Experiment: SCOLE Workshop 1984" Proceedings of a Workshop Concerning the NASA-IEEE Design Challenge, NASA Langley Research Center, Hampton, Va. 23665, December 6-7, 1984.

7. Timoshenko, S., Vibration Problems in Engineering, D. Van Nostrand Company, Inc., New York, 1937.

8. Santini, P., "Stability of Flexible Spacecrafts", Acta Astronautica, Vol. 3, 1976, pp. 685-713.

9. Armstrong, E.S., ORACLS Design System for Linear Multivariable Control, Control and Systems Theory, Vol. 10, Marcel Dekker, Inc., New York, 1980.

10. Lin, Y.H., Control of Large Space Antennas Wrap-Rib-Hoop/Column, Large Space Technology - 1981 Third Annual Technical Review, November 16-19, 1981.

11. Fan Ruying and P.M. Bainum, "The Dynamics and Control of a Space Platform Connected to a Tethered Subsatellite", Proc. of AIAA/NASA/PSN International Conference on Tethers in Space, Arlington, Va., Sept. 17-19, 1986, Tethers in Space, AAS Advances in the Astronautical Sciences, Vol. 62, pp. 277-294.

12. Larry G. Lemke, J. David Powell, and Xiaohua He, "Attitude Control of Tethered Spacecraft", The Journal of the Astronautical Sciences, Vol. 35, No. 1, Jan-March, 1987, pp. 41-55.

13. P.K. Lahshmanan, V.J. Modi, and A.K. Misra, "Dynamics and Control of the Tethered Satellite System in the Presence of Offsets", 38th IAF Congress, Brighton, U.K 10-17 Oct. 1987, Paper NO. IAF 87-316.

14. Mantion, M., Problemes de Mecanique Analytique Vuibert Universite, 75005 Paris, France, 1981.

APPENDIX A

STRUCTURAL ANALYSIS OF THE SCOLE SYSTEM

In this Appendix, the mode shape, the corresponding frequencies, and modal amplitude are derived for the SCOLE system. In this analysis, it is assumed that the beam mast has:

a) a uniform density;

b) a circular cross section;

c) a uniform distribution of stiffness;

also that the displacements and slopes are small.

Governing Differential Equations

The governing partial differential equations for the beam are comprised of two one plane bending equations, (A.1 and A.2), and one axial torsion equation, (A.3).

For the x-z plane bending, one has [7]:

$$-\frac{\partial^2 u}{\partial t^2}(z,t) = \frac{EI}{\rho A}\frac{\partial^4}{\partial z^4}u(z,t) \qquad (A.1)$$

where ρ is the density of the beam, A its cross sectional area and EI its x-z plane bending stiffness which is assumed, in what follows, to be equal to its y-z plane bending stiffness (circular shaft)

Assuming the following form for u(z,t) (separation of variables):

$$u(z,t) = p_x(t)s_x(z),$$

equation (A.1) can be rewritten as

$$-s_x(z)\frac{d^2}{dt^2}p_x(t) = \frac{EI}{\rho A}p_x\frac{d^4}{dz^4}s_x(z) \quad \text{or}$$

$$\frac{\ddot{p}_x}{p_x} = -\frac{EI}{\rho A}\frac{s_x^{(4)}}{s_x}$$

This equation is true if, and only if both sides are equal to a constant, say, $-\omega^2$, yielding

$$\ddot{p}_x + \omega_x^2 p_x = 0$$

which integrates into:

$p_x(t) = \cos(\omega_x t+\alpha)$ where α is a phase angle. From the right side,

$$s_x^{(4)} - \omega_x^2\frac{\rho A}{EI}s_x = 0$$

Letting $\beta_x'^4 = \frac{\rho A}{EI}\omega_x^2$, the general solution has the form:

$$s_x = A_1 \sin\beta_x z + B_1 \cos\beta_x z + C_1 \sinh\beta_x z + D_1 \cosh\beta_x z$$

$$u(z,t) = \cos(\omega_x t + \alpha)\{A_1 \sin\beta_x' z + B_1 \cos\beta_x' z + C_1\sinh\beta_x' z + D_1 \cosh\beta_x' z\}$$

The y-z plane bending is described by:

$$-\frac{\partial^2}{\partial t^2}(v(z,t)) = \frac{EI}{\rho A}\frac{\partial^4}{\partial z^4}(v(z,t)) \qquad (A.2)$$

Assuming v(z,t) of the form

$$v(z,t) = p_y(t)\, s_y(z)$$

After substitution, Equation (A.2) becomes

$$-s_y \ddot{p}_y = \frac{EI}{\rho A} p_y s_y^{(4)} \quad \text{or}$$

$$\frac{\ddot{p}_y}{p_y} = -\frac{EI}{\rho A}\frac{s_y^{(4)}}{s_y}$$

which is true only if both sides are equal to a constant say, $-\omega_y^2$. A reasoning similar to the one used to analyze the x-z plane bending, yields

$$v(z,t) = \cos(\omega_y t+\gamma)\{A_2 \sin\beta_y' z + B_2 \cos\beta_y' z + C_2 \sinh\beta_y' z + D_2 \cosh\beta_y' z\}$$

where $\beta_y'^4 = \frac{\rho A}{EI}\omega_y^2$

Finally, the z axis torsional bending is described by

(A.3)

where G is the modulus of rigidity of the beam. Here again, assuming the separation of the variables possible: $\phi(z,t) = p_z(t)\ \theta(z)$, and letting $\beta_z'^2 = \omega_3^2\ \rho/G$, there results:

$$\phi(z,t) = \cos(\omega_z t + \delta)\ \{A_3 \sin \beta_z' z + B_3 \cos \beta_z' z\}$$

The equations giving $u(z,t)$, $v(z,t)$, and $\phi(z,t)$ are more convenient to use when the position variable is transformed into a nondimensional form. For this reason, the variable, $\varepsilon = z/L$, where L is the length of the undeformed beam, is used. After substitution into $u(z,t)$, $v(z,t)$, and $\phi(z,t)$, those equations become:

$$u(\varepsilon,t) = \cos(\omega_x t+\alpha)\ \{A_1 \sin\beta_x \varepsilon + B_1 \cos\beta_x \varepsilon + C_1 \sinh\beta_x \varepsilon + D_1 \cosh\beta_x \varepsilon\}$$

$$v(\varepsilon,t) = \cos(\omega_y t+\gamma)\ \{A_2 \sin\beta_y \varepsilon + B_2 \cos\beta_y \varepsilon + C_2 \sinh\beta_y \varepsilon + D_2 \cosh\beta_y \varepsilon\}$$

$$\phi(\varepsilon,t) = \cos(\omega_z t + \delta)\ \{A_3 \sin\beta_z \varepsilon + B_3 \cos\beta_z \varepsilon\}$$

with, $\beta_x^4 = \dfrac{\rho A}{(EI)_x}\ \omega_x^2\ L^4$

$$\beta_y^4 = \frac{\rho A}{(EI)_y}\ \omega_y^2\ L^4$$

$$\beta_z^2 = \frac{\rho}{G}\ \omega_z^2\ L^2$$

In this investigation it is assumed that $\omega_x = \omega_y = \omega_z$ and $p_x(t) = p_y(t) = p_z(t) = p(t)$

$$\beta = \beta_x = \beta_y = \frac{GA}{EI} \beta_z L$$

or again

$$\beta_z = \frac{\beta^2}{L} \frac{EI}{GA}$$

Boundary Conditions

In our model, the offset of the mast attachment point from the center of mass of the reflector, along with its products of inertia causes a kinematic coupling between the displacements in the different degrees of freedom. The following relationships between shear, moment, and beam displacement are used in the boundary conditions [3].

$$V_x = - \frac{EI}{L^3} \frac{\partial^3}{\partial \varepsilon^3} (\varepsilon, t) = - EI \frac{\partial^3 u}{\partial z^3}(z,t)$$

$$V_y = - \frac{EI}{L^3} \frac{\partial^3 v}{\partial \varepsilon^3} (\varepsilon, t) = - EI \frac{\partial^3 v}{\partial z^3} (z,t)$$

$$M_x = -\frac{EI}{L^2}\frac{\partial^2 v}{\partial \varepsilon^2}(\varepsilon,t) = -EI\frac{\partial^2 v}{\partial z^2}$$

$$M_y = -\frac{EI\,\mu}{L^2}\frac{\partial^2 v}{\partial \varepsilon^2}(\varepsilon,t) = -EI\frac{\partial^2 \mu}{\partial z^2}$$

$$M_z = \frac{GI_p}{L}\frac{\partial \phi}{\partial \varepsilon}(\varepsilon,t) = GI_p\frac{\partial \phi}{\partial z}$$

A

where:

V_x = shear force in the x direction

V_y = shear force in the y direction

M_x, M_y, and M_z = moment components about the x, y, and z axes, respectively.

I_p = polar moment of inertia of the beam.

Let M_S be the mass of the Shuttle and M_R that of the reflector. The shear force at an end of the beam is assumed equal to the mass of the corresponding body at that end multiplied by the acceleration of that end; and if we also consider that the displacement in the x direction of a point located at z=0 is given by

$u(0,t)-Dy_0\,\Phi(0,t)$ and that in the y direction by $v(0,t)+Dx_0\,\Phi(0,t)$, (Dx_0 and Dy_0 are the displacement components of the centroid of the cross sectional area of the beam at z=0), therefore, at the Shuttle end,

$$V_x\Big|_{\varepsilon=0} = M_s\,\ddot{p}\,\{s_x(0)-Dy_o\,\theta(0)\} = -\frac{EI}{L^3}\,s_x^{(3)}(0)\,p(t)$$

$$V_y\Big|_{\varepsilon=0} = M_s\ddot{p}\{s_y(0)-Dx_0\,(0) = -\frac{EI}{L^3}\,s_y^{(3)}(0)\,p(t)$$

Taking into consideration the fact that $\ddot{p} = -\omega^2\,p(t)$ and substituting it into the shear equations yields

$$-\omega^2 M_s[\,s_x(0)-Dy_0\theta(0)\,] = -\frac{EI}{L^3}\,s_x^{(3)}(0)$$

$$-\omega^2 M_s[\,s_y(0)-Dx_0\,(0)\,] = -\frac{EI}{L^3}\,s_y^{(3)}(0)$$

but $$\omega^2 = \beta^4\,\frac{EI}{\rho AL^4}$$

After rearranging terms, one obtains

$$s_x^{(3)}(0) = \frac{M_s}{\rho AL}\,\beta^4[\,s_x(0)-Dy_0\theta(0)\,]$$

$$s_y^{(3)}(0) = \frac{M_s}{\rho AL}\beta^4[\dot{s}_y(0) - Dx_0\,\theta(0)]$$

A similar reasoning at the reflector end of the beam taking into account the equilibrium of the beam would give

$$s_x^{(3)}(1) = \frac{M_R}{\rho AL}\beta^4[-s_x(1) + Dy_L\theta(1)]$$

$$s_y^{(3)}(1) = \frac{M_R}{\rho AL}\beta^4[-s_y(1) - Dx_L\,\theta(1)]$$

Bending Moments

The next four boundary conditions involve the moments, M_{xo}, M_{yo}, M_{xL}, and M_{yL} at $z = 0$ and $z = L$, respectively, on the beam. Assuming the nonlinear coupling and all the products of inertia, except I_{xz}, to be negligible, one may write

$$M_x = I_{xx}\ddot{\theta}_x + I_{xy}\ddot{\theta}_y$$

$$M_y = I_{yy}\ddot{\theta}_y + I_{xy}\ddot{\theta}_x$$

where $\ddot{\theta}_x$ and $\ddot{\theta}_y$ are the angular accelerations of a point on the mast about the x and y axes, respectively.

since $M_x = -\frac{EI}{L^2} v^{(2)}$; $M_y = \frac{EI}{L^2} \mu^{(2)}$ from Equations (A),

and the angular displacements θ_x, and θ_y are given as

$$\theta_x = -\frac{1}{L}\frac{\partial v}{\partial \varepsilon} \quad ; \quad \text{and} \quad \theta_y = \frac{1}{L}\frac{\partial \mu}{\partial \varepsilon}$$

substitution of the general expressions for $u(\varepsilon,t)$, $v(\varepsilon,t)$, $v(\phi,t)$ and (ε,t) into the boundary conditions (A and B) at $\varepsilon = 0$ and $\varepsilon = 1$, respectively yields

$$s_y^{(2)}(0) = \frac{\beta^4}{\rho AL^3}\left(-I_{S1}\ s_y^{(1)}(0)\right)$$

$$s_x^{(2)}(0) = \frac{\beta^4}{\rho AL^3}\left(-I_{S2}\ s_x^{(1)}(0)\right)$$

(It should be recalled that the term I_{xy} as applied to the Shuttle is zero.)

$$s_y^{(2)}(1) = \frac{\beta^4}{\rho AL^3}\left[I_{R1}\ s_y^{(1)} - M_R DxDy\ s_x^{(1)}(1)\right]$$

$$s_x^{(2)}(1) = \frac{\beta^4}{\rho A L^3}[I_{R2}\ s_x^{(1)}(1) - M_R\ DxD_y\ s_y^{(1)}]$$

where $I_{S\,1}$, $I_{R\,1}$, $I_{S\,2}$, and $I_{R\,2}$ are the moments of inertia, about the x and y axes, of the Shuttle and the reflector, respectively. The x and y axes considered here pass through the respective interface points.

Torsional Moments

These moments are caused by the masses and moments of inertia, about the z axis, of the end bodies: $\Phi(z,t)\ I_{zz}$. They are countered by the beam internal moment given by

$$M_z = GI_p \frac{\partial \Phi}{\partial z}$$

Writing the equality between these two moments yields:

at the Shuttle end

$$\theta^{(1)}(0) = \frac{\beta_z^2}{\rho L I_p} I_{S3}\ \theta\ (0) \Leftrightarrow GI_p \frac{\partial \Phi}{\partial z} = \Phi(z,t) I_{zz}$$

at the reflector end

$$\theta^{(1)}(1) = \frac{\beta_z^2}{\rho L I_p}[-I_{R3}\theta(1) + M_R Dx_L\ s_y(1) - M_R\ Dy_L\ s_x(1)]$$

where I_{S3} and I_{R3} are the moments of inertia of the Shuttle and the reflector, respectively, about the z axis.

Substituting the expression for $s_x(\varepsilon)$, $s_y(\varepsilon)$, and $\theta(\varepsilon)$, and the appropriate values of ε at the boundaries into the boundary equations, the following ten linear equations are obtained. It should also be noted here that $Dx_0 = Dy_0 = 0$ since at the Shuttle end the centroid of the beam cross section coincides with the center of mass of the Shuttle.

$$-A_1 - \left(\frac{\beta M_s}{\rho AL}\right) B_1 + C_1 - \left(\frac{\beta M_s}{\rho AL}\right) D_1 = 0 \qquad (A.4)$$

$$-A_2 - \left(\frac{\beta M_s}{\rho AL}\right) B_2 + C_2 - \left(\frac{\beta M_s}{\rho AL}\right) D_2 = 0 \qquad (A.5)$$

$$A_1\left\{\frac{\beta M_R}{\rho AL} \sin\beta - \cos\beta\right\} + B_1\left\{\frac{\beta M_R}{\rho AL} \cos + \sin\right\} + C_1\left\{\frac{\beta M_R}{\rho AL} \sinh\beta - \cosh\beta\right\}$$

$$+D_1\left\{\frac{\beta M_R}{\rho AL} \cosh\beta + \sinh\beta\right\} + A_3\left\{\frac{\beta M_R}{\rho AL} Dy_L \sin\beta_z\right\} + B_3\left\{\frac{\beta M_R}{\rho AL} Dy_L \cos\beta_z\right\} = 0 \qquad (A.6)$$

$$A_2\{\frac{\beta M_R}{\rho AL}\sin - \cos\beta\} + B_2\{\frac{\beta M_R}{\rho AL}\cos\beta + \sin\beta\} + C_2\{\frac{\beta M_R}{\rho AL}\sinh\beta - \cosh\beta\}$$

$$+D_2\{\frac{\beta M_R}{\rho AL}\cosh\beta + \sinh\beta\} + A_3\{\frac{\beta M_R}{\rho AL}\ Dx_L \sin\beta_z\} + B_3\{\frac{\beta M_R}{\rho AL}\ Dx_L \cos\beta_z\} = 0 \quad (A.7)$$

$$A_2\ (\frac{\beta^3 I_{S1}}{\rho AL^3}) - B_2 + C_2(\frac{\beta^3 I_{S1}}{\rho AL^3}) \quad + D_2 = 0 \qquad (A.8)$$

$$A_1\ (\frac{\beta^3 I_{S2}}{\rho AL^3}) - B_1 + C_1(\frac{\beta^3 I_{S2}}{\rho AL^3}) \quad + D_1\ -(\frac{\beta I_{S1}}{\rho AL^3} \quad \{A_2+C_2\} = 0 \qquad (A.9)$$

$$(\beta^3\ \frac{M_R Dx\ Dy}{\rho AL^3})\ (A_1\cos\beta - B_1\sin\beta + C_1\cosh\beta + D_1\sinh\beta)$$

$$-A_2\{\frac{\beta^3}{\rho AL^3} I_{R1}\cos\beta + \sin\beta\} + B_2\{\frac{\beta^3}{\rho AL^3} I_{R1}\ \sin\beta - \cos\beta\}$$

$$-C_2\{\frac{\beta^3}{\rho AL^3} I_{R1}\cosh\beta + \sinh\beta\} - D_2\{\frac{\beta^3}{\rho AL^3} I_{R1}\ \sinh\beta + \cosh\beta\} = 0 \quad (A.10)$$

$$-A_1\{\frac{\beta^3}{\rho AL^3} I_{R2}\ \cos\beta + \sin\beta\} + B_1\{\frac{\beta^3}{\rho AL^3} I_{R2}\ \sin\beta - \cos\beta\}$$

$$+C_1\{\sinh\beta - \frac{\beta^3}{\rho AL^3} I_{R2}\ \cosh\beta\} + D_1\ \{\cosh\beta - \frac{\beta^3}{\rho AL^3} I_{R2}\ \sinh\beta\}$$

$$+ \left(\beta^3 M_R \frac{Dx\ Dy}{\rho A L^3}\right) (A_2 \cos\beta - B_2 \sin\beta_2 + C_2 \cosh\beta + D_2 \sinh\beta) = 0 \quad (A.11)$$

$$A_3 + \left(\frac{\beta_z}{\rho L I_p} I_{S3}\right) B_3 = 0 \quad (A.12)$$

$$\left(\beta_z \frac{Dy\ M_R}{\rho L I_p}\right) \{A_1 \sin\beta + B_1 \cos\beta + C_1 \sinh\beta + D_1 \cosh\beta\}$$

$$+\left(\beta_z \frac{Dx\ M_R}{\rho L I_p}\right) \{-A_2 \sin\beta + B_2 \cos\beta - C_2 \sinh\beta - D_2 \cosh\beta\}$$

$$+A_3\left\{-\frac{\beta_z I_{R3}}{\rho L I_p} \sin\beta_z + \cos\beta_z\right\} - B_3\left\{\frac{\beta_z I_{R3}}{\rho L I_p} \cos\beta_z + \sin\beta_z\right\} = 0 \quad (A.13)$$

Equations (A.4) through (A.13) can be recast in the following matrix format

$$[Z(\beta)]\{[A_1, B_1, C_1, D_1, A_2, B_2, C_2, D_2, A_3, B_3]^T\} = [0]$$

where $[Z(\beta)]$ is a 10 x 10 matrix whose entries are functions of β. Non zero solutions for A_i, B_i, C_i, and D_i exist only when the determinant of $[Z(\beta)]$ is zero.

The equations derived here being identical to those derived in reference 3, the values of A_i, B_i, C_i, and D_i obtained therein have been used (table A.1) and the

projections of the first four mode shapes plotted: Figure (A.1) through Figure (A.12).

Table A.1

Mode Number	βz	β	ω rad/sec	A_1	B_1	C_1	D_1	A_2	B_2	C_2	D_2	A_3	B_3
1	1.19	0.033	.274	.161	- .196	- .168	.195	- .0395	.069	.0584	- .0689	- .0319	.158 E-04
2	1.29	0.039	.322	.072	- .084	- .075	.084	.125	- .196	- .167	.196	.0025	-.109 E-05
3	1.97	0.092	.748	0.022	-0.059	-0.023	0.059	0.025	0.0032	-0.025	-0.0033	0.072	-.131 E-04
4	2.54	.153	1.24	0.068	-0.063	-0.068	0.063	- .105	.0940	.107	- .093	0.011	-.123 E-05

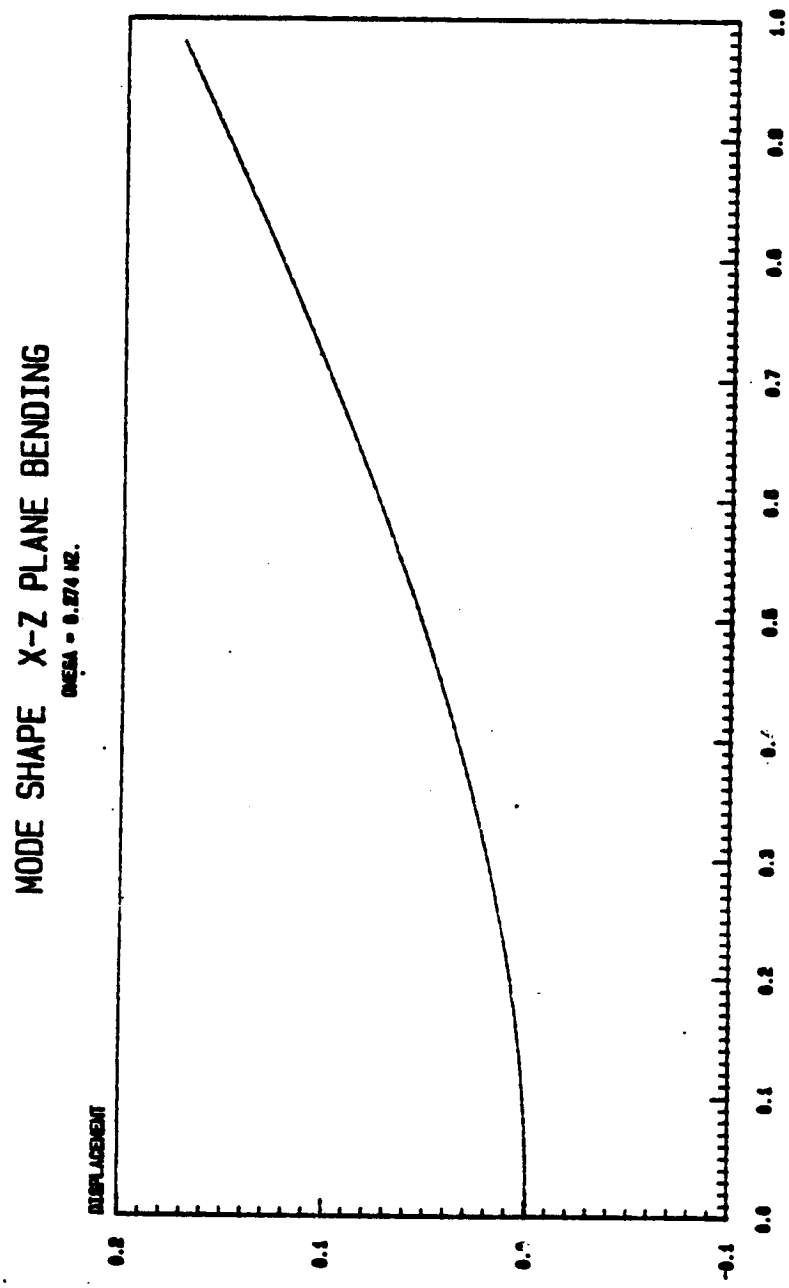

FIGURE A-1: PROJECTION OF THE FIRST MODE SHAPE ONTO THE X-Z PLANE

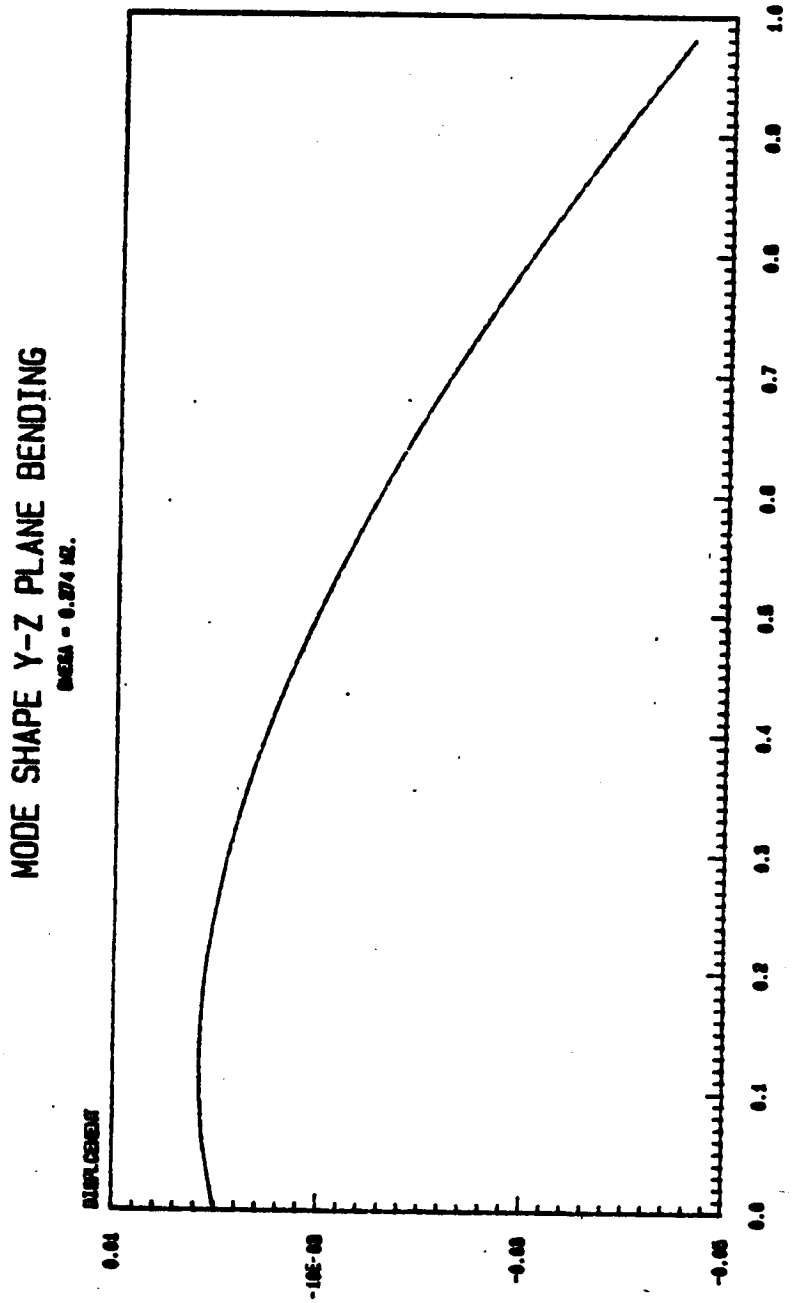

Figure A-2: PROJECTION OF THE FIRST MODE SHAPE ONTO THE Y-Z Plane

ORIGINAL PAGE IS
OF POOR QUALITY

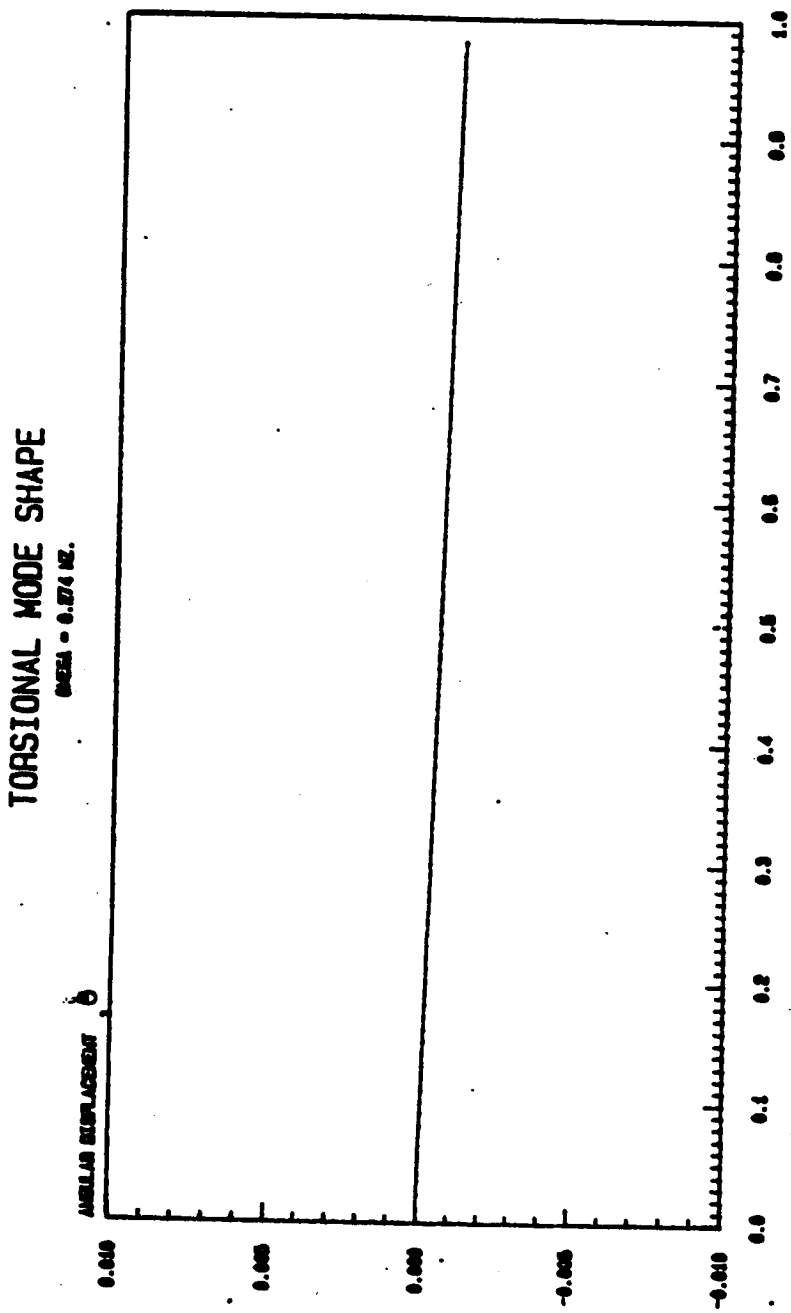

FIGURE A-3: TORSIONAL DEFLECTION OFTHE FIRST MODE SHAPE (θ IN RADIANS)

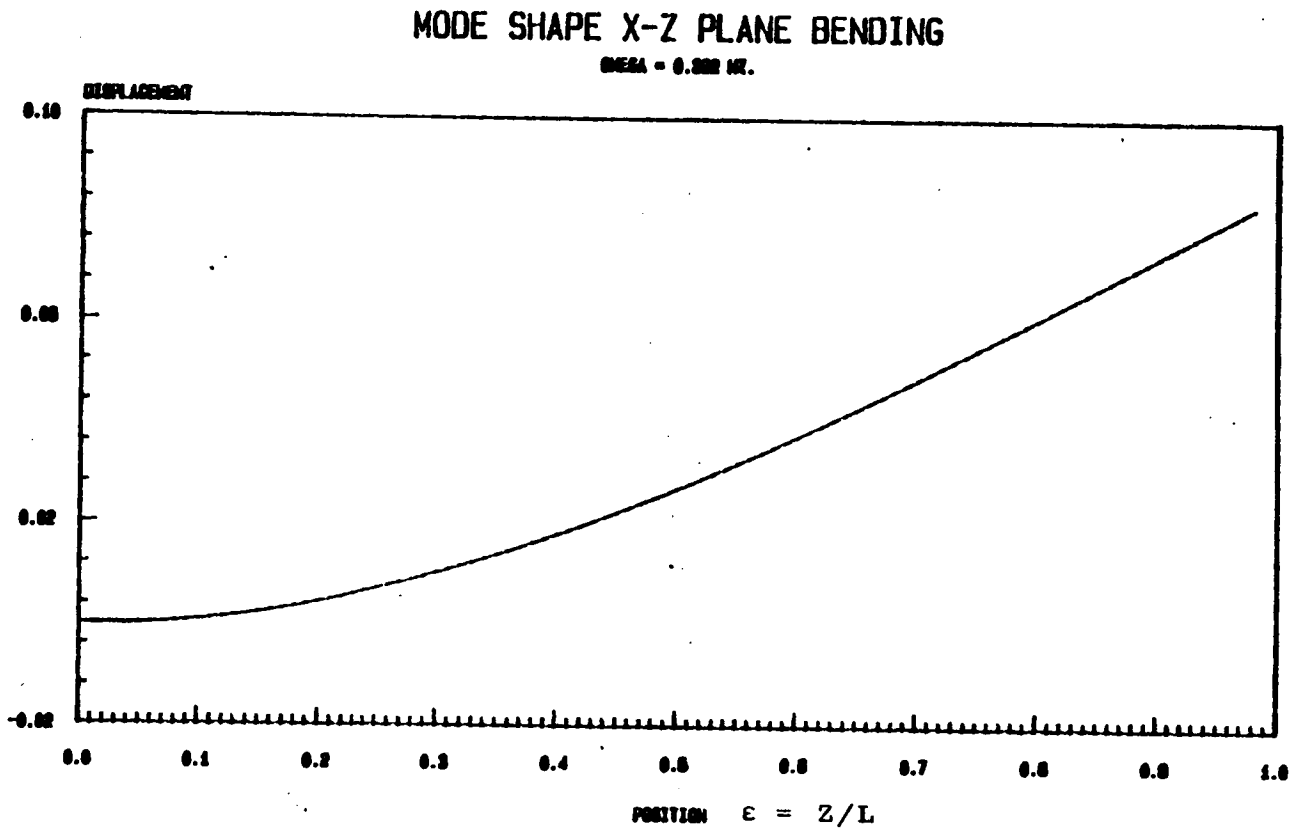

FIGURE A-4: PROJECTION OF THE SECOND MODE SHAPE ONTO THE X-Z PLANE

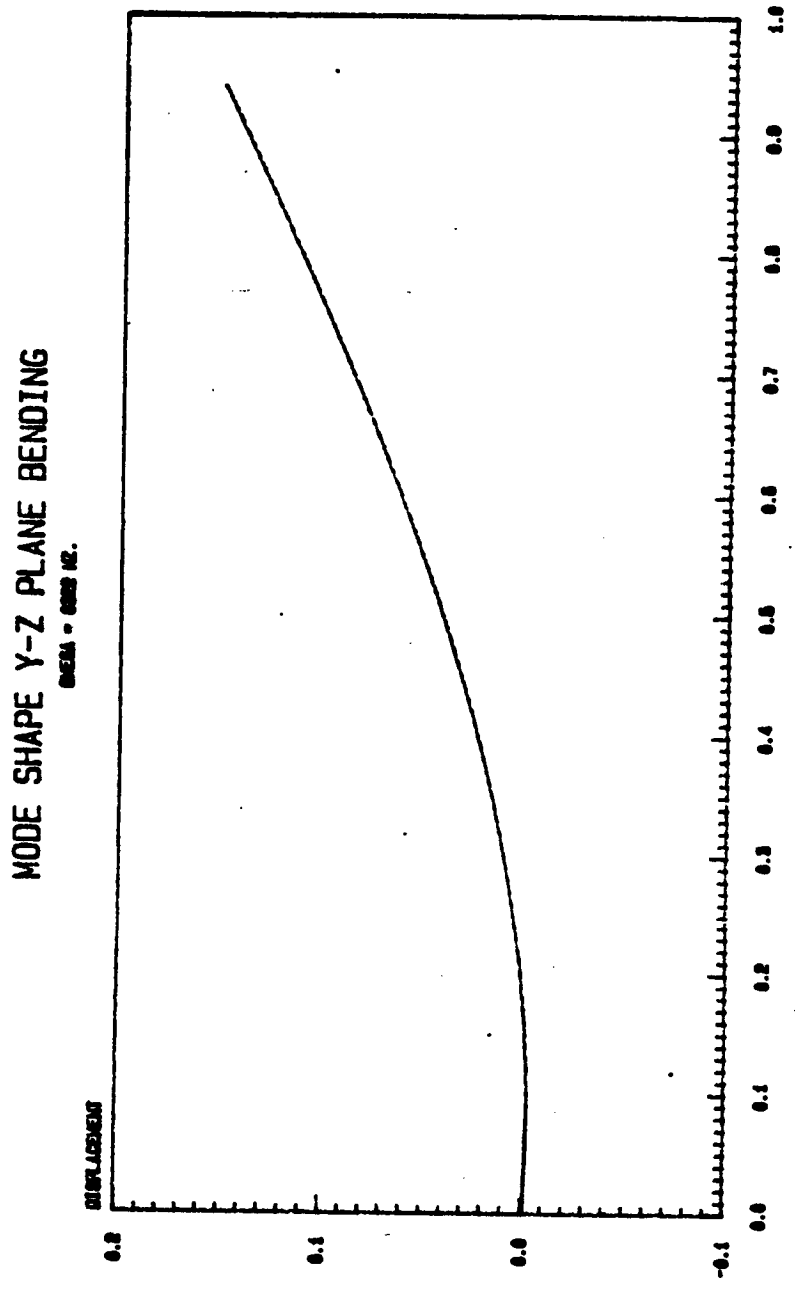

FIGURE A-5: PROJECTION OF THE SECOND MODE SHAPE ONTO THE Y-Z PLANE

ORIGINAL PAGE IS
OF POOR QUALITY

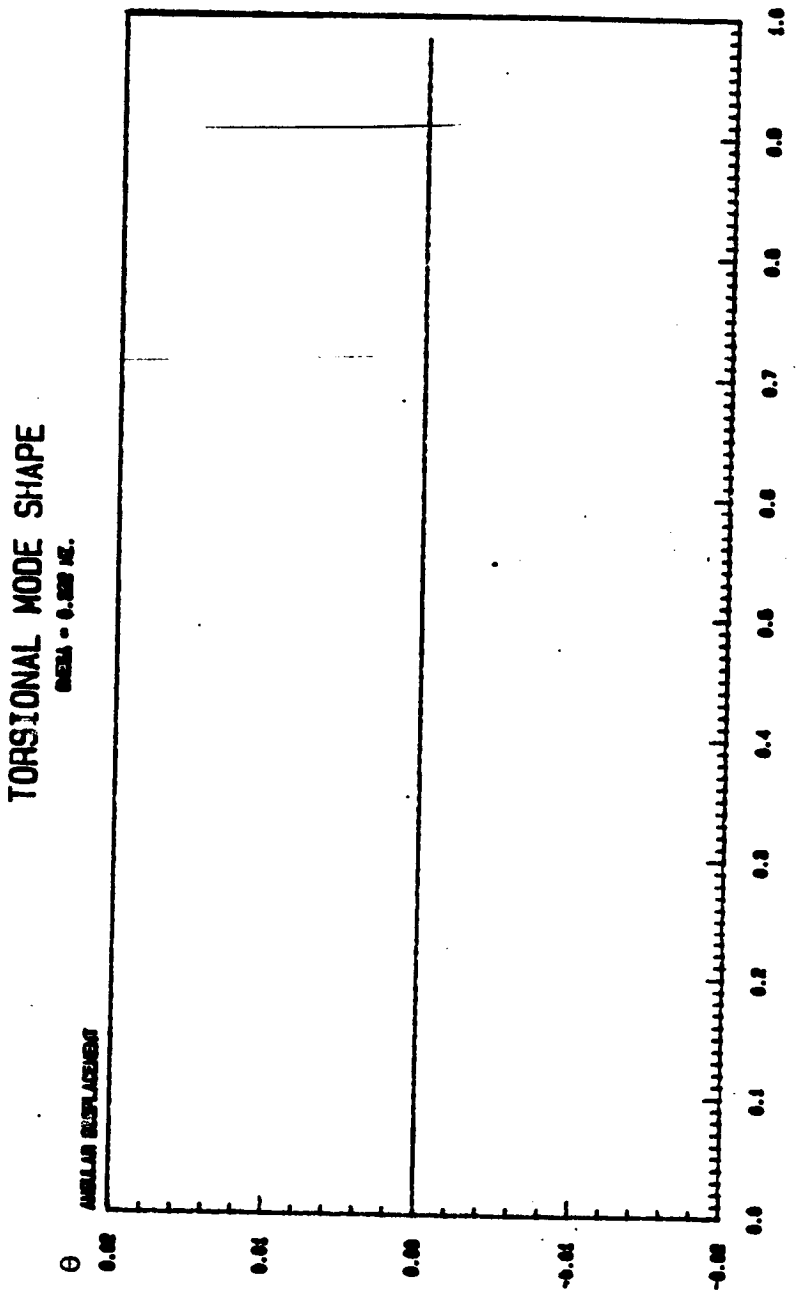

FIGURE A-6: TORSIONAL DEFLECTION OF THE SECOND MODE SHAPE (Θ IN RADIANS)

ORIGINAL PAGE IS
OF POOR QUALITY

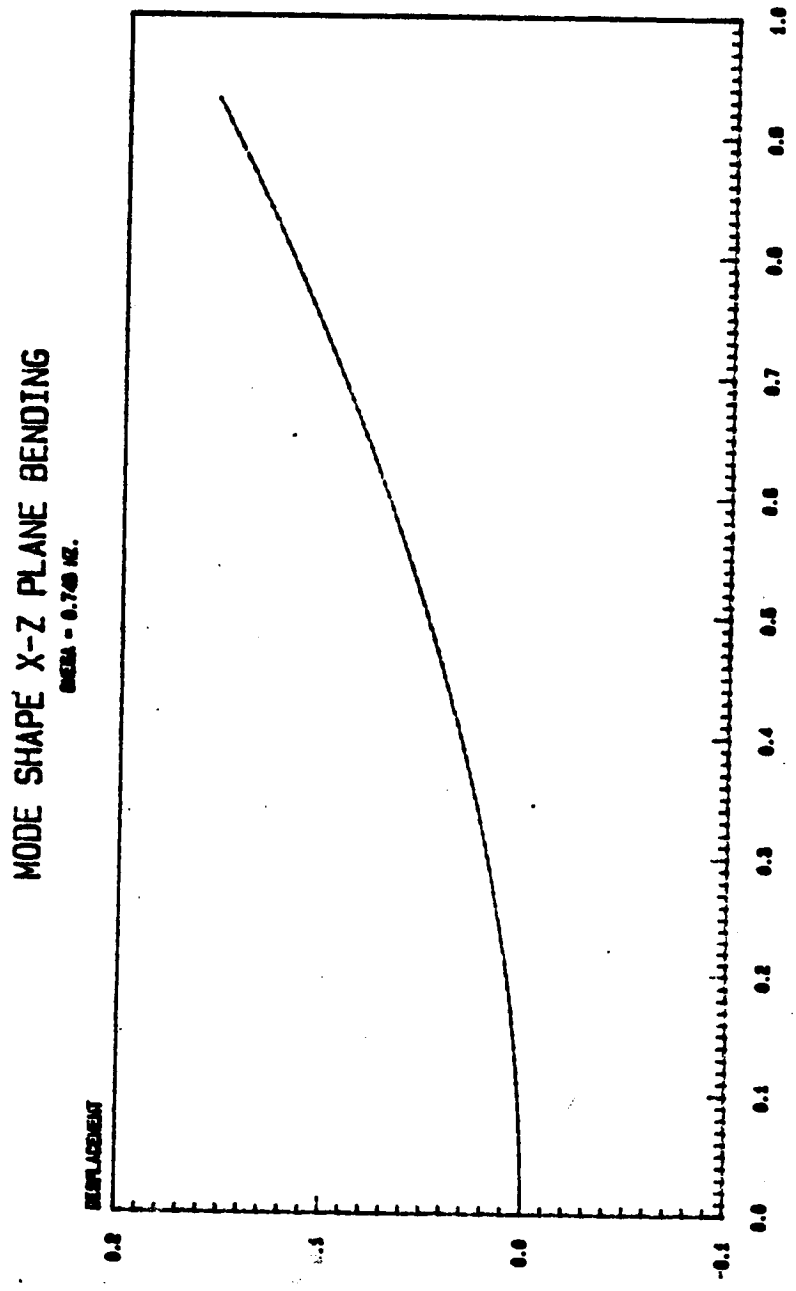

FIGURE A-7: PROJECTION OF THE THIRD MODE SHAPE ONTO THE X-Z PLANE

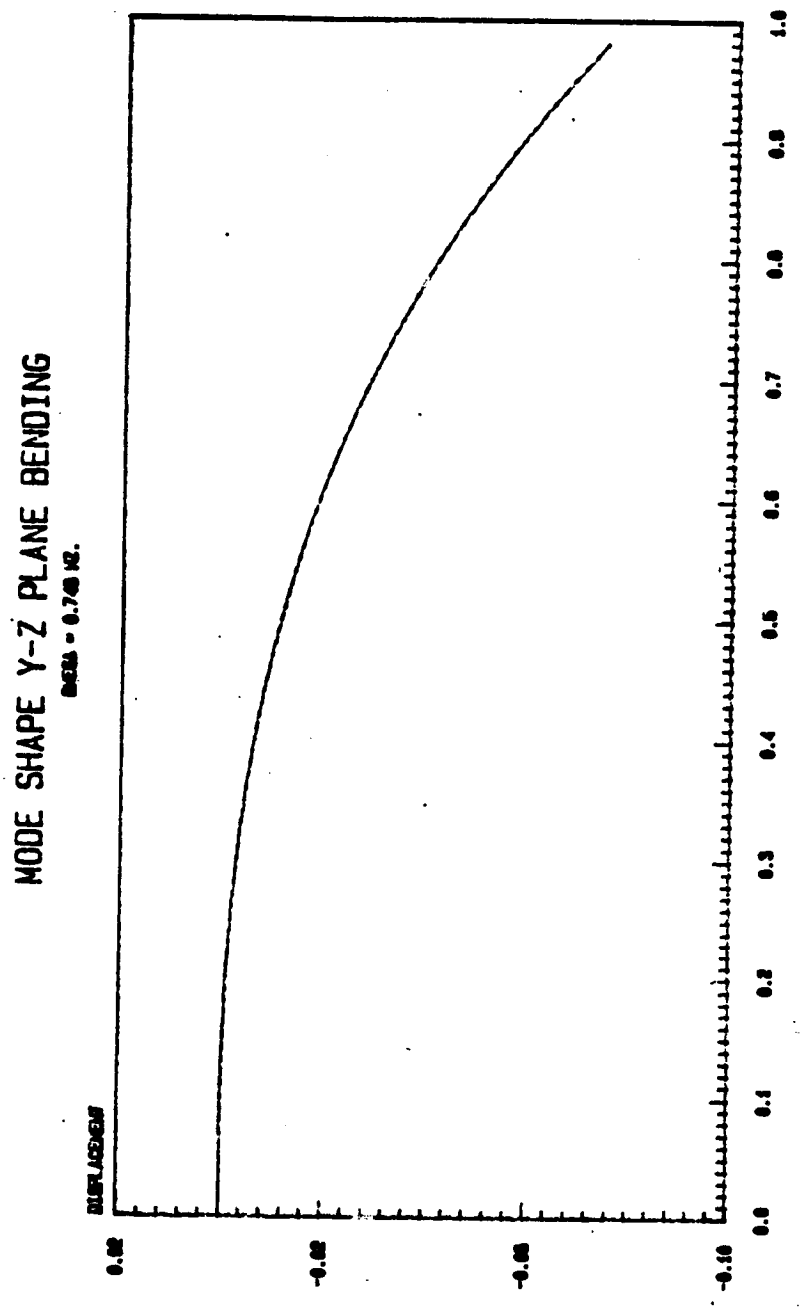

FIGURE A-8: PROJECTION OF THE THIRD MODE SHAPE ONTO THE Y-Z PLANE

ORIGINAL PAGE IS
OF POOR QUALITY

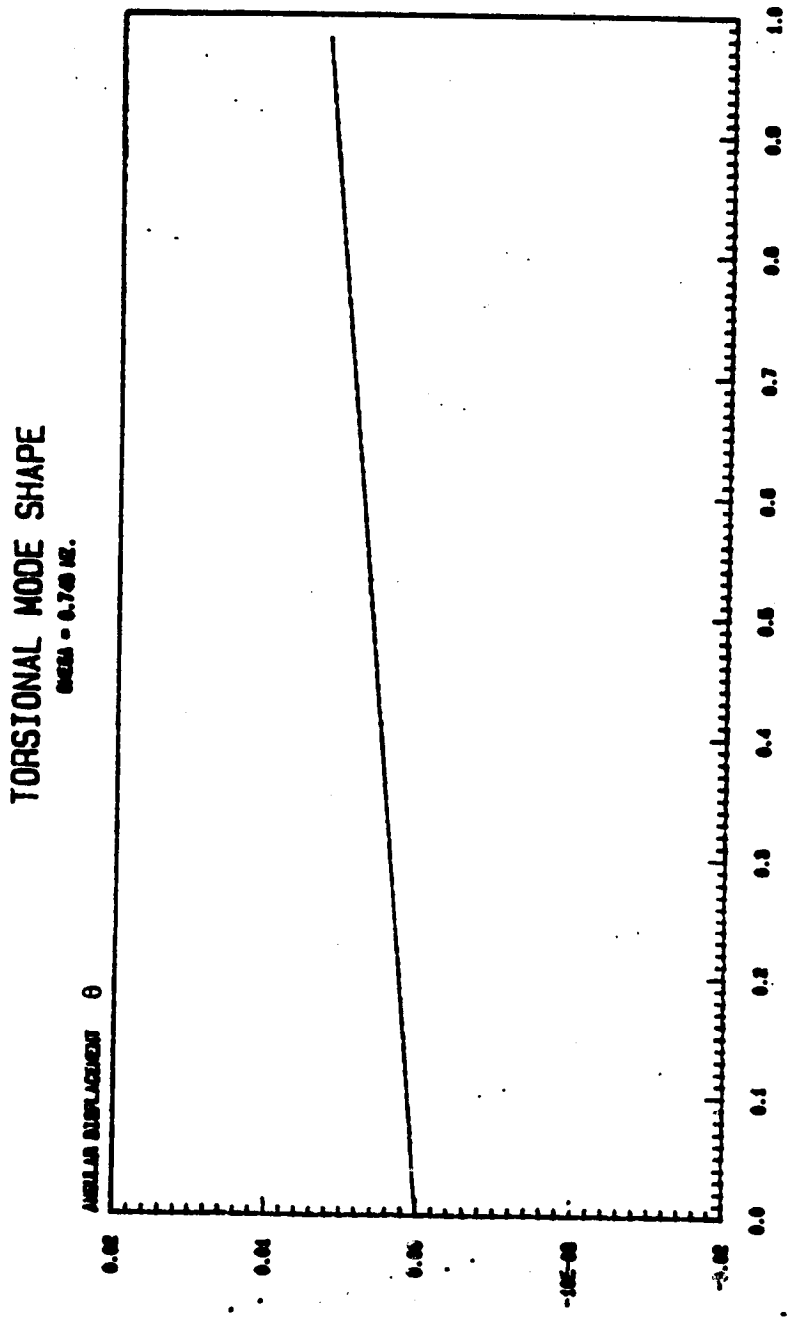

FIGURE A-9: TORSIONAL DEFLECTION OF THE THIRD MODE SHAPE (θ IN RADIANS)

ORIGINAL PAGE IS
OF POOR QUALITY

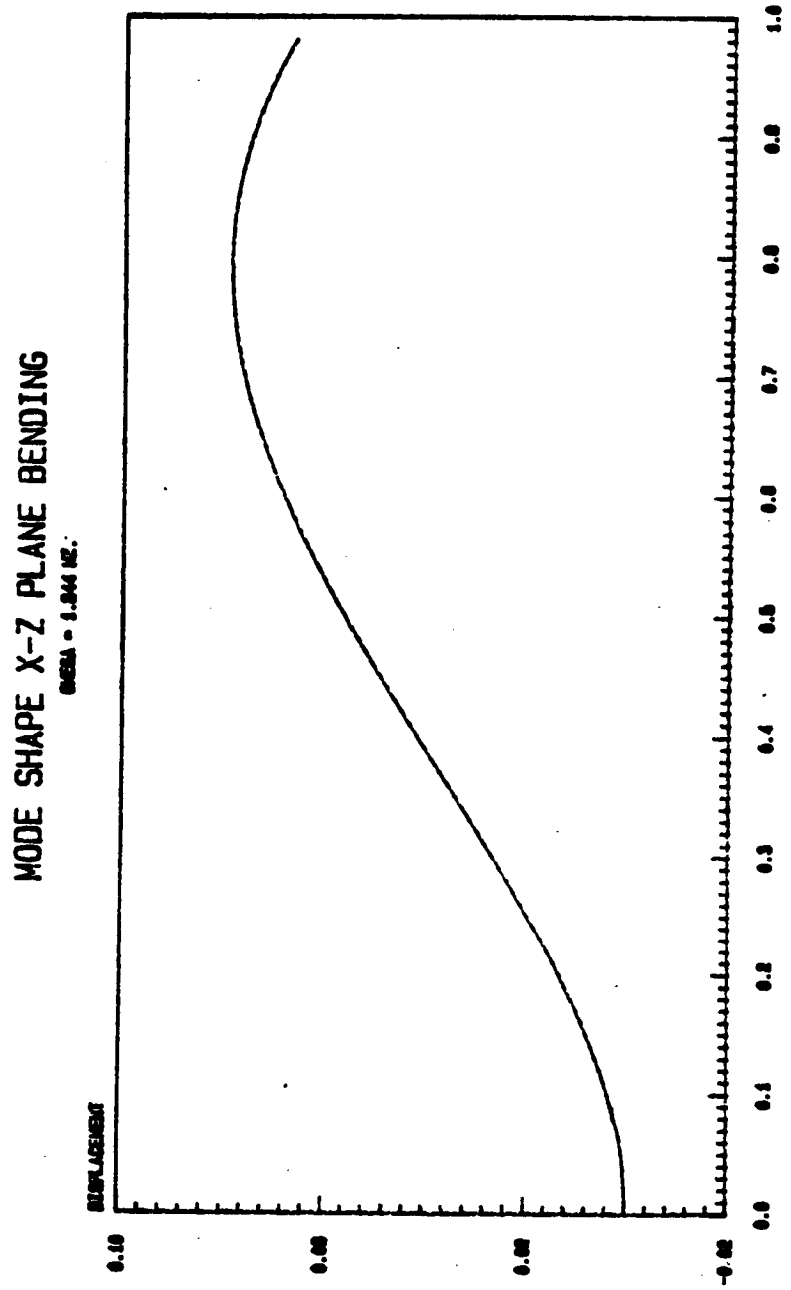

FIGURE A-10: PROJECTION OF THE FOURTH MODE SHAPE ONTO THE X-Z PLANE

ORIGINAL PAGE IS
OF POOR QUALITY

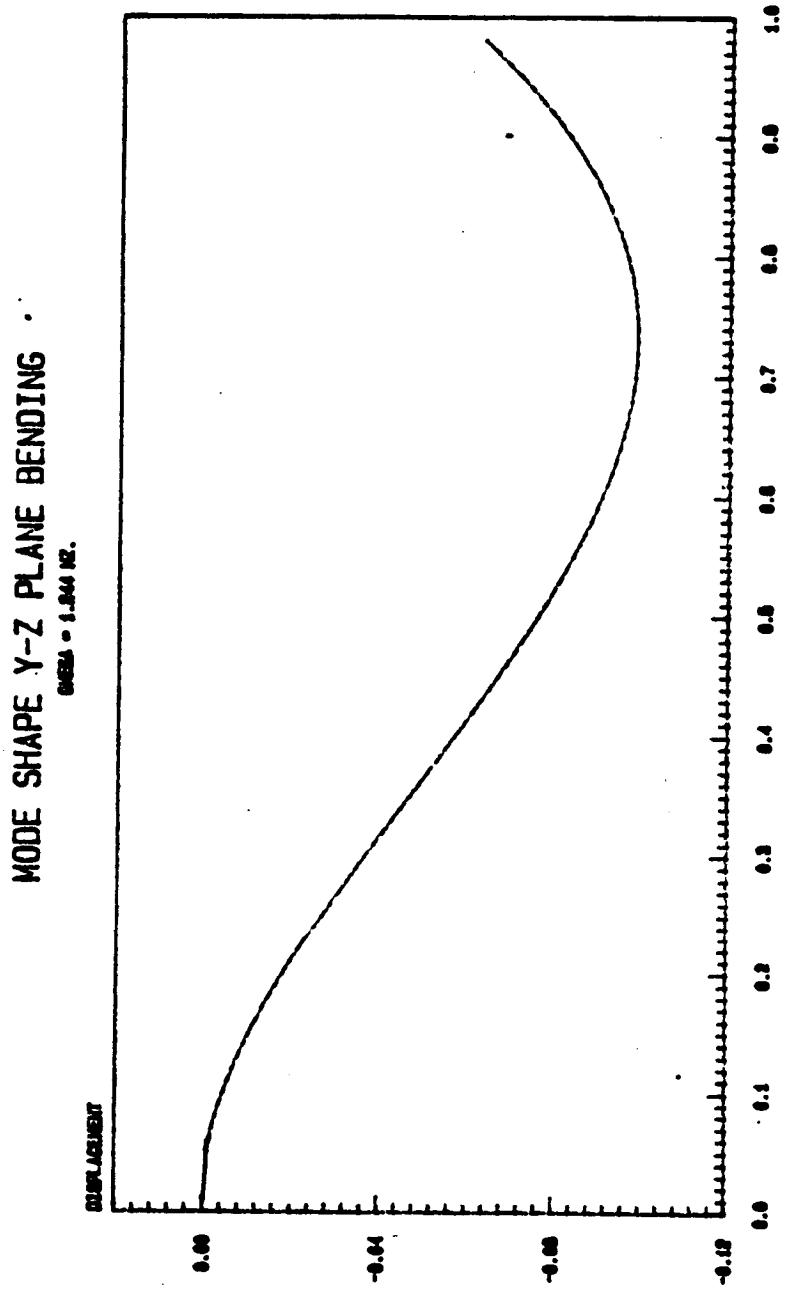

FIGURE A-11: PROJECTION OF THE FOURTH MODE SHAPE ONTO THE Y-Z PLANE

ORIGINAL PAGE IS
OF POOR QUALITY

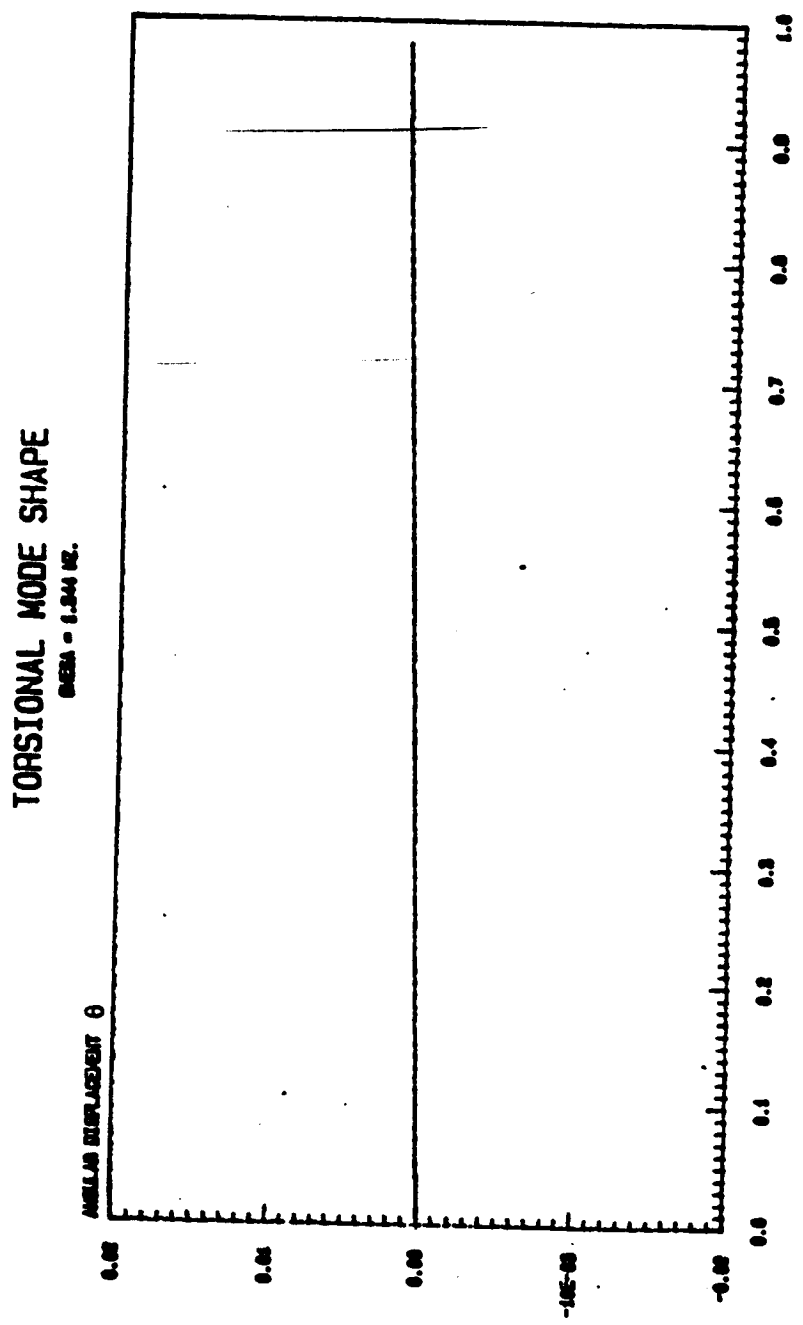

FIGURE A-12: TORSIONAL DEFLECTION OF THE FOURTH MODE SHAPE (θ IN RADIANS)

APPENDIX B

ANGULAR MOMENTUM OF A RIGID BODY

Transfer Theorem[14]

Let B be a rigid body with its center of mass located at point G and let I be some arbitrary point.

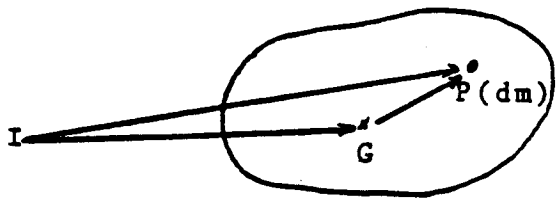

By definition, the angular momentum of B about the point I is given by:

$$\vec{H}_I = \int_M \vec{IP} \times \vec{V}(P)dm \qquad (B.1)$$

where $\vec{V}(P)$ is the inertial velocity of the dm located at point P.

The vector $\vec{IP}$ can be rewritten as

$$\vec{IP} = \vec{IG} + \vec{GP} \qquad (B.2)$$

and

$$\vec{V}(P)=\vec{V}(G) + \vec{\Omega}\times \vec{GP} \qquad (B.3)$$

where $\vec{V}(G)$ is the inertial velocity of G and $\vec{\Omega}$ is the inertial angular velocity of B.

$\vec{IP} \times \vec{V}(P)$ can therefore be expanded as

$$\vec{IP} \times \vec{V}(P) = \vec{IG} \times \vec{V}(G) + \vec{IG} \times (\times \vec{GP}) + \vec{GP} \times \vec{V}(G) + \vec{GP} \times (\vec{\Omega} \times \vec{GP}) \quad (B.4)$$

Each of the terms can be integrated as follows:

$$\int_M \vec{IG} \times \vec{V}(G)dm = \vec{IG} \times \vec{V}(G) \int_M dm = M\vec{IG} \times \vec{V}(G) \quad (B.5)$$

$$\int_M \vec{GP} \times \vec{V}(G)dm = -\vec{V}(G) \times \int_M \vec{GP}dm = \vec{0} \quad (B.6)$$

for, G is the mass center of the body B.

$$\int \vec{IG} \times (\vec{\Omega} \times \vec{GP})dm = (\vec{IG} \times \vec{\Omega}) \times \int_M \vec{GP}\, dm = \vec{0} \quad (B.7)$$

because of the reason stated above

Let now $\vec{GP} = X\hat{i} + Y\hat{j} + Z\hat{k}$ (B.8)

$$= \Omega_x\hat{i} + \Omega_y\hat{j} + \Omega_z\hat{k} \quad (B.9)$$

where $\hat{i}$, $\hat{j}$, $\hat{k}$ are any convenient reference axes fixed to B.

$$\vec{GP} \times (\vec{\Omega} \times \vec{GP}) = |\vec{GP}|^2 \vec{\Omega} - (\vec{\Omega} . \vec{GP})\vec{GP} \quad (B.10)$$

Equation (B.10) after substitution of Equations (B.8) and (B.9) becomes:

$$\vec{GP} \times (\vec{\Omega} \times \vec{GP}) = [(Y^2+Z^2)\Omega_x - XY\Omega_y - XZ\ \Omega_z]\,\hat{i} + [-XY\Omega_x + (X^2+Z^2)\Omega_y - ZY\Omega_z]\,\hat{j} + [-ZX\Omega_x - YZ\Omega_y + (X^2+Y^2)\Omega_z]\,\hat{k} \quad (B.11)$$

Because

$$\int_M (X^2+Y^2)\,dm = I_{ZZ/G}$$

$$\int_M XZ\,dm = -I_{XY/G}$$

$$\int_M XZ\,dm = -I_{ZX/G}$$

$$\int_M YZ\,dm = -I_{YZ/G}$$

$$\int (X^2+Z^2)\,dm = I_{YY/G}$$

and

$$\int (Y^2+Z^2)\,dm = I_{XX/G}$$

it can now be seen that

$$\vec{GP} \times (\vec{\Omega} \times \vec{GP})\, dm = \bar{\bar{I}}_G \vec{\Omega} \qquad \text{(B.12)}$$

which is the angular momentum of B about G. Gathering the terms yields

$$\vec{H}_I = \vec{H}_G + M\, \vec{IG} \times \vec{V}(G) \qquad \text{(B.13)}$$

APPENDIX C

GRAVITY GRADIENT TORQUE ON THE SCOLE SYSTEM

In what follows here, the gravity gradient torques will be derived for three different configurations of the SCOLE system. In the development of the expression of the gravity gradient torques for all three cases, it will be assumed, without great loss of accuracy, that the center of mass of the entire system coincides with that of the Shuttle Orbiter. Under that assumption, the unit vector, a, defining the local vertical can be expressed in the Shuttle body frame as the following functions of Euler's angles (See Chapter III, Section 1).

$$\hat{a} = \sin\theta\cos\theta\,\hat{i} - (\cos\theta\sin\psi+\sin\theta\sin\phi\cos\psi)\hat{j} + (\sin\theta\sin\phi\sin\psi - \cos\theta\cos\psi)\hat{k} \qquad (C.1)$$

Expression for the Gravity Gradient Torque, N

$$\vec{N} = 3\,\omega_0^2\,\hat{a} \times \bar{I}_{syst/G}\cdot\hat{a} \qquad (C.2)$$

where, ω_0 is the Shuttle (circular) orbital angular velocity; $\bar{I}_{syst/G}$, the inertia tensor of the system at its center of mass.

Inertia Tensor of the SCOLE Components at their Mass Centers

$$\bar{\bar{I}}_{S/G} = \begin{bmatrix} I_{S1} & 0 & -I_{S4} \\ 0 & I_{S2} & 0 \\ -I_{S4} & 0 & I_{S3} \end{bmatrix}$$

$$\bar{\bar{I}}_{M/GM} = \begin{bmatrix} \frac{ML^2}{12} & 0 & 0 \\ 0 & \frac{ML^2}{12} & 0 \\ 0 & 0 & 0 \end{bmatrix}$$

$$\bar{\bar{I}}_{R/G} = \begin{bmatrix} I_{R1} & 0 & 0 \\ 0 & I_{R2} & 0 \\ 0 & 0 & I_{R3} \end{bmatrix}$$

The total tensor of inertia about G is the sum of the inertia tensors of the components transferred at G using the parallel axis theorem.

SCOLE System Without Offset

$$\bar{\bar{I}}_{syst/G} = \begin{bmatrix} I_1 & 0 & -I_4 \\ 0 & I_2 & 0 \\ -I_4 & 0 & I_3 \end{bmatrix}$$

where

$$I_1 = I_{S1} + I_{R1} + \frac{ML^2}{3} + M_R L^2$$

$$I_2 = I_{S2} + I_{R2} + \frac{ML^2}{3} + M_R L^2$$

$$I_3 = I_{S3} + I_{R3} \quad \text{and} \quad I_4 = I_{S4}$$

Under the assumption of small angle approximation for the Euler angles, there results

$$\vec{N} = 3\omega_0^2 \{\psi (I_3 - I_2)\hat{i} + [-I_4 - \theta(I_1 - I_3)]\hat{j} + I_4 \psi \hat{k}\} \qquad (C.3)$$

SCOLE System with Offset in the "X" Direction

$$\bar{\bar{I}}_{syst/G} = \begin{bmatrix} I_1' & 0 & -I_4' \\ 0 & I & 0 \\ -I_4' & 0 & I_3' \end{bmatrix}$$

with

$$I_1' = I_1; \quad I'_4 = I_4 + M_R XL \; ; \quad I_2' = I_2 + M_R X^2$$

and $I_3' = I_3 + M_R X^2$

again

$$\vec{N} = 3\omega_0^2 \{\psi(I_3' - I_2')\hat{i} + [-I_4' - \theta(I_1' - I_3')]\hat{j} + I_4'\psi\hat{k}\} \quad (C.4)$$

Actual SCOLE Configuration in the Undeformed State

In the actual configuration, offset in both the "X" and "Y" directions, the design challenge paper[1] provided the inertia tensor of the whole system as

$$\bar{I}_{syst/G} = \begin{bmatrix} I_{xx} & -I_{yx} & -I_{xz} \\ -I_{xy} & I_{yy} & -I_{yz} \\ -I_{xz} & -I_{yz} & I_{zz} \end{bmatrix}$$

which yields

$$\vec{N} = 3\omega^2 \{-I_{yz} + \psi(I_{zz} - I_{yy}) + \theta I_{xy}]\hat{i} + [-I_{xz} + \psi I_{xy} - \theta(I_{xx} - I_{zz})]\hat{j} + (-\theta I_{yz} + \psi I_{xz})\hat{k}\} \quad (C.5)$$

APPENDIX D

Generic Mode Equations

Consider an elemental mass, dm, of the body whose instantaneous position from the center of mass of the Shuttle is $\vec{r}$. The equations of motion of dm can be written as

$$\bar{a}dm = L(\bar{q}) + \bar{f}dm + \bar{e}dm \qquad (D.1)$$

where $\bar{a}$ is the inertial acceleration of dm; $\bar{f}$, the gravitational force per unit mass; $\bar{e}$, the external force per unit mass; $\bar{q}$, the elastic displacement of dm; and L, a linear operator which, when applied to the small elastic displacement $\bar{q}$, yields the elastic forces acting on dm.

The gravitational force per unit mass, $\bar{f}$, can be expressed as [8]:

$$\bar{f} = \bar{f}_o + M\bar{r} \qquad (D.2)$$

where $\bar{f}_o$ is the gravitational force per unit mass at the center of mass of the body considered and M, a matrix operator.

In what follows, the generic mode equations will be derived based on a Newton-Euler formulation. The principal assumptions made in this development are:

1. within each component of the system, the mass and structural properties are uniformly distributed;
2. the material of each component is isotropic;
3. the system is deformed in such a manner that it experiences only small strains (within the linear range).
4. the elastic displacements are small as compared with the characteristic linear dimensions of the system;
5. the natural mode shapes of free vibrations of the system are known a priori;
6. the system is nominally earth pointing;
7. the system is considered to be closed; no mass transfer across its boundaries.

The vector equation (D.1) can be rewritten in the frame moving with each body as:

$$[\bar{a}_{Ch} + \ddot{\bar{r}} + 2\bar{\omega}\bar{x}\dot{\bar{r}} + \dot{\bar{\omega}}\bar{x}\bar{r} + \bar{\omega}\bar{x}(\bar{\omega}\bar{x}\bar{r})]\, dm = L\,(\bar{q}) + (\bar{f}+\bar{e})\, dm \qquad (D.3)$$

Note that $\dot{\vec{r}}$ and $\ddot{\vec{r}}$ are the velocity and acceleration of dm

as seen from the body fixed frame. The symbol $\vec{\omega}$ refers to the inertial angular velocity of the body. The instantaneous position vector, $\vec{r}$, of dm can be written as

$$\bar{r} = \bar{r}_o + \bar{q} \qquad (D.4)$$

where $\bar{r}_o$ is the position of vector of dm with respect to G, center of mass of the Shuttle, in the undeformed state; and $\bar{q}$ is the elastic displacement of dm. Hence,

$$\dot{\bar{r}} = \dot{\bar{q}} \quad \text{and} \quad \ddot{\bar{r}} = \ddot{\bar{q}} \qquad (D.5)$$

For small amplitude elastic displacements, one can write $\bar{q}$ as a superposition of the various modal contributions according to

$$\bar{q} = \sum_{n=1}^{\infty} A_n(t)\ \bar{\phi}_n\ (\bar{r}_o) \qquad (D.6)$$

where $A_n(t) = p_n(t)$ = modal amplitude

and $\vec{\phi}_n(r_o) = S_{xn}\,\hat{i} + S_{yn}\hat{j} + \theta_n\ \hat{k}$ (D.7)

The mode shape $\vec{\phi}_n(r_o)$ is associated with the natural frequency, ω_n, and satisfies the following conditions:

$$\int_M \bar{\phi}_m \cdot \bar{\phi}_n \, dm = \delta_{mn} M_n \qquad (D.8)$$

where M_n is the generalized mass in the nth mode.

$$L(\phi_n) = -\omega_n^2 \bar{\phi}_n \, dm \qquad (D.9)$$

$$\int_M \bar{\phi}_n \, dm = \vec{0} \qquad (D.10)$$

and

$$\int_M \vec{r}_o \times \dot{\phi}_n \, dm = \vec{0} \qquad (D.11)$$

This here assumes that the fundamental structural frequency, ω_1, is much greater than the orbital angular velocity, $\omega_o = 0.0011$ rad/s, and enables one to use, with a high degree of accuracy, the mode shape functions corresponding to a non-rotating structure.

Generic Mode Equations[8]

The generic mode equations are obtained by taking the modal components of all internal, external and inertial forces acting on the system, i.e.,

$$\int_M \bar{\phi}_n \cdot [\bar{a}_{cm} + \ddot{\bar{r}} + 2\bar{\omega}\times\dot{\bar{r}} + \dot{\bar{\omega}}\times\bar{r} + \bar{\omega}\times(\bar{\omega}\times\bar{r})] \, dm =$$

$$\int_M \phi_n \cdot [L(\bar{q})/_{dm} + \bar{f} + \bar{e}] \, dm \qquad (D.12)$$

The various terms appearing in equation (D.12) can now be expanded as follows:

$$\int_M \bar{\phi}_n \cdot \bar{a}_{cm}\, dm = \bar{a}_{cm} \cdot \int_M \bar{\phi}_n\, dm = 0 \qquad \text{(D.13)}$$

See Eq. (D.10).

$$\int_M \bar{\phi}_n \cdot \ddot{\bar{r}} dm = \int_M \bar{\phi}_n \cdot \ddot{\bar{q}}\, dm = \int_M (\bar{\phi}_n \cdot \sum_{m=1} A_m(t)\bar{\phi}_m)\, dm$$

because of the result established in Equation (D.8),

$$\int \bar{\phi}_n \cdot \ddot{\bar{r}}\, dm = \ddot{A}_n M_m \qquad \text{(D.14)}$$

$$\int_M \bar{\phi}_n \cdot (2\bar{\omega}x\dot{\bar{r}})\, dm = 2 \int_M \bar{\phi}_n \cdot (\dot{\bar{\omega}}x\bar{q})\, dm \qquad \text{(D.15)}$$

$$\bar{\phi}_n \cdot (\dot{\bar{\omega}}x\bar{r})\, dm = \int_M \bar{\phi}_n \cdot (\dot{\bar{\omega}}x\bar{r}_o)\, dm + \int_M \bar{\phi}_n \cdot (\dot{\bar{\omega}}x\bar{q})\, dm \qquad \text{(D.16)}$$

$$\int_M \bar{\phi}_n \cdot \bar{\omega}x(\bar{\omega}x\bar{r})\, dm = \int_M \bar{\phi}_n \cdot \bar{\omega}x(\bar{\omega}x\bar{r}_o)\, dm + \int_M \phi_n \cdot \bar{\omega}x(\bar{\omega}x\bar{q})\, dm \qquad \text{(D.17)}$$

$$\int_M \bar{\phi}_n \cdot L(\bar{q})_{/dm}\, dm = -\omega_n^2 A_n M_n \qquad \text{(D.18)}$$

$$\int_M \bar{\phi}_n \cdot \bar{f} dm = \int_M \bar{\phi}_n \cdot \bar{f}_o dm + \int_M \bar{\phi}_n \cdot M(\bar{r}_o) dm + \int_M \bar{\phi}_n \cdot M(\bar{q}) dm \qquad \text{(D.19)}$$

$$\int_M \bar{\phi}_n \cdot \bar{e} dm = E_n \qquad \text{(D.20)}$$

where E_n is the modal contribution of the external forces (control forces) in the nth mode.

After substitution of the values for the integrals into Equation (D.12) and rearrangement of the terms, the generic mode equations are obtained in the following form:

$$\ddot{A}_n + \omega_n^2 A_n + \Phi_n/M_n + \sum_{m=1}^{\infty} \Phi_{mn}/M_n$$

$$= [g_n + \sum_{m=1}^{\infty} g_{mn} + E_n + D_n]/M_n \qquad (D.21)$$

where

$$\Phi_n = \int_M \bar{\phi}_n \cdot [(\dot{\bar{\omega}} x \bar{r}_o) + \bar{\omega} x (\bar{\omega} x \bar{r}_o)] \, dm \qquad (D.22)$$

$$\sum_{m=1} \Phi_{mn} = \int_M \bar{\phi}_n \cdot [2\bar{\omega} x \dot{\bar{q}} + \dot{\bar{\omega}} x \bar{q} + \bar{\omega} x (\bar{\omega} x \bar{q}] \, dm \qquad (D.23)$$

$$g_n = \int_M \bar{\phi}_n \cdot M(\bar{r}_o) \, dm \qquad (D.24)$$

$$\sum_{m=1} g_{mn} = \int_M \bar{\phi}_n \cdot M(\bar{q}) dm \qquad (D.25)$$

$$E_n = \int_M \bar{\phi}_n \cdot \bar{e} \, dm \qquad (D.26)$$

and $$D_n = \int_M \phi_n \cdot \bar{f}_C \, dm \qquad (D.27)$$

Because, in Appendix A, the SCOLE system was assumed to be an unconstrained structure with end masses having

inertia, the orthogonality conditions expressed in Equations (D.10) and (D.11) result in:

$$D_n = -\int Msyst\, \bar{\phi}_n \cdot \bar{f}_0 \, dm =$$

$$-\bar{f}_o \cdot \int Msyst\, \bar{\phi}_n \, dm = \bar{0}$$

It is assumed here that the transverse displacements are small as compared with the characteristic dimensions of the system. In this first approximation analysis, terms involving the integral of $\bar{\phi}.\bar{q}$ will be assumed small as compared with terms involving $\bar{\phi}\,.\bar{r}_0$ and, thus, neglected. As a consequence of this

$$\sum_{m=1}^{\infty} \phi_{mn} = \sum_{m=1}^{\infty} g_{mn} = 0 \qquad (D.28)$$

leaving

$$A_n + \omega_n^2 A_n + \phi_n / _n = (g_n + E_n)/M_n \qquad (D.29)$$

Since the control forces consist of six actuators located in pairs at G_1, the reflector mass center, and at two points on the mast corresponding to z = -43.3 ft and z = -86.6 ft,

$$E_n = M_n F_x(s_{xn}(-L) + s_{xn}(-L/3) + s_{xn}(-2L/3))$$

$$+ M_n F_y(s_{yn}(-L) + s_{yn}(-L/3) + s_{yn}(-2L/3))$$

$$\Phi_n = \int_M \bar{\phi}_n \cdot [\dot{\bar{\omega}} \times \bar{r}_o + \bar{\omega} \times (\bar{\omega} \times \bar{r}_o)]\, dm$$

$$= \rho \{ \int_0^{-L} (s_{yn} \dot{\omega}_x z - \omega_y s_{xn} z) dz + (s_{xn} \omega_z \omega_x z + s_{yn} \omega_y \omega_z z + \theta_n \omega_z^2 z) dz$$

$$- (\omega_x^2 + \omega_y^2 + \omega_z^2) \int_0^{-L} \theta_n z \, dz \}$$

where $s_{xn} = A_{1n} \sin \beta_n z + B_{1n} \cos \beta_n z + C_{1n} \sinh \beta_n z + D_{1n} \cosh \beta_n z$

$s_{yn} = A_{2n} \sin \beta_n z + B_{2n} \cos \beta_n z + C_{2n} \sinh \beta_n z + D_{2n} \cosh \beta_n z$

and $\theta_n = A_{3n} \sin \beta' z + B_{3n} \cos \beta' z$

are the x, y components of the mode shape vector and the angular displacement of a point on the mast about the z axis, respectively

with $\beta' = \beta_n^2 \sqrt{\frac{EI}{GA}}$

Φ_n can be rewritten as

$$\Phi_n = \rho \{ \int_0^{-L} (\dot{\omega}_x + \omega_z \omega_y) s_{yn} z \, dz + \int_0^{-L} (\omega_z \omega_x - \dot{\omega}_y) s_{xn} z \, dz$$

$$- \int_0^{-L} (\omega_x^2 + \omega_y^2) \theta_n z \, dz \}$$

since $\int_0^{-L} z \sin \beta_n z \, dz = - \frac{\sin \beta_n L}{\beta_n^2} + \frac{L \cos \beta_n L}{\beta_n} = f_3 (\beta_n)$

$$\int_0^{-L} z \cos \beta_n z \, dz = \frac{\cos \beta_n L}{\beta_n^2} + \frac{L \sin \beta_n L}{\beta_2} - \frac{1}{\beta_n^2} = f_4 (\beta_n)$$

$$\int z \sinh \beta_n z \, dz = - \frac{L \cosh \beta_n L}{\beta_n} + \frac{\sinh \beta_n L}{\beta_n^2} = f_5 (\beta_n)$$

and

$$\int z \cosh \beta_n z \, dz = \frac{L \sinh \beta_n L}{\beta_n} - \frac{\cosh \beta_n L}{\beta_n^2} + \frac{1}{\beta_n^2} = f_6 (\beta_n)$$

$$\Phi_n = \rho \{ (- \frac{\sin \beta_n L}{\beta_n^2} + \frac{L \cos \beta_n L}{\beta_n}) [(\omega_z \omega_x - \dot{\omega}_y) A_{1n} + (\omega z \omega y + \dot{\omega} x) A_{2n}]$$

$$+ (\frac{L \sin \beta_n L}{\beta_n} + \frac{\cos \beta_n L - 1}{\beta_n^2}) [(\omega_z \omega_x \dot{\omega}_y) B_{1n} + (\omega_z \omega_y + \dot{\omega}_x) B_{2n}]$$

$$+\left(\frac{\sinh \beta_n L}{\beta_n^2} - \frac{L \cosh \beta_n L}{\beta_n}\right)\left[(\omega_z\omega_x - \dot{\omega}_y)C_{1n} + (\omega_z\omega_y\dot{\omega}_x)C_{2n}\right]$$

$$+\left(\frac{L \sinh \beta_n L \cosh \beta_n L - 1}{\beta_n \qquad \beta_n^2}\right)\left[(\omega_z\omega_x - \dot{\omega}_y)D_{1n} + (\omega_z\omega_y + \dot{\omega}_x)D_{1n}\right]$$

$$-\left(\frac{L \cos \beta_n' L}{\beta_n'} - \frac{\sin \beta_n' L}{\beta_n'^2}\right)(\omega_x^2 + \omega_y^2)A_{3n}$$

$$-\left(\frac{L \sin \beta_n L}{\beta_n'} + \frac{\cos \beta_n' L - 1}{\beta_n'^2}\right)(\omega_x^2 + \omega_y^2)B_{3n}$$

or

$$\Phi_n = \frac{M_n}{L}\{f_3(\beta_n)\left[(\omega_z\omega_x - \dot{\omega}_y)A_{1n} + (\omega_z\omega_y + \dot{\omega}_x)A_{2n}\right]$$

$$+ f_4(\beta_n)[\omega_z\omega_x - \dot{\omega}_y)B_{1n} + (\omega_z\omega_y + \dot{\omega}_x)B_{2n}] + f_5(\beta_n)\left[\omega_z\omega_x - \dot{\omega}_y\right)C_{1n}$$

$$+ (\omega_z\dot{\omega}_y + \dot{\omega}_x)C_{2n}] + f_6(\beta)[\omega_z\omega_x - \dot{\omega}_y)D_{1n} + (\omega_z\omega_y + \dot{\omega}_x)D_{2n}]$$

$$-(\omega_x^2 + \omega_y^2)\,[f_3(\beta_n')A_{3n} + f_4(\beta_n')\,B_{3n}]$$

With the assumed Euler angle sequence, the gravity gradient force matrix, M^o, can be derived as [8]:

$$M^o = \omega_0^2 \; T_1 \; T_2 \; B^0 \; (T_1 \; T_2)^{-1}$$

where

$$T_1 = \begin{bmatrix} 1 & 0 & 0 \\ 0 & \cos\psi & \sin\psi \\ 0 & -\sin\psi & \cos\psi \end{bmatrix} \begin{bmatrix} \cos\phi & \sin\phi & 0 \\ -\sin\phi & \cos\phi & 0 \\ 0 & 0 & 1 \end{bmatrix} \begin{bmatrix} \cos\theta & 0 & -\sin\theta \\ 0 & 1 & 0 \\ \sin\theta & 0 & \cos\theta \end{bmatrix}$$

and

$$T_2 = \begin{bmatrix} \cos x & -\sin x & 0 \\ \sin x & \cos x & 0 \\ 0 & 0 & 1 \end{bmatrix} \qquad T^{-1}{}_2 = \begin{bmatrix} \cos x & \sin x & 0 \\ -\sin x & \cos x & 0 \\ 0 & 0 & 1 \end{bmatrix}$$

$$B^0 = \begin{bmatrix} 1 & 0 & 0 \\ 0 & 1 & 0 \\ 0 & 0 & -2 \end{bmatrix}$$

$$T_1 = \begin{bmatrix} \cos\phi\cos\theta & \sin\phi & -\sin\theta\cos\phi \\ \sin\psi\sin\theta - \cos\psi\sin\phi\cos\theta & \cos\psi\cos\phi & \cos\psi\sin\phi\sin\theta + \sin\psi\cos\theta \\ \sin\phi\sin\psi\cos\theta + \cos\psi\sin\theta & -\sin\psi\cos\phi & \cos\psi\cos\theta - \sin\psi\sin\phi\sin\theta \end{bmatrix}$$

$$T_{-1} = \begin{bmatrix} \cos\phi\cos\theta & \sin\psi\sin\theta - \cos\psi\sin\phi\cos\theta & \sin\phi\sin\psi\cos\theta + \cos\psi\sin\phi \\ \sin\phi & \cos\psi\cos\phi & -\sin\psi\cos\phi \\ -\sin\theta\cos\phi & \sin\psi\cos\theta + \cos\psi\sin\phi\sin\theta & \cos\psi\cos\theta - \sin\psi\sin\phi\sin\theta \end{bmatrix}$$

Assuming here the intrinsic frame[8] of reference to coincide with the orbit frame, i.e. x = 0.

$$\text{and } M^0(\vec{r}_o) = \omega_0^2 \begin{bmatrix} M_{11} & M_{12} & M_{13} \\ M_{21} & M_{22} & M_{23} \\ M_{31} & M_{32} & M_{33} \end{bmatrix} \begin{bmatrix} 0 \\ 0 \\ z \end{bmatrix} = \omega_0^2 \begin{bmatrix} zM_{13} \\ zM_{23} \\ zM_{33} \end{bmatrix}$$

where $M_{13} = 3\omega_0^2 (S\theta C\theta C\phi C\psi - S^2\theta S\phi S\psi C\phi)$

$M_{23} = 3\omega_0^2 [S\theta C\theta S\phi(1-2C^2\psi) + S\psi C\psi(S^2\phi S^2\theta - C^2\theta)]$

and $M_{33} = \omega_0^2\{-3(S\phi S\theta S\psi - C\theta C\psi)^2 + 1\}$

Therefore

$$g_n \int_M \bar{\phi} \cdot M(r_0)\, dm = \rho \int_0^{-L} (s_{xn} z\, M_{13} + s_{yn} z\, M_{23} + z\theta_n\, M_{33})\, dz$$

$$g_n = \frac{M_n}{L} [f_3(\beta_n)(A_{1n} M_{13} + A_{2n} M_{23}) + f_4(\beta_n)(B_{1n} M_{13} + B_{2n} M_{23})$$

$$+ f_5(\beta_n)(C_{1n} M_{13} + C_{2n} M_{23}) + f_6(\beta_n)(D_{1n} M_{13} + D_{2n} M_{23})$$

$$+ f_3(\beta_n')\, A_{3n} M_{33} + f_4(\beta_n')\, B_{3n} M_{33}$$

the generic mode equations can be recast as:

$$\ddot{A}_n + \omega_n^2 A_n + \frac{1}{L}[(\omega_x \omega_z - \dot{\omega}_y - M_{13})[f_3(\beta_n) A_{1n} + f_4(\beta_n) B_{1n} + f_5(\beta_n) C_{1n}$$

$$+ f_6(\beta_n) D_{1n}] + (\omega_z \omega_y + \dot{\omega}_x - M_{23})[f_3(\beta_n) A_{2n} + f_4(\beta_n) B_{2n} + f_5(\beta_n) C_{2n}$$

$$+ f_6(\beta_n) D_{2n}] + (M_{33} - \omega_x^2 - \omega_y^2)[f_3(\beta_n') A_{3n} + f_4(\beta_n') B_{3n}] =$$

$$F_x[s_{xn}(-L) + s_{xn}(\tfrac{-L}{3}) + s_{xn}(\tfrac{-2L}{3})] + F_y[s_{yn}(-L) + s_{yn}(\tfrac{-L}{3}) + s_{yn}(\tfrac{-2L}{3})]$$

The scope of this study is limited to the stability analysis of the SCOLE system and the derivation of a control strategy for its motion about the nominal equilibrium position as derived in Chapter IV. The gravity-gradient forces acting on the system will be also calculated in that configuration.

Thus, in what follows, the Euler angles ψ, θ, and ϕ will be replaced by η_1, η_2, and η_3 with $\psi = \psi_{eq} + \eta_1$, $\theta = \theta_{eq} + \eta_2$, $\phi = \phi_{eq} + \eta_3$. After linearizing the different terms appearing in the generic mode equations, they can be rewritten, for each of the four modes included in this study, as:

$$\ddot{A}_n + \omega_n^2 A_n + \frac{1}{L}\{-(\ddot{\eta}_2 + 3\omega_0^2 \eta_2)[f_3(\beta_n) A_{1n} + f_4(\beta_n) B_{1n}$$

$$+ f_5(\beta_n) C_{1n} + f_6(\beta_n) D_{1n}] + (\ddot{\eta}_1 - 2\omega_0 \dot{\eta}_3 + 4\omega_0^2 \eta_1)[f_3(\beta_n) A_{2n} + f_4(\beta_n) B_{2n}$$

$$+ f_5(\beta_n) C_{2n} + f_6(\beta_n) D_{2n}] + 2\omega_0 \dot{\eta}_2 [f_3(\beta_n') A_{3n} + f_4(\beta_n') B_{3n}]$$

$$= F_x [V_3 s_{xn}(-L) + V_2 s_{xn}(-2L/3) + V_1 s_{xn}(-L/3)] + F_y [s_{yn}(-L) V_3 + s_{yn}(\quad) V_2 + s_{yn} x(-L/3) V_1]$$

In Chapter V, these equations (n = 1, 2, 3, and 4) will be added to the equations describing the rotational motion of the SCOLE to obtain a mathematical model of the SCOLE orbiting configuration. A modified version of equations III.22 - III.24 will then be used.